THE QUASI-BIENNIAL OSCILLATION

M. P. Baldwin,[1] L. J. Gray,[2] T. J. Dunkerton,[1] K. Hamilton,[3] P. H. Haynes,[4]
W. J. Randel,[5] J. R. Holton,[6] M. J. Alexander,[7] I. Hirota,[8] T. Horinouchi,[9] D. B. A. Jones,[10]
J. S. Kinnersley,[11] C. Marquardt,[12] K. Sato,[13] and M. Takahashi[14]

Abstract. The quasi-biennial oscillation (QBO) dominates the variability of the equatorial stratosphere (~16–50 km) and is easily seen as downward propagating easterly and westerly wind regimes, with a variable period averaging approximately 28 months. From a fluid dynamical perspective, the QBO is a fascinating example of a coherent, oscillating mean flow that is driven by propagating waves with periods unrelated to that of the resulting oscillation. Although the QBO is a tropical phenomenon, it affects the stratospheric flow from pole to pole by modulating the effects of extratropical waves. Indeed, study of the QBO is inseparable from the study of atmospheric wave motions that drive it and are modulated by it. The QBO affects variability in the mesosphere near 85 km by selectively filtering waves that propagate upward through the equatorial stratosphere, and may also affect the strength of Atlantic hurricanes. The effects of the QBO are not confined to atmospheric dynamics. Chemical constituents, such as ozone, water vapor, and methane, are affected by circulation changes induced by the QBO. There are also substantial QBO signals in many of the shorter-lived chemical constituents. Through modulation of extratropical wave propagation, the QBO has an effect on the breakdown of the wintertime stratospheric polar vortices and the severity of high-latitude ozone depletion. The polar vortex in the stratosphere affects surface weather patterns, providing a mechanism for the QBO to have an effect at the Earth's surface. As more data sources (e.g., wind and temperature measurements from both ground-based systems and satellites) become available, the effects of the QBO can be more precisely assessed. This review covers the current state of knowledge of the tropical QBO, its extratropical dynamical effects, chemical constituent transport, and effects of the QBO in the troposphere (~0–16 km) and mesosphere (~50–100 km). It is intended to provide a broad overview of the QBO and its effects to researchers outside the field, as well as a source of information and references for specialists. The history of research on the QBO is discussed only briefly, and the reader is referred to several historical review papers. The basic theory of the QBO is summarized, and tutorial references are provided.

1. INTRODUCTION

1.1. The Discovery of the Quasi-Biennial Oscillation

The first observations of equatorial stratospheric winds were made when it was discovered that debris from the eruption of Krakatau (1883) circled the globe from east to west in about 2 weeks; these winds became known as the "Krakatau easterlies." (For a more complete review of the discovery of the quasi-biennial oscillation, and subsequent developments in observations and theory, see *Maruyama* [1997] and *Labitzke and van Loon* [1999].) In 1908 the German meteorologist A. Berson launched balloons from tropical Africa and found winds blowing from west to east at about 15 km, near the tropopause, which became known as the "Berson westerlies." For nearly 50 years, there were only sporadic balloon observations [*Hamilton*, 1998a] to contradict the existence of equatorial stratospheric *easterly*

[1]NorthWest Research Associates, Inc., Bellevue, Washington.
[2]Rutherford Appleton Laboratory, Oxon, England, United Kingdom.
[3]International Pacific Research Center and Department of Meteorology, University of Hawaii, Honolulu, Hawaii.
[4]Department of Applied Mathematics and Theoretical Physics, University of Cambridge, Cambridge, England, United Kingdom.
[5]National Center for Atmospheric Research, Boulder, Colorado.
[6]Department of Atmospheric Sciences, University of Washington, Seattle, Washington.
[7]NorthWest Research Associates, Colorado Research Associates Division, Boulder, Colorado.
[8]Department of Geophysics, Kyoto University, Kyoto, Japan.
[9]Radio Atmospheric Science Center, Kyoto University, Uji, Japan.
[10]Division of Engineering and Applied Sciences, Harvard University, Cambridge, Massachusetts.
[11]Qwest, Seattle, Washington.
[12]GeoForschungsZentrum Potsdam, Potsdam, Germany.
[13]National Institute of Polar Research, Arctic Environment Research Center, Tokyo, Japan.
[14]Center for Climate System Research, University of Tokyo, Tokyo, Japan.

Copyright 2001 by the American Geophysical Union.

Reviews of Geophysics, 39, 2 / *May 2001*
pages 179–229
8755-1209/01/1999RG000073*$15.00*
Paper number 1999RG000073

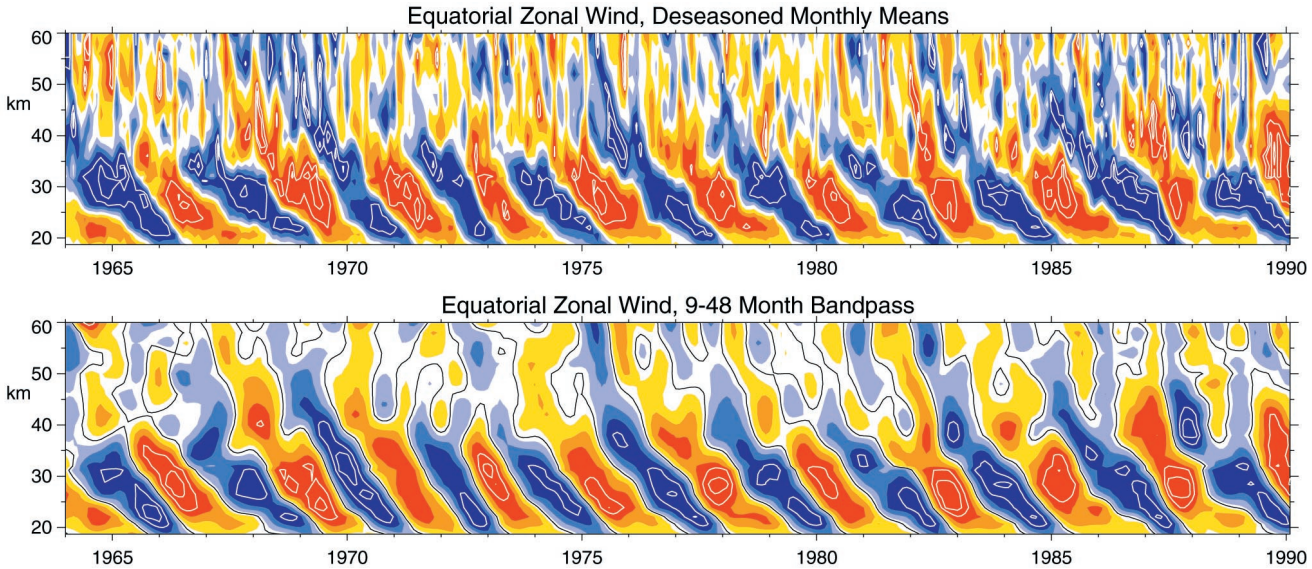

Plate 1. (top) Time-height section of the monthly-mean zonal wind component (m s^{-1}), with the seasonal cycle removed, for 1964–1990. Below 31 km, equatorial radiosonde data are used from Canton Island (2.8°N, January 1964 to August 1967), Gan/Maledive Islands (0.7°S, September 1967 to December 1975), and Singapore (1.4°N, January 1976 to February 1990). Above 31 km, rocketsonde data from Kwajalein (8.7°N) and Ascension Island (8.0°S) are shown. The contour interval is 6 m s^{-1}, with the band between −3 and +3 unshaded. Red represents positive (westerly) winds. After *Gray et al*. [2001]. In the bottom panel the data are band-pass filtered to retain periods between 9 and 48 months.

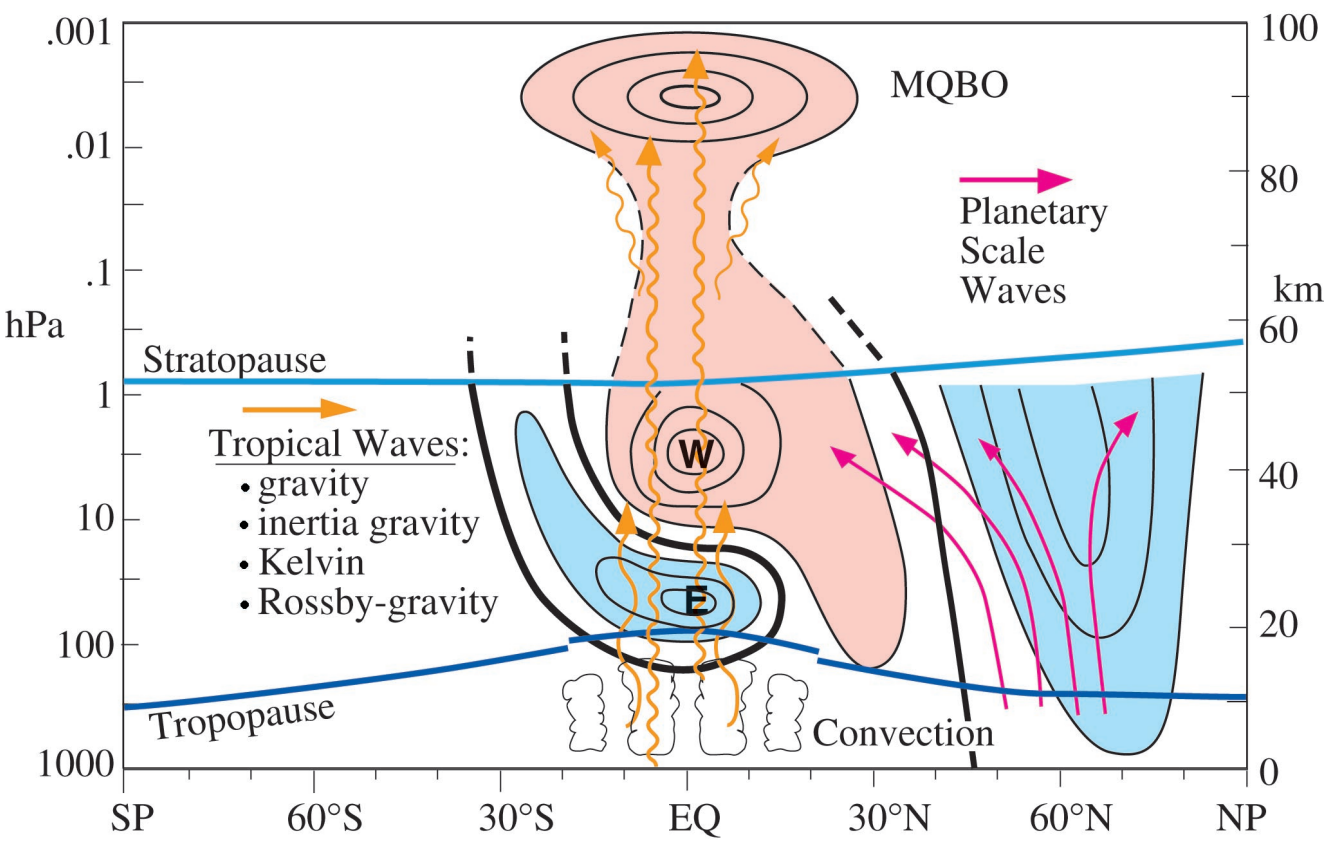

Plate 2. Dynamical overview of the QBO during northern winter. The propagation of various tropical waves is depicted by orange arrows, with the QBO driven by upward propagating gravity, inertia-gravity, Kelvin, and Rossby-gravity waves. The propagation of planetary-scale waves (purple arrows) is shown at middle to high latitudes. Black contours indicate the difference in zonal-mean zonal winds between easterly and westerly phases of the QBO, where the QBO phase is defined by the 40-hPa equatorial wind. Easterly anomalies are light blue, and westerly anomalies are pink. In the tropics the contours are similar to the observed wind values when the QBO is easterly. The mesospheric QBO (MQBO) is shown above ~80 km, while wind contours between ~50 and 80 km are dashed due to observational uncertainty.

winds overlying *westerly* winds. (Italicized terms are defined in the glossary, after the main text. The meteorological term "easterlies" describes winds that blow from the east, while "westerlies" blow from the west. Unfortunately, the terms *eastward* (to the east) and *westward* (to the west) are used commonly in discussions of wave propagation and flow and have the opposite meaning of easterly and westerly. Throughout this review we will use both descriptions, as found in the literature.) *Palmer* [1954] used upper air sounding data, gathered to study fallout from nuclear testing on the Marshall Islands, to find that the transition between the Berson westerlies and Krakatau easterlies varied from month to month and year to year. However, the data were insufficient to show any periodicity. By using observations from Christmas Island (2.0°N), *Graystone* [1959] contoured 2 years of wind speeds in the time-height plane, which showed gradually descending easterly and westerly wind regimes.

Discovery of the QBO must be credited to the independent work of R. J. Reed in the United States and R. A. Ebdon in Great Britain. In a paper entitled "The circulation of the stratosphere" presented at the fortieth anniversary meeting of the American Meteorological Society, Boston, January 1960, Reed announced the discovery, using rawinsonde (balloon) data at Canton Island (2.8°S), of "alternate bands of easterly and westerly winds which originate above 30 km and which move downward through the stratosphere at a speed of about 1 km per month." Reed pointed out that the bands "appear at intervals of roughly 13 months, 26 months being required for a complete cycle." This work was later published as *Reed et al*. [1961]. *Ebdon* [1960] also used data from Canton Island, spanning 1954–1959, to show that the wind oscillation had an apparent 2-year period. *Ebdon and Veryard* [1961] used additional data from Canton Island (January 1954 to January 1960) at 50 hPa (hectopascals, equal to millibars) to show that the wind fluctuated with a period of 25–27 months, rather than exactly 2 years. They extended the earlier study of Ebdon to include other equatorial stations and concluded that the wind fluctuations occurred simultaneously around the equatorial belt and estimated that the wind regimes (when the equatorial winds are easterly or westerly) took about a year to descend from 10 to 60 hPa. *Veryard and Ebdon* [1961] extended this study to find a dominant period of 26 months and observed similar fluctuations in temperature.

With the observation of a longer-period cycle starting in 1963, *Angell and Korshover* [1964] coined the term "quasi-biennial oscillation," which gained acceptance and was abbreviated QBO. Many of the dynamical aspects of the QBO are best illustrated by a time-height cross section of monthly-mean equatorial *zonal* (longitudinal) wind (Plate 1). Ideally, such a diagram would be of the zonally averaged zonal wind, but the approximate longitudinal symmetry of the QBO [*Belmont and Dartt*, 1968] allows rawinsonde observations from a single station near the equator to suffice. The alternating wind regimes repeat at intervals that vary from 22 to 34 months, with an average period of slightly more than 28 months. Westerly shear zones (in which westerly winds increase with height) descend more regularly and rapidly than easterly shear zones. The amplitude of $\sim$20 m s^{-1} is nearly constant from 5 to 40 hPa but decreases rapidly as the wind regimes descend below 50 hPa. Rawinsonde observations are used up to 10 hPa, and rocketsondes (meteorological rockets) are used above that. The QBO amplitude diminishes to less than 5 m s^{-1} at 1 hPa, near the stratopause. The amplitude of the QBO is approximately Gaussian about the equator with a 12° half width and little phase dependence on latitude within the tropics [*Wallace*, 1973]. Although the QBO is definitely not a biennial oscillation, there is a tendency for a seasonal preference in the phase reversal [*Dunkerton*, 1990] so that, for example, the onset of both easterly and westerly wind regimes occurs mainly during Northern Hemisphere (NH) late spring at the 50-hPa level. The three most remarkable features of the QBO that any theory must explain are (1) the quasi-biennial periodicity, (2) the occurrence of zonally symmetric westerly winds at the equator (conservation of angular momentum does not allow zonal-mean advection to create an equatorial westerly wind maximum), and (3) the downward propagation without loss of amplitude.

1.2. The Search for an Explanation of the QBO

At the time of discovery of the QBO, there were no observations of tropical atmospheric waves and there was no theory predicting their existence. The search for an explanation for the QBO initially involved a variety of other causes: some internal feedback mechanism, a natural period of atmospheric oscillation, an external process, or some combination of these mechanisms. All these attempts failed to explain features such as the downward propagation and maintenance of the amplitude of the QBO (and hence increase in energy density) as it descends.

Apparently, forcing by zonally asymmetric waves is required to explain the equatorial westerly wind maximum. *Wallace and Holton* [1968] tried to drive the QBO in a numerical model through heat sources or through extratropical *planetary-scale waves* propagating toward the equator. They showed rather conclusively that lateral momentum transfer by planetary waves could not explain the downward propagation of the QBO without loss of amplitude. They made the crucial realization that the only way to reproduce the observations was to have a driving force (a momentum source) which actually propagates downward with the mean equatorial winds.

Booker and Bretherton's [1967] seminal paper on the absorption of *gravity waves* at a *critical level* provided the spark that would lead to an understanding of how the QBO is driven (see *Lindzen* [1987] for a historical review of the development of the theory of the QBO). It was Lindzen's leap of insight to realize that vertically prop-

agating gravity waves could provide the necessary wave forcing for the QBO. *Lindzen and Holton* [1968] showed explicitly in a two-dimensional (2-D) model how a QBO could be driven by a broad spectrum of vertically propagating gravity waves (including phase speeds in both westward and eastward directions) and that the oscillation arose through an internal mechanism involving a two-way feedback between the waves and the background flow. The first part of the feedback is the effect of the background flow on the propagation of the waves (and hence on the momentum fluxes). The second part of the feedback is the effect of the momentum fluxes on the background flow. Lindzen and Holton's model represented the behavior of the waves and their effect on the background flow through a simple parameterization. The modeled oscillation took the form of a downward propagating pattern of easterly and westerly winds. An important corollary to Lindzen and Holton's work was that the period of the oscillation was controlled, in part, by the wave momentum fluxes, and hence a range of periods was possible. The fact that the observed oscillation had a period close to a subharmonic of the annual cycle was therefore pure coincidence.

It was a bold assertion to ascribe the forcing of the QBO to eastward and westward propagating equatorial gravity waves, considering that most observational evidence of waves was yet to come. The theory of equatorial waves was first developed during the late 1960s, in parallel with the theory of the QBO. The solutions included a Rossby mode, and a mode which became known as the (mixed) *Rossby-gravity* mode. A third solution, an eastward propagating gravity mode, was called the equatorial *Kelvin* mode. *Maruyama* [1967] displayed observations consistent with a westward propagating Rossby-gravity mode. *Wallace and Kousky* [1968a] first showed observations of equatorial Kelvin waves in the lower stratosphere and noted that the wave produced an upward flux of westerly momentum, which could account for the westerly acceleration associated with the QBO. A net easterly acceleration is contributed by Rossby-gravity waves [*Bretherton*, 1969].

Holton and Lindzen [1972] refined the work of *Lindzen and Holton* [1968] by simulating, in a 1-D model, a QBO driven by vertically propagating Kelvin waves, which contribute a westerly force, and Rossby-gravity waves, which contribute an easterly force. The observed amplitudes of these waves, though small, were arguably (given the paucity of equatorial wave observations) large enough to drive the QBO. The Holton and Lindzen mechanism continued to be the accepted paradigm for the QBO for more than 2 decades.

The conceptual model of the QBO, which formed the basis of the *Lindzen and Holton* [1968] model, was strongly supported by the ingenious laboratory experiment of *Plumb and McEwan* [1978], which used a salt-stratified fluid contained in a large annulus. The bottom boundary of the annulus consisted of a flexible membrane that oscillated up and down to produce vertically propagating gravity waves traveling clockwise and counterclockwise around the annulus. For waves of sufficient amplitude, a wave-induced mean flow regime was established that was characterized by downward progressing periodic reversals of the mean flow. This experiment, which remains one of the most dramatic laboratory analogues of a large-scale geophysical flow, showed that the theoretical paradigm for the QBO was consistent with the behavior of a real fluid system.

While the observed amplitudes of Kelvin and mixed Rossby-gravity waves may be sufficient to drive a QBO in idealized models of the atmosphere, *Gray and Pyle* [1989] found it necessary to increase the wave amplitudes by a factor of 3 over those observed to achieve a realistic QBO in a full radiative-dynamical-photochemical model. *Dunkerton* [1991a, 1997], and *McIntyre* [1994] pointed out that the observed rate of tropical upwelling (about 1 km per month) effectively requires that the QBO wind regimes propagate downward much faster than was thought, relative to the background air motion, because the whole of the tropical stratosphere is moving upward. This fact more than doubles the required momentum transport by vertically propagating equatorial waves. Observations indicate that mixed Rossby-gravity and Kelvin waves cannot provide sufficient forcing to drive the QBO with the observed period. *Dunkerton* [1997] reasoned that additional momentum flux must be supplied by a broad spectrum of gravity waves similar to those postulated by *Lindzen and Holton* [1968].

Although the QBO is a tropical phenomenon, it influences the global stratosphere, as first shown by *Holton and Tan* [1980]. Through modulation of winds, temperatures, extratropical waves, and the circulation in the *meridional plane*, the QBO affects the distribution and transport of trace constituents and may be a factor in stratospheric ozone depletion. Thus an understanding of the QBO and its global effects is necessary for studies of long-term variability or trends in trace gases and aerosols.

2. AN OVERVIEW OF THE QBO AND ITS GLOBAL EFFECTS

2.1. Zonal Wind

A composite of the QBO in equatorial zonal winds (Figure 1) [*Pawson et al.*, 1993] shows faster and more regular downward propagation of the westerly *phase* and the stronger intensity and longer duration of the easterly phase. The mean period of the QBO for data during 1953–1995 is 28.2 months, slightly longer than the 27.7 months obtained from the shorter record of *Naujokat* [1986]. The standard deviation about the composite QBO is also included in Figure 1, showing maxima in variability close to the descending easterly and westerly shear zones (larger for the westerly phase). This mainly reflects deviations in the duration of each phase (as seen in Plate 1).

Dunkerton [1990] showed that the QBO may be some-

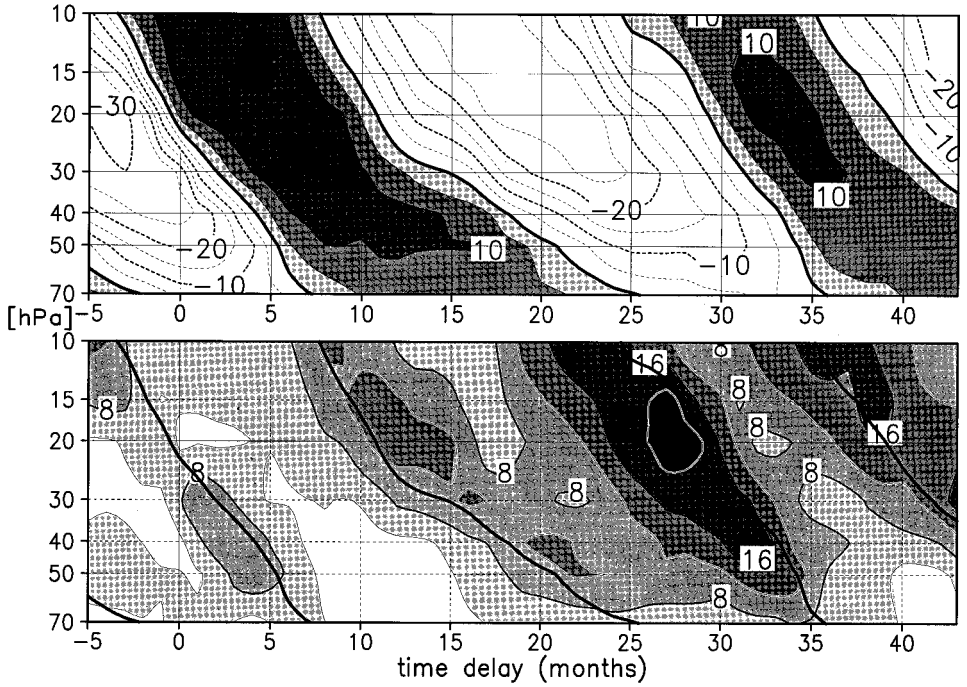

Figure 1. A composite plot of the quasi-biennial oscillation (QBO) according to the easterly-westerly transition at 20 hPa. The transition month was chosen as the first month when westerlies were present at 20 hPa. Westerlies are shaded, and the darkness increases at intervals of 5 m s^{-1} (which is the contour interval). The time axis extends from 5 months before the east-west transition at 20 hPa until 42 months afterward. The regularity of the QBO is shown by the existence of a second westerly phase, which onsets at 20 hPa about 29 months after the initial onset. The lower panel shows the standard deviation about this mean QBO, with a contour interval/shading level of 4 m s^{-1}. The largest variability occurs in the neighborhood of the shear lines and is due to the variable period of the QBO and the fact that the duration of each phase at any level is long compared with the transition time.

what synchronized to the annual cycle, demonstrating that the onset of the easterly regime at 50 hPa tends to occur during NH late spring or summer. His analysis is updated in Figure 2, which shows the onset of each wind regime at 50 hPa. The easterly and westerly transitions both show a strong preference to occur during April–June.

The latitudinal structure of the QBO in zonal wind is shown in Figure 3, derived from long time series of wind observations at many tropical stations [*Dunkerton and Delisi*, 1985]. The amplitude of the QBO is latitudinally symmetric, and the maximum is centered over the equator, with a meridional half width of approximately 12°. Similar QBO structure is derived from assimilated meteorological analyses, but the amplitude is often underestimated in comparison with rawinsonde measurements [*Pawson and Fiorino*, 1998; *Randel et al.*, 1999].

Plate 2 provides an overview of the QBO, its sources, and its global dynamical effects, as well as a foundation for the discussion of the details of the QBO in the following sections. The diagram spans the troposphere, stratosphere, and mesosphere from pole to pole and shows schematically the differences in zonal wind be-

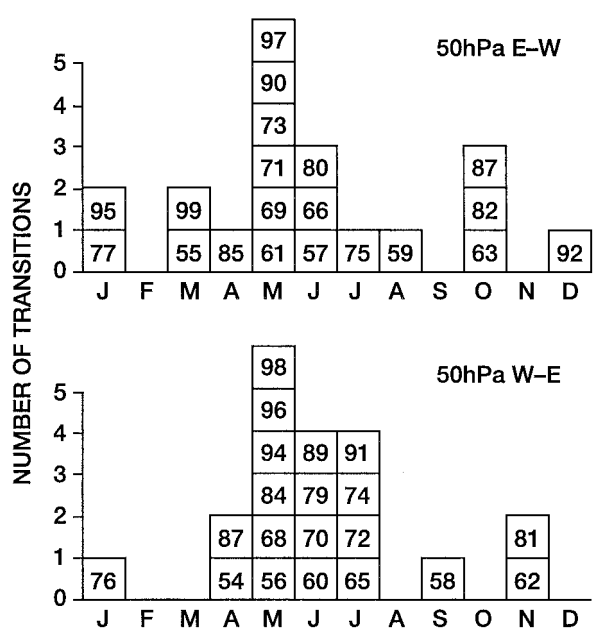

Figure 2. Histograms of the number of transitions (zero crossings) at 50 hPa grouped by month. Individual years are listed in the boxes. Easterly to westerly transitions are displayed in the top panel, while westerly to easterly transitions are shown in the bottom panel. After *Pawson et al.* [1993].

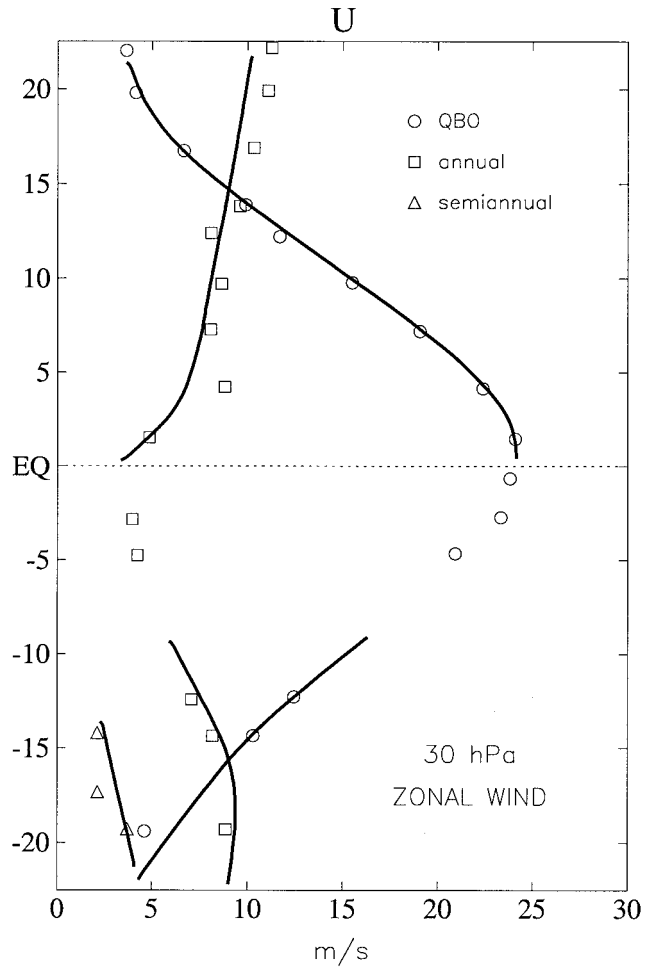

Figure 3. Harmonic analysis of 30-hPa zonal wind, showing the amplitude of the annual cycle (squares), semiannual cycle (triangles), and residual deseasoned component (circles). Symbols show individual rawinsonde station amplitudes. Solid lines are based on binned data. Reprinted from *Dunkerton and Delisi* [1985] with permission from the American Meteorological Society.

tween the 40-hPa easterly and westerly phases of the QBO.

Convection in the tropical troposphere, ranging from the scale of mesoscale convective complexes (spanning more than 100 km) to planetary-scale phenomena, produces a broad spectrum of waves (orange wavy arrows), including gravity, *inertia-gravity*, Kelvin, and Rossby-gravity waves (see section 3). These waves, with a variety of vertical and horizontal wavelengths and phase speeds, propagate into the stratosphere, transporting easterly and westerly zonal momentum. Most of this zonal momentum is deposited at stratospheric levels, driving the zonal wind anomalies of the QBO. For each wave the vertical profile of the zonal wind determines the critical level at or below which the momentum is deposited. The critical levels for these waves depend, in part, on the shear zones of the QBO. Some gravity waves propagate through the entire stratosphere and produce a QBO near the mesopause known as the mesospheric QBO, or MQBO (section 6).

In the tropical lower stratosphere the time-averaged wind speeds are small, so the easterly minus westerly composite in Plate 2 is similar in appearance to the actual winds during the easterly phase of the QBO. At high latitudes, there is a pronounced annual cycle, with strong westerly winds during the winter season. To the north of the equator in the lower stratosphere, tropical winds alter the effective waveguide for upward and equatorward propagating planetary-scale waves (curved purple arrows). The effect of the zonal wind structure in the easterly phase of the QBO is to focus more wave activity toward the pole, where the waves converge and slow the zonal-mean flow. Thus the polar vortex north of ~45°N shows weaker westerly winds (or easterly anomaly, shown in light blue). The high-latitude wind anomalies penetrate the troposphere and provide a mechanism for the QBO to have a small influence on tropospheric weather patterns (section 6).

2.2. Temperature and Meridional Circulation

The QBO exhibits a clear signature in temperature, with pronounced signals in both tropics and extratropics. The tropical temperature QBO is in thermal wind balance with the vertical shear of the zonal winds, expressed for the equatorial β-*plane* as

$$\frac{\partial u}{\partial z} = \frac{-R}{H\beta}\frac{\partial^2 T}{\partial y^2} \tag{1a}$$

[*Andrews et al.*, 1987, equation 8.2.2], where u is the zonal wind, T is temperature, z is *log-pressure height* (approximately corresponding to geometric altitude), y is latitude, R is the gas constant for dry air, $H \approx 7$ km is the nominal (constant) scale height used in the log-pressure coordinates, and β is the latitudinal derivative of the Coriolis parameter. For QBO variations centered on the equator with meridional scale L, thermal wind balance at the equator is approximated as

$$\frac{\partial u}{\partial z} \sim \frac{R}{H\beta}\frac{T}{L^2}. \tag{1b}$$

The equatorial temperature anomalies associated with the QBO in the lower stratosphere are of the order of ±4 K, maximizing near 30–50 hPa. Figure 4 compares time series (after subtraction of the seasonal cycle) of 30-hPa temperature measurements at Singapore with the corresponding zonal wind vertical shear in the 30- to 50-hPa level, showing good correlation (see also Plate 1). The slope of $\partial u/\partial z$ versus temperature estimated from regression is consistent with a meridional scale $L \sim$ 1000–1200 km (~10° of latitude) [*Randel et al.*, 1999].

Smaller anomalies extend downward, with QBO variations of the order of ±0.5 K observed near the tropopause [*Angell and Korshover*, 1964]. The QBO temperature anomalies also extend into the middle and upper stratosphere, where they are out of phase with the lower

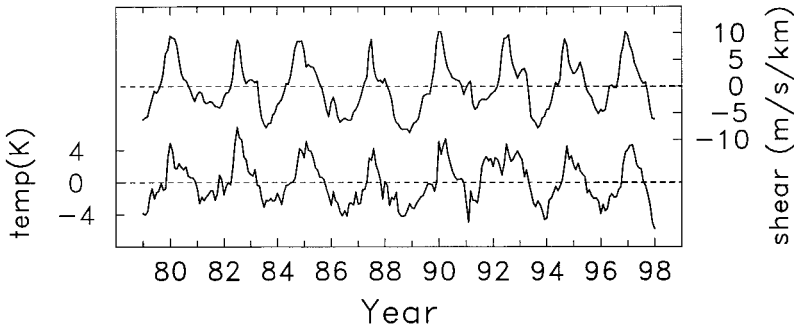

Figure 4. Equatorial temperature anomalies associated with the QBO in the 30- to 50-hPa layer (bottom curve) and vertical wind shear (top curve).

stratosphere anomalies. Figure 5 shows an example of temperature anomalies associated with an easterly phase of the QBO during NH winter 1994, derived from UK Meteorological Office (UKMO) stratospheric assimilation data extending to 45 km. Although these data probably underestimate the magnitude of the temperature QBO (the retrievals average over a layer deeper than the temperature anomaly), the out-of-phase vertical structure is a robust feature also observed in long time records of satellite radiance measurements [*Randel et al.*, 1999].

Besides the equatorial maximum in QBO temperature, satellite data reveal coherent maxima over 20°–40° latitude in each hemisphere, which are out of phase with the tropical signal. This is demonstrated in Figure 6, which shows regression of stratospheric temperatures over 13–22 km (from the microwave sounding unit channel 4) onto the 30-hPa QBO winds, for the period 1979–1999. One remarkable aspect of the extratropical temperature anomalies is that they are seasonally synchronized, occurring primarily during winter and spring in each hemisphere. Nearly identical signatures are observed in column ozone measurements (section 5), and this seasonally synchronized extratropical variability is a key and intriguing aspect of the global QBO. Because low-frequency temperature anomalies are tightly coupled with variations in the mean meridional circulation, global circulation patterns associated with the QBO are also highly asymmetric at solstice (arrows in Figure 5). The temperature patterns in Figure 6 furthermore show signals in both polar regions, which are out of phase with the tropics, and maximize in spring in each hemisphere. Although these polar signals are larger than the subtropical maxima, and probably genuine, they are not statis-

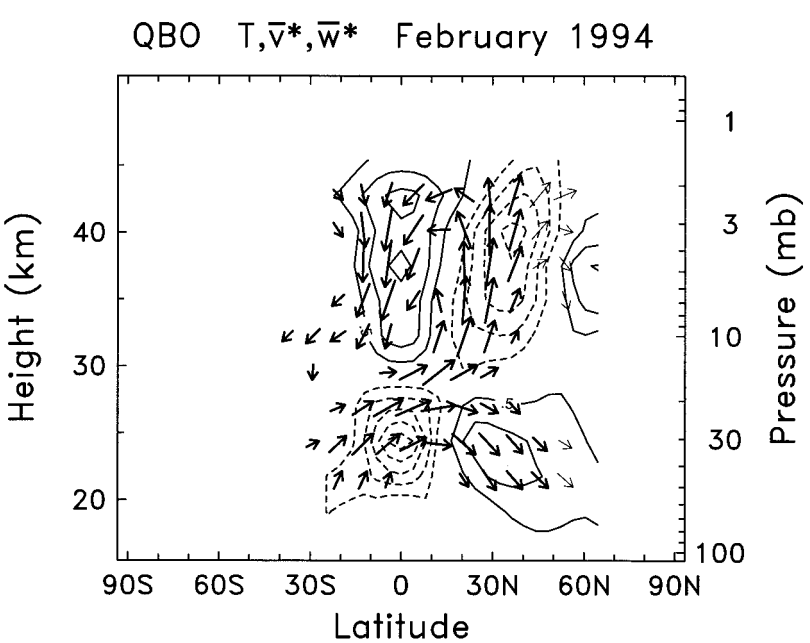

Figure 5. Cross sections of QBO anomalies in February 1994. Temperature anomalies are contoured (±0.5, 1.0, 1.5 K, etc., with negative anomalies denoted by dashed contours), and components of the residual mean circulation ($\bar{v}^*$, $\bar{w}^*$) are as vectors (scaled by an arbitrary function of altitude). Reprinted from *Randel et al.* [1999] with permission from the American Meteorological Society.

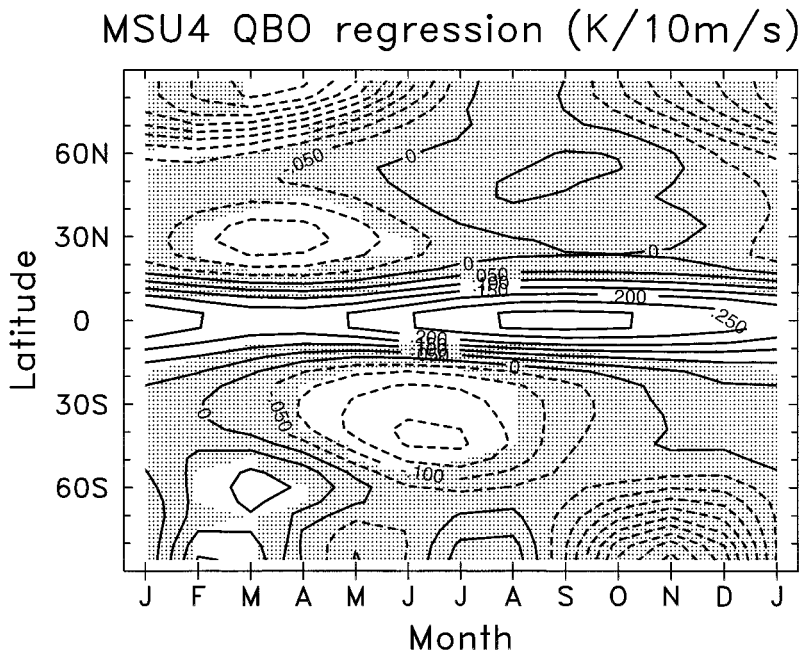

Figure 6. QBO regression using 13- to 22-km Microwave Sounding Unit temperature data for 1979–1998. Shading denotes regions where the statistical fits are not different from zero at the 2σ level. Updated from *Randel and Cobb* [1994].

tically significant in this 1979–1998 record because of large natural variability in polar regions during winter and spring.

The modulation by the QBO of zonal-mean wind (Plate 1) is coupled to modulation of the zonally averaged mean meridional circulation. The climatological circulation is characterized by large-scale ascent in the tropics, broad poleward transport in the stratosphere, and compensating sinking through the extratropical tropopause [*Holton et al.*, 1995]. The transport of chemical trace species into, within, and out of the stratosphere is the result of both large-scale circulations and mixing processes associated with waves. Chemical processes, such as those resulting in ozone depletion, not only depend on the concentrations of trace species, but may also depend critically on temperature. Since the QBO modulates the global stratospheric circulation, including the polar regions, an understanding of the effects of the QBO not only on dynamics and temperature but also on the distribution of trace species is essential in order to understand global climate variability and change.

Many long-lived trace species, such as N_2O and CH_4, originate in the troposphere and are transported into the stratosphere through the tropical tropopause. Plate 3 provides a summary of the influence of the QBO on the mean meridional circulation and the transport of chemical trace species. In Plate 3 the contours illustrate schematically the isopleths of an idealized conservative, long-lived, vertically stratified tracer during the NH winter when the equatorial winds are easterly near 40 hPa (matching Plate 2). Upwelling is reflected in the broad tropical maximum in tracer density in the middle to upper stratosphere. The extratropical anomalies caused by the QBO result in deviations from hemispheric symmetry, some of which are also due to the seasonal cycle of planetary-wave mixing.

The bold arrows in Plate 3 illustrate circulation anomalies associated with the QBO (the time-averaged circulation has been removed), which is here assumed to be easterly at 40 hPa. At the equator the QBO induces ascent (relative to the mean tropical upwelling) through the tropopause, but descent in the middle to upper stratosphere. The lower stratospheric circulation anomaly is nearly symmetric about the equator, while the circulation anomaly in the middle stratosphere is larger in the winter hemisphere (see section 5). This asymmetry is reflected in the asymmetric isopleths of the tracer. In addition to advection by the mean meridional circulation, the tracer is mixed by wave motions (approximately on isentropic, or constant potential temperature, surfaces). This mixing is depicted by the wavy horizontal arrows. The descent from the middle stratosphere circulation anomaly creates a "staircase" pattern in the tracer isopleths between the equator and the subtropics (near 5 hPa). A second stairstep in the midlatitude winter hemisphere is formed by isentropic mixing in the region of low potential vorticity gradient which surrounds the polar vortex, known as the *surf zone* [*McIntyre and Palmer*, 1983]. Mixing may also occur equatorward of the subtropical jet axis in the upper stratosphere, as illustrated by the wavy line near 3 hPa and 10°–20°N [*Dunkerton and O'Sullivan*, 1996]. Anomalous transport from the Southern Hemisphere (SH) to the NH near the stratopause is associated with enhanced extratropical plane-

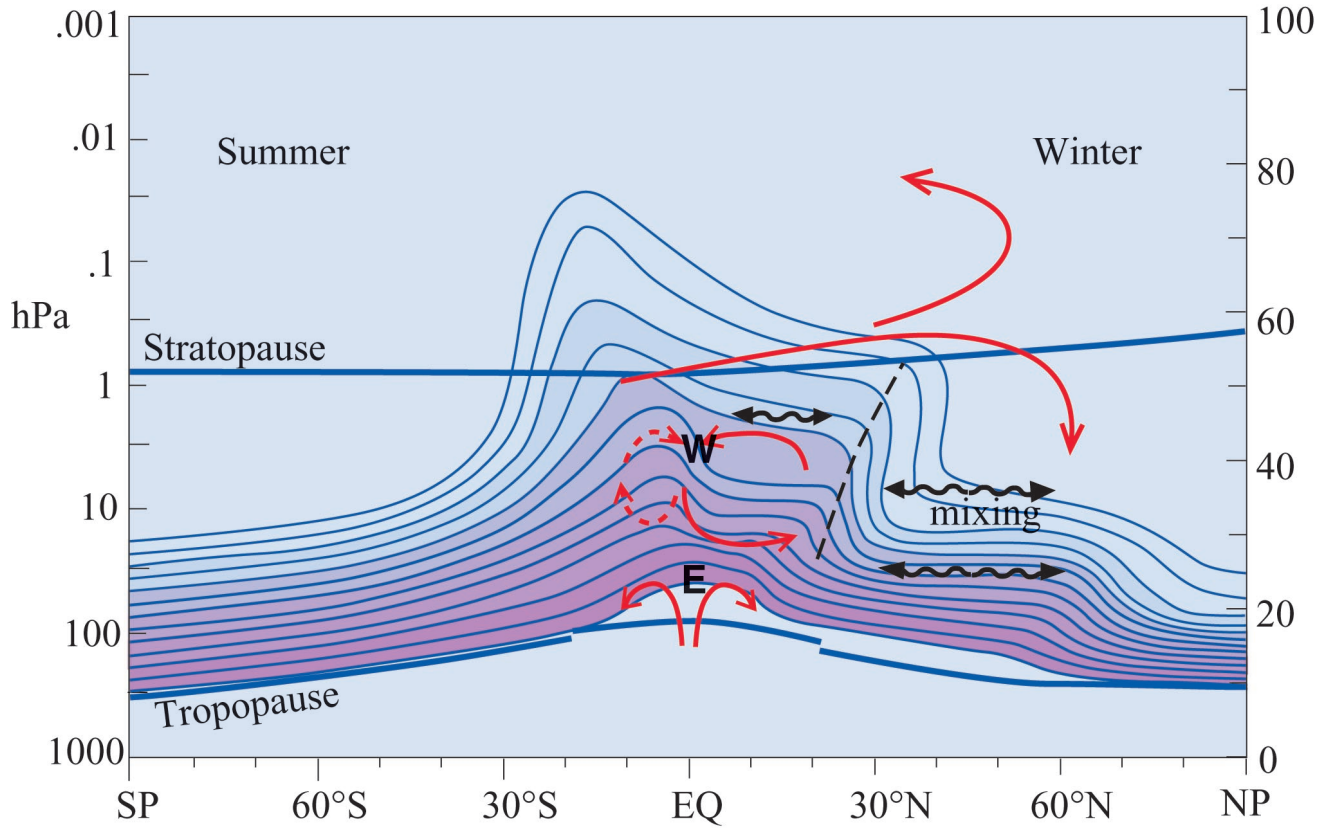

Plate 3. Overview of tracer transport by QBO wind anomalies and mean advection. Contours illustrate schematically the isopleths of a conservative tracer during northern winter when the QBO is in its easterly phase at 40 hPa (matching Plate 2). Tropical upwelling causes the broad maximum in tracer density in the middle to upper equatorial stratosphere, while the QBO causes deviations from hemispheric symmetry near the equator. Red arrows near the equator depict circulation anomalies of the QBO. The circulation anomaly in the equatorial lower stratosphere is approximately symmetric, while the anomaly in the upper stratosphere is much stronger in the winter hemisphere. The descent near the equator (~5 hPa) and ascent to the north (~5 hPa, 10°N) combine to produce a "staircase" pattern. A second stairstep is formed in midlatitudes by horizontal mixing.

tary wave driving (Plate 2). The detailed effects of the QBO on tracer transport are discussed in section 5.

3. DYNAMICS OF THE QBO

3.1. QBO Mechanism

Since the QBO is approximately longitudinally symmetric [*Belmont and Dartt*, 1968], it is natural to try to explain it within a model that considers the dynamics of a longitudinally symmetric atmosphere. In a rotating atmosphere the temperature and wind fields are closely coupled, and correspondingly, both heating or mechanical forcing (i.e., forcing in the momentum equations) can give rise to a velocity response. Although, as noted in section 1, the current view is that mechanical forcing, provided by wave momentum fluxes, is essential for the QBO, the coupling between temperature and wind fields must be taken into account to explain many aspects of the structure.

The essence of the mechanism for the oscillation may be demonstrated in a simple representation of the interaction of vertically propagating gravity waves with a background flow that is itself a function of height [*Plumb*, 1977]. Consider two discrete upward propagating internal gravity waves, forced at a lower boundary with identical amplitudes and equal but opposite zonal phase speeds. The waves are assumed to be quasi-linear (interacting with the mean flow, but not with each other), steady, hydrostatic, unaffected by rotation, and subject to linear damping. The superposition of these waves corresponds exactly to a single "standing" wave. As each wave component propagates vertically, its amplitude is diminished by damping, generating a force on the mean flow due to convergence of the vertical flux of zonal momentum. This force locally accelerates the mean flow in the direction of the dominant wave's zonal phase propagation. The momentum flux convergence depends on the rate of upward propagation and hence on the vertical structure of zonal-mean wind. With waves of equal amplitude but opposite phase speed, zero mean flow is a possible equilibrium, but unless vertical diffu-

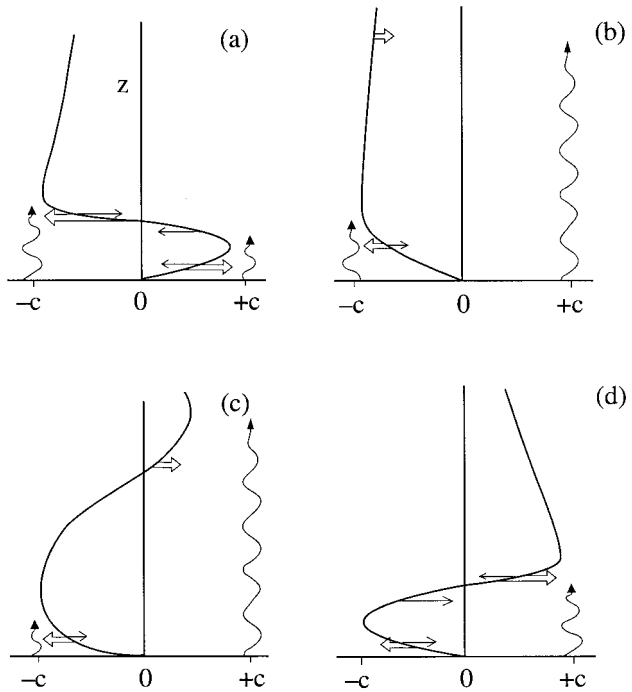

Figure 7. Schematic representation of the evolution of the mean flow in *Plumb*'s [1984] analog of the QBO. Four stages of a half cycle are shown. Double arrows show wave-driven acceleration, and single arrows show viscously driven accelerations. Wavy lines indicate relative penetration of eastward and westward waves. After *Plumb* [1984]. Reprinted with permission.

sion is strong, it is an unstable equilibrium; any small deviation from zero will inevitably grow with time.

Plumb [1977] showed that the zonal-mean wind anomalies descend in time, as illustrated in Figure 7. Each wave propagates vertically until its group velocity is slowed, and the wave is damped as it encounters a shear zone where $|\bar{u} - c|$ is small ($\bar{u}$ is the zonal-mean wind and c is the zonal phase speed of the wave). As the shear zone descends (Figure 7a) the layer of eastward winds becomes sufficiently narrow that viscous diffusion destroys the low-level eastward winds. This leaves the eastward wave free to propagate to high levels through westward mean flow (Figure 7b), where dissipation and the resulting eastward acceleration gradually build a new eastward regime that propagates downward (Figures 7c and 7d).

The process just described repeats, but with westerly shear descending above easterly shear, leading to the formation of a low-level easterly jet. When the easterly jet decays, the westward wave escapes to upper levels, and a new easterly shear zone forms aloft. The entire sequence, as described, represents one cycle of a nonlinear oscillation. The period of the oscillation is determined, among other things, by the eastward and westward momentum flux input at the lower boundary and by the amount of atmospheric mass affected by the waves. In *Plumb*'s [1977] *Boussinesq* formulation the QBO period is inversely proportional to momentum flux. The same is true in a quasi-compressible atmosphere, but the decrease in atmospheric density with height results in a substantially shorter period.

Simple representations such as Plumb's capture the essential wave mean-flow interaction mechanism leading the QBO. However, they cannot explain why the QBO is an equatorial phenomenon (notwithstanding its important links to the extratropics). One reason the QBO is equatorially confined may be that it is driven by equatorially trapped waves. However, it is also possible that the QBO is driven by additional waves and is confined near the equator for another, more fundamental, reason. Some simple insights on this point come from considering the equations for the evolution of a longitudinally symmetric atmosphere subject to mechanical forcing. A suitable set of model equations for such a longitudinally symmetric atmosphere is as follows:

$$\frac{\partial u}{\partial t} - 2\Omega \sin \phi v = F \tag{2}$$

$$2\Omega \sin \phi \frac{\partial u}{\partial z} + \frac{R}{aH}\frac{\partial T}{\partial \phi} = 0 \tag{3}$$

$$\frac{\partial T}{\partial t} + w\frac{HN^2}{R} = -\alpha T \tag{4}$$

$$\frac{1}{a \cos \phi}\frac{\partial}{\partial \phi} v \cos \phi + \frac{1}{\rho_0}\frac{\partial}{\partial z}(\rho_0 w) = 0 \tag{5}$$

Here ϕ is latitude, Ω is the angular frequency of the Earth's rotation, a is the radius of the Earth, and ρ_0 is a nominal basic state density proportional to exp $(-z/H)$. In (4), N^2 is the square of the buoyancy frequency (a measure of static stability), defined as

$$N^2 \equiv \frac{R}{H}\left(\frac{dT_0}{dz} + \frac{\kappa T_0}{H}\right),$$

where T_0 is a reference temperature profile depending only on z and $\kappa = R/c_p$, where c_p is the specific heat of air at constant pressure. Finally, u is the longitudinal component of wind, T is the temperature deviation from T_0, and v and w are the latitudinal and vertical components, respectively, of velocity.

Equation (2) states that the longitudinal acceleration is equal to the applied force F (here assumed to be a given function of latitude, height, and time), plus the *Coriolis* force associated with the latitudinal velocity. The Coriolis force is the important effect of rotation; the response to an applied force is not simply an equivalent acceleration. Instead, part of the applied force is balanced by a Coriolis force; how much depends on how large a latitudinal velocity is excited. Equation (3) is the thermal wind equation coupling the longitudinal velocity field and the temperature field, which follows from the assumption that the flow is in hydrostatic and geostrophic balance. Equation (4) states that the rate of change of temperature is equal to the diabatic heating plus the

adiabatic temperature change associated with vertical motion. Here the diabatic heating is represented by the term $-\alpha T$, where α is a constant rate, representing long-wave heating or cooling. Equation (5) is the mass-continuity equation.

Equation (2)–(5) may be regarded as predictive equations for the unknowns $\partial u/\partial t$, $\partial T/\partial t$, v, and w. They may be combined to give a single equation for one of the unknowns, with a single forcing term containing the force F. It is convenient to follow *Garcia* [1987] and assume that the time dependence is purely harmonic. Thus we write $F(\phi, z, t) = \mathrm{Re}\,(\hat{F}(\phi, z)e^{i\omega t})$ and consider the response in the longitudinal velocity u, assumed to be of the form $u(\phi, z, t) = \mathrm{Re}\,(\hat{u}(\phi, z)e^{i\omega t})$. Equations (2)–(5) then can be transformed to a single equation

$$\frac{1}{\cos\phi}\frac{\partial}{\partial\phi}\left(\frac{1}{\cos\phi}\frac{\partial}{\partial\phi}\left(\frac{\cos\phi}{\sin\phi}\hat{u}\right)\right) + \frac{1}{\rho_0}\frac{\partial}{\partial z}\left(\rho_0\left(1+\frac{\alpha}{i\omega}\right)\frac{4\Omega^2a^2}{N^2}\frac{\sin\phi}{\cos\phi}\frac{\partial\hat{u}}{\partial z}\right) = \frac{1}{i\omega}\frac{1}{\cos\phi}\frac{\partial}{\partial\phi}\left(\frac{1}{\cos\phi}\frac{\partial}{\partial\phi}\left(\frac{\cos\phi}{\sin\phi}\hat{F}\right)\right). \quad (6)$$

The operator acting on $\hat{u}$ on the left-hand side of the equation is elliptic, consistent with the well-known property of rotating, stratified systems that localized forcing gives rise to a nonlocal response. For an oscillation with period 2 years, $\omega \approx 10^{-7}\ \mathrm{s}^{-1}$. The Newtonian cooling rate α is, for the lower stratosphere, generally taken to be about $5 \times 10^{-7}\ \mathrm{s}^{-1}$, corresponding to a timescale of about 20 days. Hence the factor $1 + \alpha/(i\omega)$ appearing in the second term on the left-hand side may be approximated by $\alpha/(i\omega)$.

A scale analysis of (6) shows that when rotational effects are weak, i.e., when $\sin\phi$ is small, the dominant balance is between the forcing term and the first term on the left-hand side. This implies that the acceleration is equal to the applied force. More generally, the second term on the left-hand side will play a major role in the balance, implying that the Coriolis force must be substantially canceling the applied force in (2). Following *Haynes* [1998], a quantitative comparison of the two terms on the left-hand side of (6) may be performed by assuming a height scale D and a latitudinal scale L for the velocity response. Then, at low latitudes, noting that $\sin\phi$ scales as ϕ and hence as L/a, the ratio of the second term on the left-hand side of (6) to the first is $4\Omega^2L^4\alpha/(a^2D^2N^2\omega)$. It follows that if $L \ll (aDN/(2\Omega))^{1/2}(\omega/\alpha)^{1/4}$, then the acceleration is approximately equal to the applied force. This might be called the "tropical response"; it occurs if the latitudinal scale L is small enough. On the other hand, if $L \gg (aDN/(2\Omega))^{1/2}(\omega/\alpha)^{1/4}$, then the applied force is largely canceled by the Coriolis torque and most of the response to the applied force appears as a mean meridional circulation. This might be called the "extratropical response" (though clearly the scaling would require modification if it were to be applied well away from the equator).

The physical reason for the distinction between the tropical and extratropical responses is the link between velocity and temperature fields in a rotating system, expressed by (3), together with the temperature damping implied by (4). At high latitudes an applied force, varying on sufficiently long timescales, will tend to be canceled by the Coriolis force due to a mean meridional circulation. This circulation will induce temperature anomalies, upon which the thermal damping will act, effectively damping the velocity response and limiting its amplitude. At low latitudes, on the other hand, the force will give rise to an acceleration, there will be relatively little temperature response, and thermal damping will have little effect on the velocity response. It is as if low-latitude velocities have a longer "memory" than high-latitude velocities; anomalies at low latitudes take longer to dissipate [*Scott and Haynes*, 1998]. Thus the QBO mechanism might be expected to work only at low latitudes. The *Lindzen and Holton* [1968] experiments in a 2-D model showed that the Coriolis torque reduced the amplitude of the wind oscillation away from the equator. *Haynes* [1998] went further to suggest that the transition from the tropical regime to the extratropical regime may set the latitudinal width of the QBO, rather than, for example, the latitudinal scale of the waves that provide the necessary momentum flux. Simulations in a simple numerical model where the momentum forcing is provided by a latitudinally broad field of small-scale gravity waves, designed not to impose any latitudinal scale, predicted a transition scale at about 10°.

To summarize, a long-period oscillation that requires the zonal velocity field to respond directly to a wave-induced forced is likely to work only in the tropics, since elsewhere the force will tend to be balanced by the Coriolis torque due to a meridional circulation. For this reason, 1-D models, which omit Coriolis torques altogether, can capture the tropical oscillation. However, they cannot simulate the latitudinal structure that arises in part from the increase of Coriolis torques with latitude.

3.2. Waves in the Tropical Lower Stratosphere

There exists a broad spectrum of waves in the tropics, many of which contribute to the QBO. On the basis of observations of wave amplitudes, we now believe that a combination of Kelvin, Rossby-gravity, inertia-gravity, and smaller-scale gravity waves provide most of the momentum flux needed to drive the QBO [*Dunkerton*, 1997]. All of these waves originate in the tropical troposphere and propagate vertically to interact with the QBO. Convection plays a significant role in the generation of tropical waves. Modes are formed through lateral propagation, refraction, and reflection within an equatorial waveguide, the horizontal extent of which depends on wave properties, for example, turning points where

wave intrinsic frequency equals the local inertial frequency.

Equatorward propagating waves originating outside the tropics, such as planetary Rossby waves from the winter hemisphere, may have some influence in upper levels of the QBO [*Ortland*, 1997]. The lower region of the QBO (~20–23 km) near the equator is relatively well shielded from the intrusion of extratropical planetary waves [*O'Sullivan*, 1997].

Vertically propagating waves relevant to the QBO are either those with slow vertical group propagation undergoing absorption (due to radiative or mechanical damping) at such a rate that their momentum is deposited at QBO altitudes, or those with fast vertical group propagation up to a critical level lying within the range of QBO wind speeds [*Dunkerton*, 1997]. The height at which momentum is deposited depends on the vertical group velocity (supposing for argument's sake that the damping rate per unit time is independent of wave properties). Waves with very slow group propagation are confined within a few kilometers of the tropopause [*Li et al.*, 1997]. On the other hand, waves with fast vertical group velocity and with phase speeds lying outside the range of QBO wind speeds propagate more or less transparently through the QBO.

Long-period waves tend to dominate spectra of horizontal wind and temperature. However, higher-frequency waves contribute more to momentum fluxes than might be expected from consideration of temperature alone. We can organize the waves relevant to the QBO into three categories: (1) Kelvin and Rossby-gravity waves, which are equatorially trapped; periods of $\gtrsim$3 days; wave numbers 1–4 (zonal wavelengths $\gtrsim$10,000 km); (2) inertia-gravity waves, which may or may not be equatorially trapped; periods of ~1–3 days; wave numbers ~4–40 (zonal wavelengths ~1000–10,000 km); and (3) gravity waves; periods of $\lesssim$1 day; wave number >40 (zonal wavelengths ~10–1000 km) propagating rapidly in the vertical. (Waves with very short horizontal wavelengths $\lesssim$10 km tend to be trapped vertically at tropospheric levels near the altitude where they are forced and are not believed to play a significant role in middle atmosphere dynamics.)

The observations reviewed below suggest that intermediate and high-frequency waves help to drive the QBO. However, uncertainties remain in the wave momentum flux spectrum, with regard to actual values of flux and the relative contribution from various parts of the spectrum. Although the momentum flux in mesoscale waves is locally very large, it is necessary to know the spatial and temporal distribution of these waves in order to assess their role in the QBO. Available observations are insufficient for this purpose. For intermediate-scale waves, it is unclear what fraction of the waves is important to the QBO without a more precise estimate of their phase speeds, modal structure, and absorption characteristics. Twice-daily rawinsondes provide an accurate picture of vertical structure but have poor horizontal and temporal coverage. Their description of horizontal structure is inadequate, and temporal aliasing may occur, obscuring the true frequency of the waves.

The QBO, in principle, depends on wave driving from the entire tropical belt, but the observing network can only sample a small fraction of horizontal area and time. Thus it is uncertain how to translate the information from local observations of intermediate and small-scale waves into a useful estimate of QBO wave driving on a global scale. Ultimately, satellite observations will provide the needed coverage in space and time. These observations have already proven useful for planetary-scale equatorial waves and small-scale extratropical gravity waves with deep vertical wavelength. Significant improvement in the vertical resolution of satellite instruments and their ability to measure or infer horizontal wind components will be necessary, however, before such observations are quantitatively useful for estimates of momentum flux due to intermediate and small-scale waves in the QBO region.

3.2.1. Kelvin and Rossby-gravity waves. Kelvin and Rossby-gravity waves were detected using rawinsonde observational data by *Yanai and Maruyama* [1966] and *Wallace and Kousky* [1968b]; these discoveries were important to the development of a modified theory of the QBO by *Holton and Lindzen* [1972]. For reviews of early equatorial wave observations, see *Wallace* [1973], *Holton* [1975], *Cornish and Larsen* [1985], *Andrews et al.* [1987], and *Dunkerton* [1997]. Interpretation of disturbances as equatorial wave modes relies on a comparison of wave parameters (e.g., the relation of horizontal scale and frequency), latitudinal structure (e.g., symmetric or antisymmetric about the equator), and phase relationship between variables (e.g., wind components and temperature) with those predicted by theory. The identification of equatorial modes is relatively easy in regions with good spatial coverage so that coherent propagation may be observed.

Long records of rawinsonde data from high-quality stations have been used to derive seasonal and QBO-related variations of Kelvin and Rossby-gravity wave activity near the equator [*Maruyama*, 1991; *Dunkerton*, 1991b, 1993; *Shiotani and Horinouchi*, 1993; *Sato et al.*, 1994; *Wikle et al.*, 1997]. The QBO variation of Kelvin wave activity observed in fluctuations of zonal wind and temperature is consistent with the expected amplification of these waves in descending westerly shear zones. Annual variation of Rossby-gravity wave activity is observed in the lowermost equatorial stratosphere and may help to explain the observed seasonal variation of QBO onsets near 50 hPa [*Dunkerton*, 1990].

Equatorially trapped waves have been observed in temperature and trace constituent data obtained from various satellite instruments. Most of these studies dealt with waves in the upper stratosphere relevant to the stratopause *semiannual oscillation* (SAO); a few, however, also observed waves in the equatorial lower stratosphere relevant to the QBO [e.g., *Salby et al.*, 1984;

Randel, 1990; *Ziemke and Stanford*, 1994; *Canziani et al.*, 1995; *Kawamoto et al.*, 1997; *Shiotani et al.*, 1997; *Mote et al.*, 1998; *Canziani and Holton*, 1998]. It is difficult to detect the weak, shallow temperature signals associated with vertically propagating equatorial waves, and satellite sampling usually recovers only the lowest zonal wave numbers (e.g., waves 1–6). Nevertheless, satellite observations are valuable for their global view, complementing the irregular sampling of the rawinsonde network.

Two-dimensional modeling studies [*Gray and Pyle*, 1989; *Dunkerton*, 1991a, 1997] showed that Kelvin and Rossby-gravity waves are insufficient to account for the required vertical flux of momentum to drive the QBO. The required momentum flux is much larger than was previously assumed because the tropical stratospheric air moves upward with the Brewer-Dobson circulation. When realistic equatorial upwelling is included in models, the required total wave flux for a realistic QBO is 2–4 times as large as that of the observed large-scale, long-period Kelvin and Rossby-gravity waves. Three-dimensional simulations [e.g., *Takahashi and Boville*, 1992; *Hayashi and Golder*, 1994; *Takahashi*, 1996] described in section 3.3.2 confirm the need for additional wave fluxes. Therefore it is necessary to understand better from observations the morphology of smaller-scale inertia-gravity and gravity waves and their possible role in the QBO.

3.2.2. Inertia-gravity waves. Eastward propagating equatorial inertia-gravity waves are seen in westerly shear phases of the QBO, while westward propagating waves are seen in easterly shear phases. Observational campaigns using rawinsondes have provided data with high temporal and vertical resolution, so that analysis is possible both for temporal and vertical phase variations.

Cadet and Teitelbaum [1979] conducted a pioneering study on inertia-gravity waves in the equatorial region, analyzing 3-hourly rawinsonde data at 8.5°N, 23.5°W during the Global Atmospheric Research Project Atlantic Tropical Experiment (GATE). The QBO was in an easterly shear phase. They detected a short vertical wavelength (<1.5 km) inertia-gravity wave-like structure having a period of 30–40 hours. The zonal phase velocity was estimated to be westward.

Tsuda et al. [1994a, 1994b] conducted an observational campaign focusing on waves in the lower stratosphere at Watukosek, Indonesia (7.6°S, 112.7°E), for 24 days in February–March 1990 when the QBO was in a westerly shear phase. Wind and temperature data were obtained with a temporal interval of 6 hours and vertical resolution of 150 m. Figure 8 shows a time-height section of temperature fluctuations with periods shorter than 4 days. Clear downward phase propagation is observed in the lower stratosphere (above about 16 km altitude). The vertical wavelength is about 3 km, and the wave period is about 2 days. Similar wave structure was seen also for zonal (u) and meridional wind (v) fluctuations. The amplitudes of horizontal wind and temperature fluctuations were about 3 m s^{-1} and 2 K, respectively.

On the basis of hodographic analysis, assuming that these fluctuations are due to plane inertia-gravity waves, *Tsuda et al.* [1994b] showed that most wave activity propagated eastward and upward in the lower stratosphere. Similar characteristics were observed in their second campaign, in Bandung, Indonesia (107.6°E, 6.9°S), during another westerly shear phase of the QBO (November 1992 to April 1993) [*Shimizu and Tsuda*, 1997].

Statistical studies of equatorial inertia-gravity waves have been made using operational rawinsonde data at Singapore (1.4°N, 104.0°E). *Maruyama* [1994] and *Sato et al.* [1994] analyzed the year-to-year variation of 1- to 3-day wave activity in the lower stratosphere using data from Singapore spanning 10 years. Extraction of waves by their periods is useful since the ground-based wave frequency is invariant during the wave propagation in a steady background field. The QBO can be considered sufficiently steady for these purposes for inertia-gravity waves having periods shorter than several days.

Maruyama [1994] analyzed the covariance of zonal wind and the time derivative of temperature for 1- to 3-day components and estimated the vertical flux of zonal momentum per unit density $\overline{u'w'}$ using the following relation derived from the thermodynamic equation for adiabatic motions:

$$\overline{\frac{\partial T'}{\partial t} u'} = -\left[\frac{\bar{T}N^2}{g}\right] \frac{c}{\hat{c}} \overline{u'w'}, \tag{7}$$

where T is temperature, t is time, u and w are the zonal and vertical components of wind velocity, c is the ground-based horizontal phase speed, $\hat{c} = c - \bar{u}$ is the intrinsic horizontal phase speed, $\bar{u}$ is the background wind speed, and the overbar indicates a time average. Since $\hat{c}$ is not obtained from the observational data, this estimate is possible only when $\bar{u}$ is small enough to assume $\hat{c}/c \sim 1$. Maruyama showed that the momentum flux $\overline{u'w'}$ is largely positive and that the magnitude is comparable to that of long-period Kelvin waves in the westerly shear phase of the QBO.

Sato et al. [1994] examined the interannual variation of power and cross spectra of horizontal wind and temperature fluctuations in the period range of 1–20 days at Singapore. They found that spectral amplitudes are maximized around the tropopause for all components in the whole frequency band, although the altitudes of the tropopause maxima are slightly different. The T and u spectra are maximized around a 10-day period, corresponding to Kelvin waves. In the lower stratosphere the wave period shortens, for example, 9 days at 20 km to 6 days at 30 km. On the other hand, v spectra are maximized around 5 days, slightly below the tropopause, corresponding to Rossby-gravity waves. The Rossby-gravity wave period also becomes shorter with increasing altitude in the lower stratosphere, consistent with the analysis of *Dunkerton* [1993] based on rawinsonde data at several locations over the tropical Pacific. An impor-

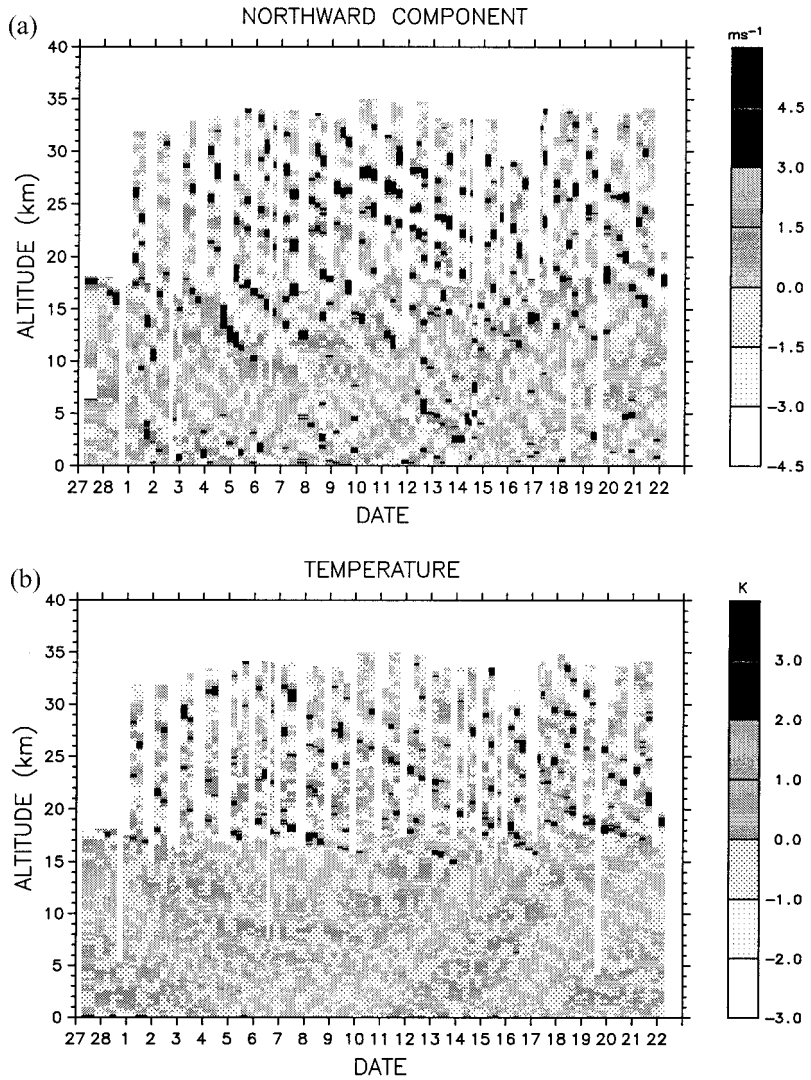

Figure 8. A time-height section of short-period (<4 days) (a) northward velocity component and (b) temperature, at Watukosek, Indonesia (7.6°S, 112.7°E), for 24 days in February to March 1990. From *Tsuda et al*. [1994b].

tant fact is that spectral amplitudes are as large at periods shorter than 2–3 days as for long-period Kelvin waves and Rossby-gravity waves.

The activity of inertia-gravity and Kelvin waves is observed to be synchronized with the QBO. Plate 4 shows power and cross spectra as a function of time averaged over the height region 20–25 km in the lower stratosphere. A low-pass filter with cutoff of 6 months was applied in order to display the relation with the QBO more clearly. Dominant peaks in the power spectra of T and u are observed in the 1- to 3-day period range during both phases of the QBO and around the 10-day period in the westerly shear phase of the QBO. The latter peak corresponds to Kelvin waves.

The quadrature spectra $Q_{Tu}(\omega)$ correspond to the covariance of zonal wind and time derivative of temperature. Thus large negative values observed around a 10-day period in the westerly shear phase show the positive $\overline{u'w'}$ associated with Kelvin waves [*Maruyama*, 1991, 1994]. Such a tendency is not clear at shorter periods in the quadrature spectra. Clear synchronization with the QBO is seen in the cospectra $C_{Tu}(\omega)$ in the whole range of frequencies. Positive and negative values appear in the westerly and easterly shear phases, respectively, though the negative values are weak around the 10-day period. This feature cannot be explained by the classical theory of equatorial waves in a uniform background wind [*Matsuno*, 1966], which predicts that the covariance of T and u should be essentially zero.

Dunkerton [1995] analyzed theoretically and numerically the covariance of T and u for 2-D (plane) inertia-gravity waves in a background wind having vertical shear and derived the following relation:

$$\overline{T'u'} = \left[\frac{\bar{T}N}{2gk|\hat{c}|}\right]\bar{u}_z|\overline{u'w'}| \tag{8}$$

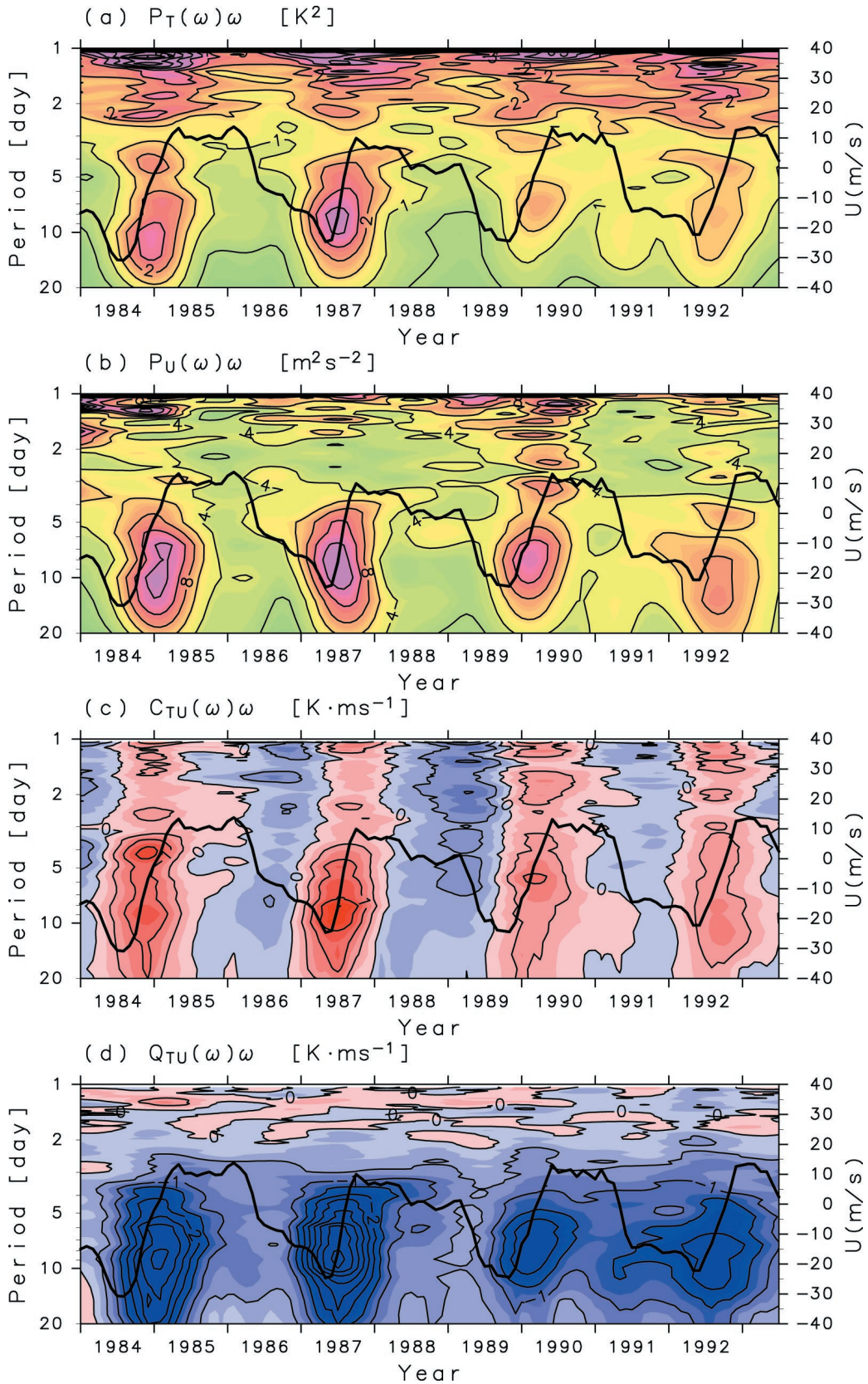

Plate 4. Power spectra for (a) T and (b) u fluctuations at Singapore as a function of time, averaged over 20–25 km. Contour interval 0.5 K^2, and 2 $(m\ s^{-1})^2$, respectively. (c) Cospectra and (d) quadrature spectra of T and u components. Contour interval 0.5 K $(m\ s^{-1})$. Red and blue colors show positive and negative values, respectively. The bold solid line represents a QBO reference time series. After *Sato et al.* [1994].

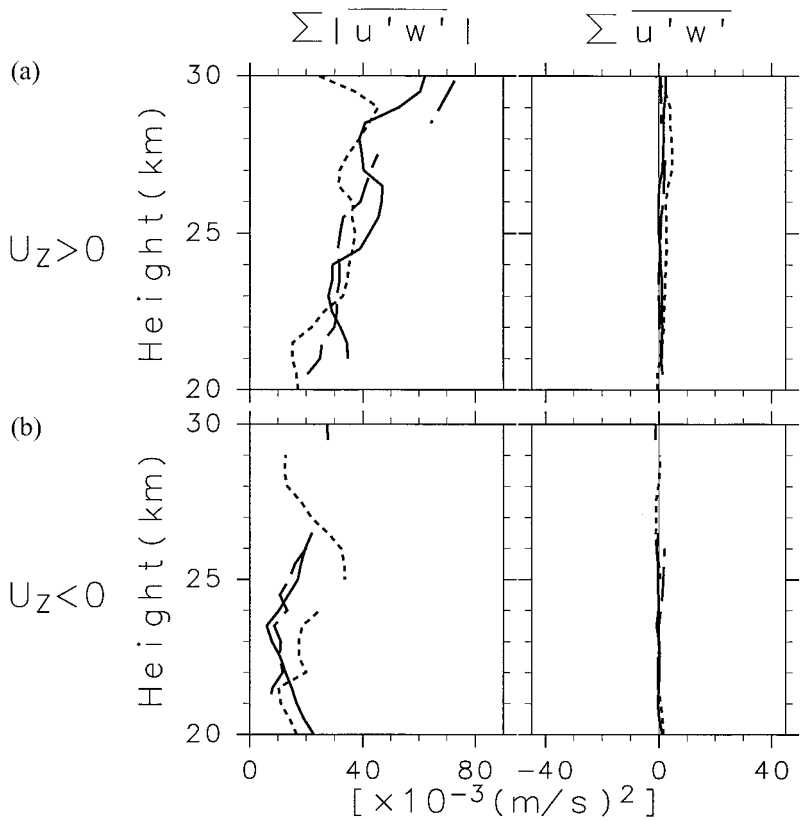

Figure 9. Momentum flux estimates for short-period (1–3 days) component in the (a) westerly and (b) easterly shear phases. Left panels show indirect estimates corresponding to a sum of absolute values of positive and negative momentum fluxes. Right panels show direct estimates corresponding to net momentum fluxes. From *Sato and Dunkerton* [1997].

for slowly varying, steady, conservative, incompressible waves. This theory was extended to 3-D equatorially trapped waves (T. J. Dunkerton, manuscript in preparation, 2001). According to (8), the covariance is proportional to the vertical shear and vertical flux of horizontal momentum, or radiation stress. The sign of the covariance is determined by the vertical shear, independent of the horizontal and vertical direction of inertia-gravity wave propagation. This is qualitatively consistent with the observation in Plate 4c.

Sato and Dunkerton [1997] estimated momentum fluxes associated with 1- to 3-day period waves directly and indirectly based on the quadrature and cospectra of T and u components at Singapore obtained by *Sato et al.* [1994]. Unlike Kelvin waves, which propagate only eastward, inertia-gravity waves can propagate both eastward and westward. Thus the net momentum flux estimate from quadrature spectra as obtained by *Maruyama* [1994] may be a residual after cancelation between positive and negative values. On the other hand, cospectra correspond to the sum of absolute values of positive and negative momentum fluxes. Using an indirect estimate of momentum fluxes from cospectra and a direct estimate from quadrature spectra, positive and negative parts of momentum fluxes can be obtained separately.

The direct estimate of momentum flux for Kelvin waves (5- to 20-day period) is 2–9 $\times$ 10^{-3} m^2 s^{-2} and accords with the indirect estimate within the estimation error, supporting the validity of the indirect method. Note that momentum flux is properly measured in pascals (Pa), equal to air density times the product of velocity components. In most QBO literature the density term is ignored, and the resulting "flux" is described in units of m^2 s^{-2}. Near the tropical tropopause the density is about 0.1 in MKS units, providing an easy conversion between the two definitions of flux.

The result for 1- to 3-day periods is shown in Figure 9, assuming plane inertia-gravity waves. The indirect estimate of momentum flux for 1- to 3-day-period components in westerly shear is 20–60 $\times$ 10^{-3} m^2 s^{-2}, while the direct estimate is only 0–4 $\times$ 10^{-3} m^2 s^{-2}. For easterly shear, the indirect estimate is 10–30 $\times$ 10^{-3} m^2 s^{-2}, while the direct estimate is almost zero. The discrepancy between the indirect and direct estimates indicates a large cancelation between positive and negative momentum fluxes.

There is ambiguity in the indirect estimate according to the assumed wave structure. If equatorially trapped modes are assumed, the values should be reduced by 30–70%. On the other hand, if there is aliasing from higher-frequency waves (with periods shorter than 1 day, for twice-daily data such as rawinsonde data at Singa-

pore), the actual momentum flux should be much larger than shown in Figure 9. Even considering these ambiguities, it appears that intermediate-frequency period gravity or inertia-gravity waves have significant momentum flux compared with Kelvin and Rossby-gravity waves.

According to the analysis of *Sato and Dunkerton* [1997], momentum fluxes associated with eastward and westward propagating gravity waves are almost equal, though eastward propagating gravity waves are slightly dominant in the eastward shear phases. This fact does not contradict the result from observational campaigns by *Cadet and Teitelbaum* [1979] and *Tsuda et al*. [1994b] that eastward (westward) propagating gravity waves are dominant in the time-height sections of u and T components in the eastward (westward) shear phase. Observations confirm that it is more likely to observe waves with short vertical wavelengths (corresponding to small intrinsic frequencies) if those waves propagate eastward in eastward shear or westward in westward shear. For two waves with equal momentum flux but different intrinsic frequencies, the amplitudes of u and T are larger for the wave having smaller intrinsic frequency. Westward (eastward) propagating gravity waves having small intrinsic phase speeds, i.e., small vertical wavelengths, probably would not be found in the eastward (westward) shear phase because such waves would have encountered critical levels or been absorbed at lower levels. Westward (eastward) gravity waves having large intrinsic phase speeds carrying significant momentum flux can exist but may not be recognized in the rawinsonde data because their vertical wavelengths are too long and their amplitudes in u and T are too small. Thus, in the eastward (westward) shear phase, only eastward (westward) propagating gravity waves have small intrinsic phase speeds and hence small vertical wavelengths that are observable.

Bergman and Salby [1994] calculated equatorial wave activity propagating into the stratosphere based on high-resolution imagery of the global convective pattern and some simple assumptions about the relation of cloud variations to the properties of the waves that would be generated. Figure 10 shows the geographical distribution of the vertical component of *Eliassen-Palm flux* that they derived. The components with periods shorter than 2 days have large Eliassen-Palm flux, compared with longer-period waves. The short-period wave generation is large over the African and American continents and in a broad area from the Indian Ocean to the western tropical Pacific.

The analysis of *Bergman and Salby* [1994] does not provide a quantitative estimate of actual wave fluxes but supports the idea that intermediate and small-scale waves contribute significantly to the QBO. From their analysis we note, first, that the contribution is large relative to that of planetary-scale equatorial waves, by a factor of about 2.5, and second, that most of the activity in smaller-scale waves is associated with zonal phase speeds lying in the range of QBO wind speeds [*Dunkerton*, 1997].

The excitation of inertia-gravity waves by deep tropical convection occurs either through a process of self-organization, in which waves and convection support one another, or (more simply) as a result of irregular, seemingly random activity as convective elements impinge on a stratified layer above. Self-organization of waves and convection occurs mainly on longer horizontal and temporal scales [*Takayabu et al*., 1996; *Wada et al*., 1999; *Wheeler and Kiladis*, 1999].

3.2.3. Gravity waves. Deep convection is a dominant source for high-frequency gravity waves in the tropics. Numerical simulations of convection that include stratospheric altitudes [*Fovell et al*., 1992; *Alexander et al*., 1995; *Alexander and Holton*, 1997] generate high-frequency gravity waves that appear prominently above convective clouds (Figure 11). Theory predicts a close association of high-frequency waves in the lower stratosphere and the convective systems that generate them because the energy propagation direction is most vertically oriented for waves with high intrinsic frequency,

$$\hat{\omega} = N \cos \theta, \tag{9}$$

where θ is the angle between the vertical and lines of constant phase or direction of the group velocity vector. In these simulations, high-frequency waves carry significant momentum flux, suggesting they could play a prominent role in driving the QBO [*Alexander and Holton*, 1997].

Observational studies have identified large-amplitude, high-frequency gravity waves in the midlatitude stratosphere directly above deep tropospheric convection [*Röttger*, 1980; *Larsen et al*., 1982; *Sato*, 1992, 1993; *Sato et al*., 1995]. *Sato* [1993] was able to estimate the vertical momentum flux carried by the waves. These observations found significant values of 0.03 Pa, equivalent to about 0.3 $m^2 s^{-2}$, an order of magnitude larger than the estimated time-averaged, zonal-mean flux needed for tropical gravity waves to be important to the QBO [*Dunkerton*, 1997].

High-frequency gravity waves have also been detected in aircraft observations in the lower stratosphere. NASA's ER-2 aircraft flies at altitudes up to ~20 km and has participated in numerous campaigns that included tropical flights in the stratosphere. Observations of winds and temperatures on board have been used to detect gravity waves. *Pfister et al*. [1986, 1993a, 1993b] detected waves with short horizontal wavelength <150 km in temperature and horizontal wind fields associated with cumulus convection over Panama and northern Australia. *Pfister et al*. [1993a, 1993b] proposed a "convective topography" mechanism for generating these waves and used a model to estimate the vertical momentum flux that could be generated by this mechanism and the impact such waves might have on the QBO momen-

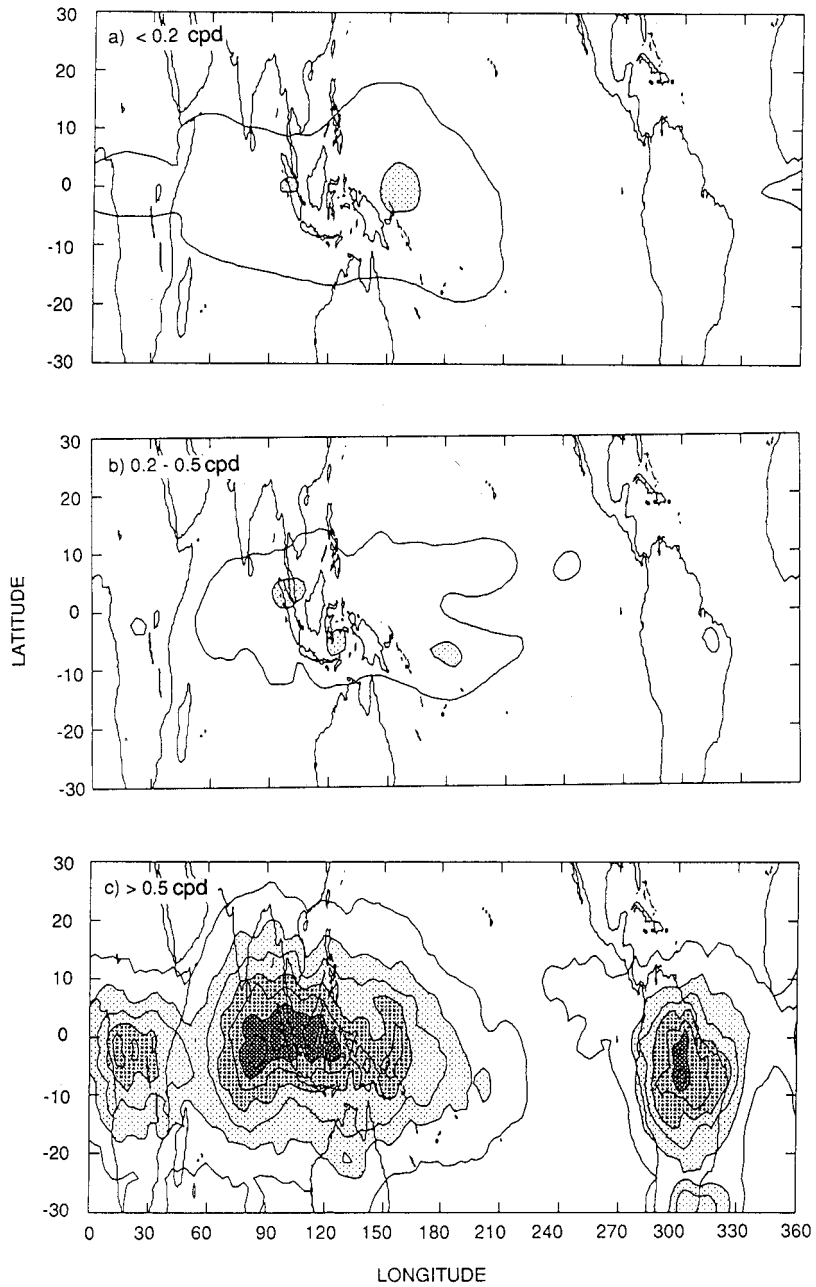

Figure 10. Geographical distribution of vertical component of Eliassen-Palm flux for equatorial waves with periods (a) longer than 5 days, (b) of 2–5 days, and (c) shorter than 2 days, estimated based on high-resolution imagery of the global convective pattern constructed from six satellites. Shown here is the frequency-integrated absolute value of the Eliassen-Palm flux. Units are arbitrary, and contour increments are linear. Reprinted from *Bergman and Salby* [1994] with permission from the American Meteorological Society.

tum budget. The calculated effect was small (<10%) compared with estimates of planetary-scale wave driving. Other forcing mechanisms may be active, however, and the effects of high-frequency waves would be underestimated in these calculations [*Dunkerton*, 1997]. The estimates are also uncertain because of the unknown geographical distribution and occurrence frequency of convectively forced gravity waves based on only a few case studies.

Alexander and Pfister [1995] used observations of both the horizontal and vertical winds together to estimate momentum flux along an ER-2 flight path over deep convection north of Australia. The momentum flux emphasizes shorter-period waves. Very large values ~0.1 Pa were observed over the deepest, highest clouds. More extensive correlations of these data with cloud top temperature were reported by *Alexander et al.* [2000] and are shown in Figure 12. These results suggested that large values of momentum flux are correlated with deep convection and have magnitudes similar to waves generated

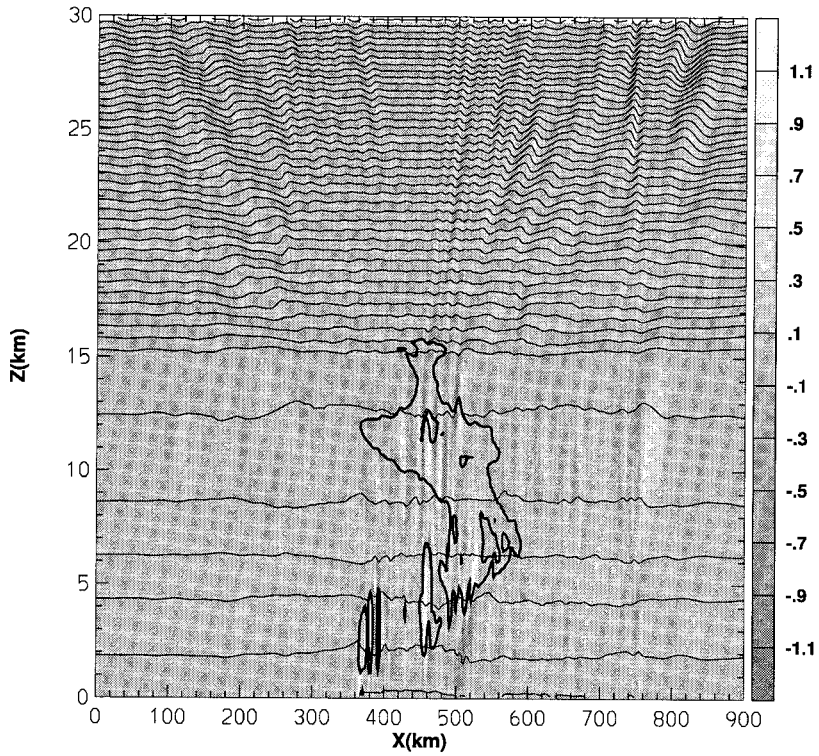

Figure 11. Stratospheric gravity waves above a simulation of tropical convection. The shading shows vertical velocities. The scale runs ± 1.2 m s^{-1} to enhance the wave perturbations in the stratosphere, but maximum values in the troposphere exceed ± 5 m s^{-1}. Potential temperature contours at 10-K intervals (thin lines) and the outline of the storm cloud (bold lines) are also shown. Reprinted from *Alexander and Holton* [1997] with permission from the American Meteorological Society.

in 2-D simulations of tropical convection [*Alexander and Holton*, 1997]. A more recent observational study suggests smaller momentum fluxes in other regions [*Alexander et al.*, 2000]. While the geographical and seasonal distributions of such fluxes are uncertain, the results nonetheless suggest a potentially important role for high-frequency gravity waves in the QBO.

The gravity waves observed in the low-latitude (~12°S) rawinsonde analyses described by *Allen and Vincent* [1995] showed a seasonal cycle suggesting convection as an important source during the December–February monsoon season. These results represented only 1 year of observations; however, subsequent analysis of data from Cocos Island, also at ~12°S, spanning 6 years showed a similar correlation with the monsoon season, but it is modulated by QBO winds [*Vincent and Alexander*, 2000]. The months with peak momentum flux were found to coincide with the strongest easterly winds. At these times the waves also propagate predominantly eastward. Parallel theoretical calculations of gravity

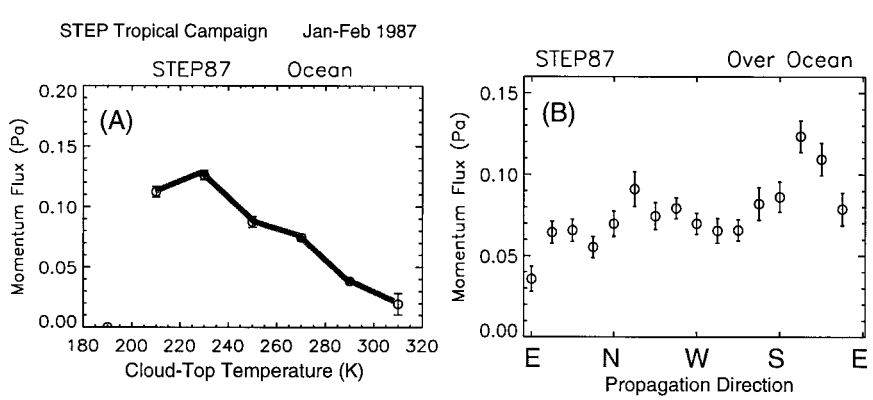

Figure 12. (a) Gravity wave momentum flux in the stratosphere versus underlying cloud-top temperature for oceanic flights north of Australia during January–February 1987. (b) The directional distribution of the momentum fluxes in these observations. From *Alexander et al.* [2000].

wave propagation and interaction with the background flow qualitatively support the convective topography mechanism because of the anisotropy observed in wave propagation direction and because the altitude where the waves are generated was inferred to be very high, close to the tropopause. *Karoly et al*. [1996] also observed a correlation between inertia-gravity wave activity and deep convection in tropical sounding data.

3.3. Numerical Models of the QBO

3.3.1. One-dimensional models. One-dimensional models, in which wind and wave fields are functions of height only, have been used to explore many aspects of QBO behavior relevant to the real atmosphere. Sometimes the one-dimensionality may be justified, as in the work of *Holton and Lindzen* [1972], by integrating the dynamical equations in latitude to derive evolution equations for the zonal flow integrated across the tropics. This approach is acceptable for Kelvin waves, which are known to depend primarily on the near-equatorial wind and which generate a simple profile of the mean-flow forcing. Other equatorial waves, however, are significantly affected by latitudinal shear and produce more complicated latitudinal profiles of mean-flow forcing [*Andrews and McIntyre*, 1976; *Boyd*, 1978; *Dunkerton*, 1983a]. High-frequency gravity waves propagate mostly vertically, and their interaction with the mean flow is more easily described in a 1-D model. For these waves the latitudinal dependence of sources is important, however, owing to the seasonally varying distribution of tropical convection [*Allen and Vincent*, 1995]. For these and other reasons the utility of 1-D models is limited and their value lies in their simplicity rather than their realism. For example, *Plumb* [1977] considered nonrotating gravity waves in order to demonstrate a number of basic properties of QBO behavior.

One-dimensional models have been used to investigate several aspects of QBO wave forcing, including the effect of scale-dependent radiative damping of the waves [*Hamilton*, 1981], effects of laterally propagating Rossby waves [*Dunkerton*, 1983b], the effects of self-acceleration of wave phase speed and of wave saturation [*Tanaka and Yoshizawa*, 1987], upwelling of the tropical Hadley circulation [*Saravanan*, 1990], and interannual variations of forcing [*Geller et al*., 1997]. One-dimensional models are also useful for interpreting the results of more complex 2-D or 3-D models [*Dunkerton*, 1997].

3.3.2. Two-dimensional models. Many important aspects of the QBO behavior can be considered using models that represent only latitudinal and vertical variations. This applies self-evidently to questions concerning latitudinal structure, but also to wider questions concerning the interaction of the QBO with the annual cycle and the effect of the QBO on tracer distributions (to be discussed in more detail in section 5).

The first detailed 2-D model analysis of the latitudinal structure, including the mean meridional circulation, was that by *Plumb and Bell* [1982b], who assumed that the wave momentum fluxes were due to equatorial Kelvin waves and Rossby-gravity waves. For the wind field at any instant they calculated the height-latitude structure of the waves on the basis of a linear, steady state calculation [*Plumb and Bell*, 1982a]. These momentum and heat fluxes were used to force the longitudinally symmetric dynamical equations including thermal damping through a Newtonian cooling term, with the structure of the waves being recalculated at each time step. Their attempt to simulate the QBO in this manner was broadly successful, except that they were limited to cases where the amplitude of the oscillation was only about half of that observed. *Dunkerton* [1985] and *Takahashi* [1987] used different strategies for calculating the wave momentum fluxes and succeeded in simulating oscillations of realistic amplitude. The 2-D models showed explicitly that the QBO meridional circulation anomaly was in the sense of sinking at the equator in westerly shear zones and rising at the equator in easterly shear zones. In westerly shear zones the thermal wind equation (1b) implies a maximum in temperature at the equator which is maintained against thermal damping by adiabatic warming due to sinking motion. The opposite holds in easterly shear zones. The pattern of shear zones and meridional circulations is shown schematically in Figure 13.

The models mentioned above were focused on the equatorial regions and did not include a realistic seasonal cycle in winds or temperatures. A realistic QBO was achieved by *Gray and Pyle* [1989] in a full radiative-dynamical model (which therefore had a realistic seasonal cycle) only by increasing their parameterized wave momentum forcing by a factor of 3 larger than could be justified by Kelvin and Rossby-gravity waves alone. This additional forcing, now thought to be due to gravity and inertia-gravity waves, was required in order that QBO wind regimes propagate downward despite climatological upwelling in the tropics [*Dunkerton*, 1997].

Mengel et al. [1995] obtained a QBO-like oscillation in a 2-D middle atmosphere model in which eddy momentum transport was due solely to the *Hines* [1997] gravity wave parameterization. Although the QBO simulated in this model was weak and sensitive to vertical diffusion, the parameterization's striking ability to reproduce the entire phase structure of observational equatorial oscillations [*Burrage et al*., 1996] emphasizes the importance of gravity waves that have a wide range of phase speeds and whose amplitude grows with height.

The 2-D simulations by *Gray and Pyle* [1989] demonstrated that the influence of the QBO extends to all latitudes. For example, the QBO circulation with rising or sinking at the equator is compensated by an opposing circulation off the equator, which gives rise to a temperature anomaly in the subtropics and midlatitudes of opposite sign to that at the equator (see also *Plumb and Bell* [1982b] and *Dunkerton* [1985]). A significant interhemispheric asymmetry in the timing and amplitude of

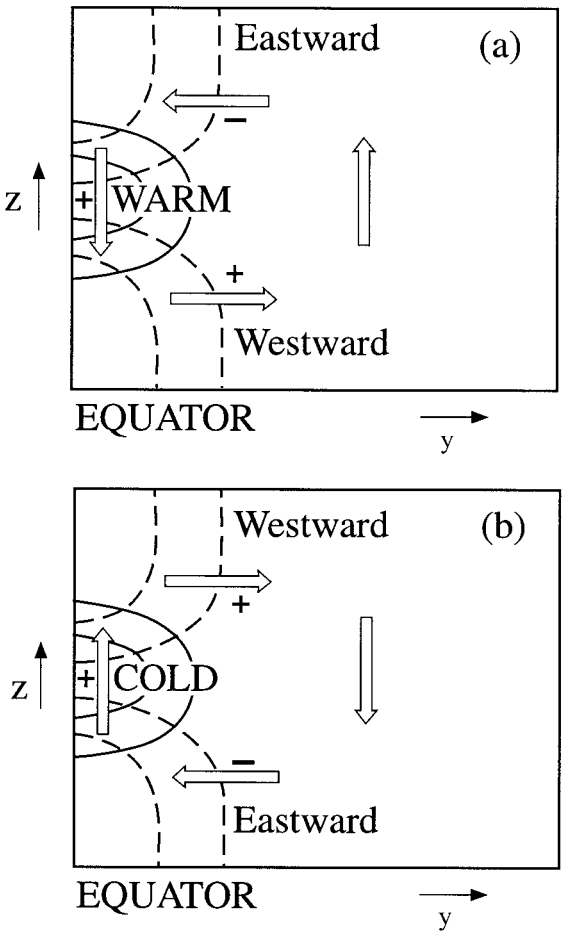

Figure 13. Schematic latitude-height sections showing the mean meridional circulation associated with the equatorial temperature anomaly of the QBO. Solid contours show temperature anomaly isotherms, and dashed contours are zonal wind isopleths. Plus and minus signs designate signs of zonal wind accelerations driven by the mean meridional circulation. (a) Westerly shear zone. (b) Easterly shear zone. After *Plumb and Bell* [1982b]. Printed with permission from the Royal Meteorological Society.

the subtropical anomalies is also present, due to the interaction of the QBO with the seasonal cycle [*Gray and Dunkerton*, 1990]. The QBO-induced meridional velocity in the winter hemisphere and, correspondingly, the vertical velocity in the subtropical winter hemisphere are substantially larger than those in the summer hemisphere, particularly above ~25 km [*Jones et al.*, 1998; *Kinnersley*, 1999], probably due in part to asymmetric subtropical angular momentum gradients at solstice.

The meridional circulation affects chemical tracers such as ozone and gives rise to strong QBO signals in such tracers at all latitudes, with significant interhemispheric asymmetry (see section 5). However, there may also be a significant feedback of the ozone QBO on the dynamics of the QBO, since changes in ozone have radiative implications and, in particular, have a direct effect on short-wave heating. The effect of including the coupling between ozone-QBO anomalies and heating rates tends to reduce the heating rate that would otherwise be calculated from a given temperature anomaly in the lower stratosphere [*Hasebe*, 1994; *Li et al.*, 1995; *Kinnersley and Pawson*, 1996; *Randel et al.*, 1999]. *Hasebe* [1994] argued that this effect must be taken into account in order to explain the observed phase relation in the lower stratosphere between the QBO signals in ozone and wind. In the upper stratosphere the ozone heating enhances the QBO vertical velocity.

Plumb and Bell [1982b] noted that the advective effects of the meridional circulation can account for the observed asymmetry in the descent of easterlies and westerlies (without any need for asymmetry in the waves providing easterly and westerly momentum fluxes). Downward advection of momentum associated with the westerly shear zone enhances the descent of the westerlies, while the upward advection of momentum associated with easterly shear inhibits the descent of easterlies. An additional advective effect, since vertical velocities are greatest near the equator, is to narrow latitudinally the region of strongest westerly acceleration and to broaden that of strongest easterly acceleration [*Hamilton*, 1984; *Dunkerton and Delisi*, 1985; *Dunkerton*, 1985; *Takahashi*, 1987; *Dunkerton*, 1991a].

3.3.3. Three-dimensional models. In the 1-D and 2-D models discussed above, the waves that contribute to the driving of the QBO must be parameterized. Three-dimensional models offer the possibility of explicit simulation of the waves, without any need for simplifying assumptions that allow parameterization. In "mechanistic" models, waves are artificially forced (e.g., by imposed heating fields or imposed lower boundary perturbations). One particular issue where mechanistic models have given important insight concerns whether the easterly momentum forcing needed to account for the equatorial QBO can be supplied entirely by Rossby-gravity waves. A 3-D mechanistic model simulation by *Takahashi and Boville* [1992] in which a Kelvin wave and Rossby-gravity wave were forced at the lower boundary gave a good representation of the QBO in the lower stratosphere. However, the amplitudes of the Kelvin wave and, particularly, the Rossby-gravity wave were considerably stronger than the observed values. This result added to the evidence that a much broader spectrum of waves is needed.

In general circulation models (GCMs) the waves are generated spontaneously in the model (although that is not to say that the generation processes are necessarily realistic). For various reasons, the ability to simulate a realistic QBO is a stringent requirement on a GCM. First, the large apparent contribution of the QBO to interannual variability in the entire middle atmosphere, not just at low latitudes (see section 4), means that ultimately, if a GCM that includes the middle atmosphere is to be regarded as realistic, it must represent the QBO. Second, since the QBO is believed to be partially driven by waves excited by cumulus convection (on a whole range of scales), the ability or inability of a model

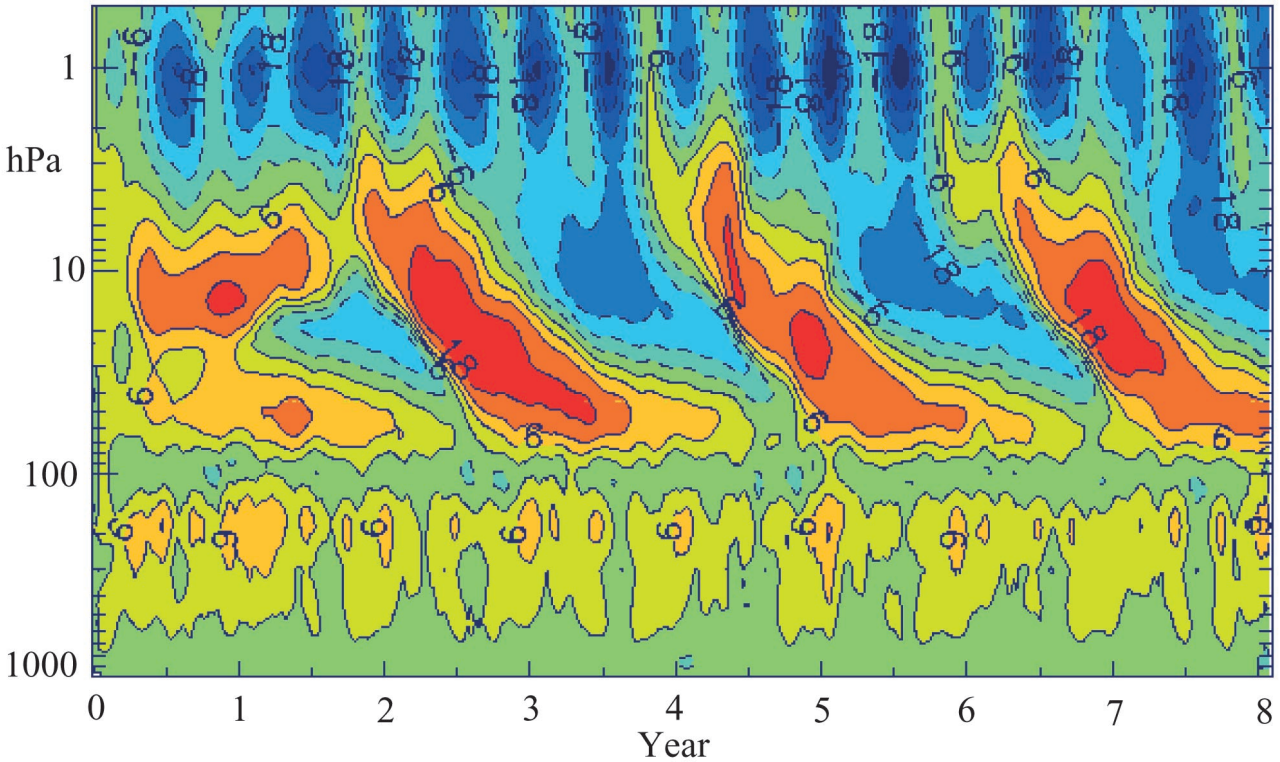

Plate 5. Time-height section of the zonal-mean zonal wind over the equator simulated by *Takahashi* [1999]. The time coordinate ranges from day 0 (January 1, with a 360-day model year) to day 1830. The contour interval is 6 m s^{-1}. Red and blue shading represent westerly and easterly winds, respectively.

to simulate the QBO might also have implications for the simulated tropical tropospheric circulation.

Until relatively recently, no GCM had successfully simulated the QBO (or an analogous long-period, wave-driven "QBO-like" oscillation) even if the GCMs included Kelvin and Rossby-gravity waves of realistic amplitude (Community Climate Model, Version 2 (CCM2) [*Boville and Randel*, 1992] or SKYHI [*Hayashi and Golder*, 1994]). Simulation of the QBO evidently puts demanding requirements on a GCM. Here we present an overview of the successful simulations and discuss the main features upon which a successful simulation depends.

The first realistic simulation of the QBO in a GCM was made by *Takahashi* [1996]. He used the Center for Climate System Research/National Institute of Environmental Studies (CCSR/NIES) GCM with horizontal resolution of T21 (triangular truncation at total wave number 21, equivalent to a grid spacing of about 600 km, or $5\frac{1}{2}°$ of latitude) and a vertical grid spacing of 500 m in the stratosphere. This fine vertical resolution allowed waves with small vertical wavelength to propagate vertically and interact with the mean flow; most previous GCMs had a vertical grid spacing of 2 km or more in the stratosphere.

All GCMs, for numerical reasons, include some kind of horizontal diffusion or its equivalent. In this case, to obtain a QBO it was necessary also to reduce the coefficient of the fourth-order horizontal diffusion by 1 order of magnitude from its standard value. The model then produced a QBO-like oscillation with a period of 1.5 years. Other simulations have been made by *Horinouchi and Yoden* [1998] (aquaplanet GCM, period 1.1 years); *Hamilton et al.* [1999] (SKYHI, period 1 year); and *Untch* [1998] (European Centre for Medium-Range Weather Forecasts (ECMWF), realistic period). Plate 5 shows the most realistic simulation to date [*Takahashi*, 1999], with a period of 2.3 years, using a horizontal resolution of T42. The horizontal diffusion coefficient had to be reduced by a factor of 4 from its standard value.

Although several GCMs have produced simulations of the QBO, there is no simple set of criteria that guarantees a successful simulation. Realistic simulations are difficult and time consuming because the simulations depend on the subtle interaction of several factors. The simulation of a QBO in a GCM requires fine vertical resolution in the stratosphere, a small diffusion coefficient, moderate to high horizontal resolution, and a convection scheme that generates sufficient waves to drive the QBO.

The vertical grid spacing in the stratosphere must be sufficient to resolve the waves and their interaction with the mean flow. The values used in simulations of the QBO range from 500 m [*Takahashi*, 1996] to 1500 m [*Untch*, 1998]. High horizontal resolution is not always

required. The *Takahashi* [1996] simulation used a horizontal resolution of only T21. In a T63 simulation, *Untch* [1998] found that a QBO developed, but then disappeared due to a long-term westerly drift in the upper stratosphere. The drift was eliminated, and the QBO persisted in a T159 simulation. *Hamilton et al*. [1999] found that a horizontal resolution of 2° × 2.4° was needed.

Development of an oscillation can be prevented by horizontal diffusion that smoothes the meridional structure of the zonal flow. All of the successful QBO simulations have diffusion timescales longer than the period of the simulated QBO-like oscillation. Waves propagating upward into the stratosphere are also damped by the diffusion. *Takahashi* [1996] showed that a decrease in the diffusion coefficient increased the power of waves in the stratosphere while having little effect on the troposphere.

As in the real atmosphere, it appears that a broad spectrum of waves supplies the necessary forcing in these simulations. For example, *Takahashi et al*. [1997] suggested that the easterly acceleration of the model QBO was due to gravity waves as well as Rossby waves from the NH winter and Rossby-gravity waves, while westerly acceleration was due to Kelvin and gravity waves. In contrast, in the *Takahashi* [1999] model, gravity waves were the dominant forcing for the QBO.

Horinouchi and Yoden [1998] also did a thorough wave analysis. The frequency distribution of momentum flux and its magnitude were roughly consistent with the observational estimates of *Sato and Dunkerton* [1997] for Singapore (see section 3.2). In particular, the Kelvin and Rossby-gravity waves played a small role.

The tropospheric source of the waves, which is dominated by latent heat release due to cumulus convection, is a crucial characteristic. Since most GCMs approximately reproduce the climatological mean precipitation, the low-frequency components of latent heating will be similar. However, the transient characteristics of cumulus convection, which are important for wave excitation, differ greatly among models.

All of the successful QBO simulations employed the moist convective adjustment scheme except for the model of *Untch* [1998], which used the *Tiedtke* [1989] scheme. The moist convective adjustment scheme tends to produce intermittent grid-scale cumulus convection. The *Takahashi* [1996] T21 model also produced a QBO-like oscillation when the scheme was replaced by the prognostic Arakawa-Schubert scheme [*Nagashima et al*., 1998], which also tends to produce highly transient grid-scale heating pulses. However, some cumulus parameterizations produce little transient cumulus convection. For example, convection due to the *Zhang and McFarlane* [1995] scheme in the National Center for Atmospheric Research (NCAR) CCM3 (which has not successfully simulated the QBO) results in a momentum flux to the stratosphere that is quite weak, even though the time-averaged precipitation is realistic.

A final factor that may affect the ability of a GCM to simulate a QBO is tropical upwelling due to the Brewer-Dobson circulation. As noted in section 3.3.1, strong upwelling tends to slow the descent of the QBO. The upwelling in the *Takahashi* [1999] model, which had a realistic period, was a little weaker than the observational estimates of *Mote et al*. [1996]. The *Takahashi* [1996] and *Horinouchi and Yoden* [1998] models, which had shorter periods, had unrealistically weak upwelling. It is possible that in some models, unrealistically strong upwelling may prevent the simulation of a QBO, while in other models, unrealistically weak upwelling may result in a shorter QBO period than observed.

The most important factor in reproducing the QBO is probably the use of a fine vertical resolution to resolve equatorial gravity waves. The horizontal diffusion should be weak enough not to prevent the evolution of the mean flow oscillation and not to be the primary damping mechanism for the waves. Transient characteristics of tropical cumulus convection are also important since they determine the excitation of the waves. Despite the recent success, those models that reproduced the QBO might have overly active cumulus convection and hence excessively large amplitude of gravity waves with resolved scales. Thus a parameterization of subgrid-scale gravity waves due to convection, supplementing the forcing due to resolved waves, might be necessary in order to produce a QBO with the same spectrum of waves that drives it in the real atmosphere.

4. DYNAMICAL EFFECTS IN THE EXTRATROPICAL STRATOSPHERE

Any connection between the equatorial QBO and the extratropical atmosphere must be viewed in the context of the seasonal cycle and variability of the extratropical stratosphere. Compared with the troposphere, the zonal-mean circulation in the extratropical stratosphere undergoes a much stronger seasonal cycle with an actual reversal of winds from winter to summer. During the winter season the high-latitude stratosphere cools, forming a deep, strong westerly vortex. The strong westerlies are replaced by easterlies with increasing solar heating in the spring and summer.

In both hemispheres the smoothly varying seasonal cycle described above is modified by the effects of planetary Rossby waves (hereinafter referred to simply as planetary waves) which are forced in part by land-sea contrasts and surface topography. These waves propagate vertically and meridionally into the winter stratosphere (Plate 2), but are evanescent in the mean easterly winds of the summer hemisphere [*Charney and Drazin*, 1961; *Andrews et al*., 1987].

The NH has much greater land-sea contrast and larger mountain ranges than the SH, resulting in larger-amplitude tropospheric planetary waves. Consequently, the northern winter stratosphere tends to be much more

disturbed by planetary waves than the southern winter stratosphere. Large-amplitude waves can rapidly disrupt the northern polar vortex, even in midwinter, replacing westerly winds with easterly winds in high latitudes and causing the polar stratosphere to dramatically warm. Such events are called major stratospheric warmings. The transition from westerlies to easterlies in the springtime usually occurs in conjunction with a planetary wave event and is called the final warming. In the NH the timing of the final warming is highly variable and tends to occur during March or April. In the SH the final warming occurs in November and December, with less interannual variability [*Waugh and Randel*, 1999].

In the NH the planetary wave amplitudes are just large enough for midwinter sudden warmings to occur during some years but not others. Thus the northern stratosphere is sensitive to the effects of vertically propagating planetary waves, resulting in large interannual variability in the strength of the polar vortex. It appears that this sensitivity to the upward and equatorward propagation of planetary waves allows the equatorial QBO to influence the polar stratosphere by modulating the flux of wave activity or Eliassen-Palm flux [e.g., *Dunkerton and Baldwin*, 1991].

The definitive identification of an extratropical QBO signal has been difficult due to the brevity and limited height range of data sets. In the NH, data up to 10 hPa appear to be reliable beginning in the 1950s. Above the 10-hPa level, and in the SH lower stratosphere, the lack of rawinsonde coverage has limited the production of reliable gridded data to the period beginning in the late 1970s, when satellite temperature retrievals began. Most of the literature on the extratropical influence of the QBO has focused on the NH simply because the data record is longer and more reliable. Part of the difficulty in identifying a NH QBO signal is that the QBO accounts for only a fraction of the variance. In addition to the variability of tropospheric forcing, other signals, such as the 11-year solar cycle, volcanic eruptions, and sea surface temperature anomalies, appear to influence the variability of the extratropical stratosphere.

Holton and Tan [1980, 1982] presented strong evidence that the QBO influences the extratropical northern stratosphere by using gridded data for 16 NH winters (1962–1977) to form easterly and westerly phase composites of 50-hPa geopotential. They showed that geopotential height at high latitudes is significantly lower during the westerly phase of the QBO. They also found a statistically significant modulation of the springtime zonal wind in the SH. In the NH, *Labitzke* [1987] and *Labitzke and van Loon* [1988] found a strong relation to the 11-year solar cycle during January and February, suggesting that solar influence modifies the signal during late winter. *Naito and Hirota* [1997] confirmed their findings and also showed that a robust QBO signal is present during November and December.

4.1. Mechanism for Extratropical Influence

As discussed previously in section 3.1, in purely zonally symmetric flow there is a nonlocal response to a localized momentum forcing. One possible mechanism for an extratropical effect of the QBO is therefore through such a response. However, the response to near-equatorial forcing is strongly confined to tropical and subtropical latitudes [*Plumb*, 1982], and this mechanism therefore cannot account for the observed QBO modulation of the NH polar vortex. The mechanism now favored involves zonally asymmetric planetary waves. Typically, the dominant direction of wave activity propagation for tropospheric planetary waves is upward and equatorward, and vertical propagation is limited to the waves with largest spatial scales (primarily waves 1 and 2) [*Charney and Drazin*, 1961]. In the high-latitude stratosphere these waves distort the vortex from zonal symmetry, and if amplitudes are large enough, the vortex can be displaced from the pole or disrupted so that easterlies replace westerlies near the pole. Concomitant with large wave amplitude is the "breaking" of planetary waves [*McIntyre and Palmer*, 1983, 1984], leading to erosion of the vortex and weaker westerly winds.

The vertical and meridional propagation of planetary waves depends on the latitude-height structure of the zonal-mean wind, which may be thought of as refracting the waves as they propagate out of the troposphere. Quasi-stationary waves cannot propagate in easterly winds, and the phase of the QBO in the tropics and subtropics alters the effective *wave guide* and position of the boundary between easterly and westerly zonal-mean winds: the critical line for waves with zero phase speed.

If the mean flow in the tropical stratosphere is westerly, planetary waves are able to penetrate into the tropics and even across the equator without encountering a critical line. By contrast, when the mean flow in the tropical stratosphere is easterly, planetary waves encounter a critical line on the winter side of the equator. Thus, when there are easterly winds in the tropics, the effective wave guide for planetary wave propagation is narrower, and as a result, wave activity at middle and high latitudes in the winter hemisphere tends to be stronger. Stronger planetary waves in high latitudes lead to greater wave-induced drag on the mean flow, reduced westerly winds, and hence a warmer polar stratosphere.

4.2. Observations of Extratropical Influence

The effect of the QBO on the strength of the northern winter stratospheric vortex may be seen by comparing composites of extratropical zonal-mean wind during easterly and westerly phases of the QBO. The QBO phase must be defined precisely, and typically the equatorial zonal-mean wind at a particular level is used. *Holton and Tan* [1980] defined the QBO phase using equatorial winds at the 50-hPa level, but other authors have used 45, 40, and 30 hPa. The motivation for picking a particular wind level is to optimize the extratropical signal. In Figures 14–16 the QBO phase was defined

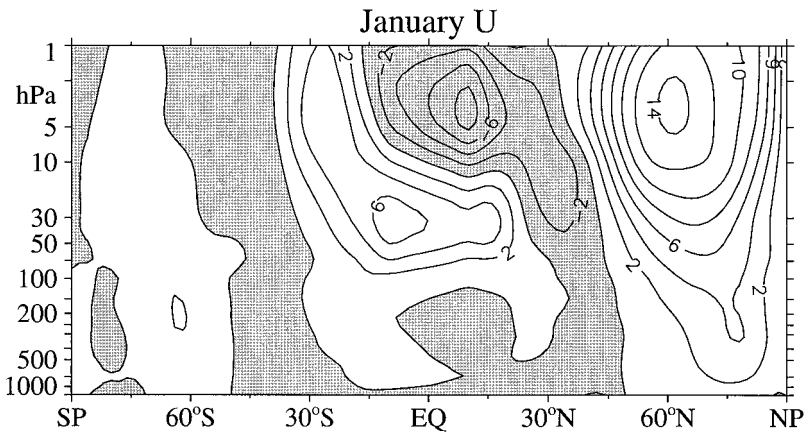

Figure 14. January latitude-height zonal-mean wind difference between the average of all years with westerly QBO and those with easterly QBO, during 1964–1996. The phase of the QBO is optimized for the Northern Hemisphere (NH) and is defined using the empirical orthogonal function technique of *Baldwin and Dunkerton* [1998b]; it is nearly equivalent to using 40-hPa equatorial winds. The contour interval is 2 m s^{-1}, and negative values are shaded. From *Baldwin and Dunkerton* [1998b].

using the first two empirical orthogonal functions (EOFs) of the vertical variations of equatorial winds [*Wallace et al.*, 1993; *Baldwin and Dunkerton*, 1998a]. The QBO definition was adjusted to optimize the extratropical signal in either the NH or SH. The resulting definition of the QBO phase is very similar to the 40-hPa equatorial wind for the NH composites and the 25-hPa wind for the SH composites.

Figure 14 illustrates the difference in zonal-mean wind between westerly and easterly QBO composites, using National Centers for Environmental Prediction (NCEP) analyses for the period 1978–1996. The difference is formed by calculating separate averages of the January wind data for the two phases of the QBO and then taking the difference between these averages. The zonal winds were derived from the geopotential fields using the balance method [*Robinson*, 1986; *Hitchman et al.*, 1987; *Randel*, 1987]. Although this method works well in the extratropics, it is not possible to derive accurate winds in the tropics, where winds have been interpolated between 10°N and 10°S, making the QBO too weak. The northern signal is dominated by a modulation of the polar vortex which extends from the surface to the 1-hPa level. Differences are of the opposite sign south of ~40°N and blend into the upper branch of the tropical QBO.

The features in Figure 14 are not confined to the middle stratospheric levels where the equatorial QBO is defined. Rather, the most prominent features are found above 10 hPa. Correlation analysis of zonal-mean wind in the latitude-height plane [*Baldwin and Dunkerton*, 1991] suggests that the upper level features, including those in the SH near 30°S, are a result of modulation by the QBO of the cross-equatorial (summer to winter) branch of the mean meridional circulation. It is reasonable to suppose that this circulation is weakly modulated by the Holton-Tan oscillation. For example, during the westerly phase of the QBO, polar temperatures are relatively low, implying a weaker cross-equatorial flow and a weak westerly anomaly near 30°S (Figure 14). The feature near 30°S may be interpreted not only as a direct effect of the QBO, but a remote effect of the Holton-Tan wave driving communicated by the mean meridional circulation, as described by (6). This behavior is also seen in numerical models (see section 4.3 and Figure 17).

The statistical significance of the NH winter QBO signal has been addressed by several authors and was treated in detail by *Baldwin and O'Sullivan* [1995]. The details of such an analysis (definition of the QBO, selection of winter months, level of data) are critical to the outcome of statistical tests. For example, the effect of the QBO is observed to be large in December and January but weaker in February. Using 1964–1993 NCEP data for December–January–February at levels up to 10 hPa, they showed that the effect of the QBO (defined by the 40-hPa Singapore wind) is statistically significant at the 0.001 level using 10-hPa geopotential, as measured by the field significance test of *Barnston and Livezey* [1987]. In zonal-mean wind composites the statistical significance of the effect of the QBO increases with height, at least through 10 hPa, with much higher significance at 10 hPa than at 30 hPa.

The NH dipole pattern illustrated in Figure 14 is not unique to the influence of the QBO; it represents the leading mode of variability of the northern winter stratosphere [*Nigam*, 1990; *Dunkerton and Baldwin*, 1992]. During winter the QBO appears to excite the "northern annular mode" (NAM) (also called the Arctic Oscillation) [*Thompson and Wallace*, 1998, 2000]. NH QBO composites (of geopotential, wind, temperature, etc.) tend to reflect the degree to which the QBO excites the NAM. One phase of the NAM is represented by a cold, strong vortex, while the opposite phase is represented by

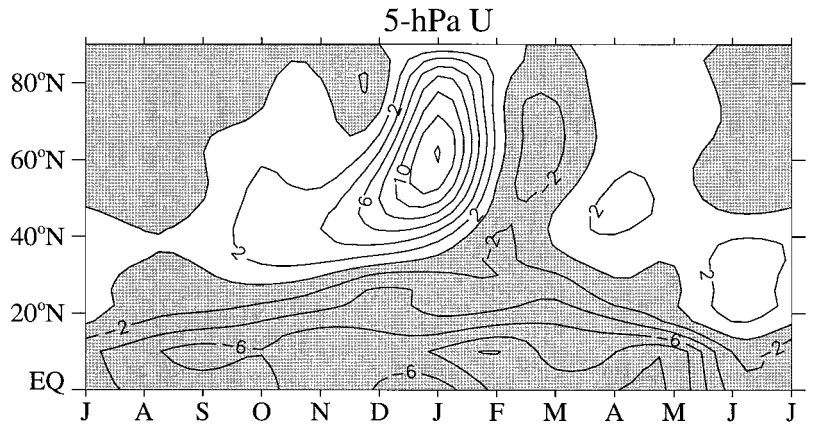

Figure 15. NH 5-hPa month-latitude zonal-mean wind difference between the average of all years with westerly QBO and those with easterly QBO, during 1964–1996. The phase of the QBO is defined as in Figure 14, and the data are monthly means. The contour interval is 2 m s^{-1}, and negative values are shaded. From *Baldwin and Dunkerton* [1998b].

a weaker vortex and higher polar temperatures. The dipole in Figure 14 is much more prominent in the stratosphere and weaker in the troposphere. The connection to the stratosphere is limited to the winter season, but the tropospheric NAM is observed during all seasons. The tropospheric aspects of the NAM and the tropospheric patterns associated with the QBO will be discussed in section 6.2.

Figure 15 illustrates the 5-hPa seasonal development of the NH zonal wind composite difference. The extratropical signal begins during autumn in midlatitudes and reaches a high-latitude maximum during January. The late winter (February and March) composite difference is opposite in sign, but small, north of 40°. The abrupt diminution of the signal indicates that the QBO modulates the strength of the northern winter polar vortex until midwinter but has little effect on the timing of the final warming.

Major stratospheric warmings are defined as a reversal of the zonal-mean wind at 10 hPa, 60°N to easterly, and higher temperature at the pole than the zonal average at 10 hPa, 60°N. The Holton-Tan effect implies that major warmings should be more common when the QBO is easterly. Unfortunately, such a simple measure is not robust because the definitions of both QBO phase (east/west) and warming (yes/no) are arbitrary. Using NCEP reanalyzed data from 1958–1999, and a 40-hPa definition of the QBO phase, there were six westerly warmings and 10 easterly warmings. However, if the "Berlin" hand-analyzed data are used with a 45-hPa definition of the QBO, and major warmings are defined synoptically, there were 10 westerly warmings and 11 easterly warmings (K. Labitzke, personal communication, 2000). The disparity between these results illustrates that this procedure is too sensitive to the definitions of QBO phase and warmings. Composites, as in Figures 14 and 15, are more robust, can be used in both hemispheres, and provide a quantitative measure of the Holton-Tan effect.

The SH polar vortex is much stronger, longer-lived, and more quiescent than its NH counterpart. During winter, planetary waves generally do not disrupt the southern vortex in the lower to middle stratosphere. It is not surprising that the observations indicate that the QBO does not significantly modulate the strength of the Antarctic vortex in winter. As shown in Figure 16, at 5 hPa the QBO modulates the strength of winds in midlatitudes during late autumn, as in the NH. However, unlike the NH, throughout winter and early spring the modulation is apparent only in midlatitudes. The observed seasonality of the QBO modulation of the extratropical circulation in both hemispheres is consistent with the hypothesis that planetary waves play a vital role in the mechanism for the modulation. The striking difference between Figures 15 and 16 is that in the SH, the largest influence of the QBO occurs during late spring (November), at the time of the final warming. In the SH the October vortex is of the same magnitude as the NH vortex in January. Since planetary wave amplitudes are much smaller in the SH, the effect of the QBO is seen only at the vortex periphery until the vortex is relatively small.

4.3. Model Simulations of Extratropical Influence

It is difficult to formulate a simple quantitative model for the mechanism of the extratropical QBO (analogous, say, to the Holton-Lindzen model [*Holton and Lindzen*, 1972] for interaction of the equatorial mean flow with vertically propagating waves). The main complications are (1) the planetary waves propagate both vertically and meridionally, and (2) the effects of critical lines on planetary wave propagation are not easy to predict theoretically. Lacking a simple theory, the effects of the QBO on extratropical waves and mean circulation have been studied extensively in detailed numerical simulation experiments with models of varying complexity.

The effect of the QBO on sudden warmings was

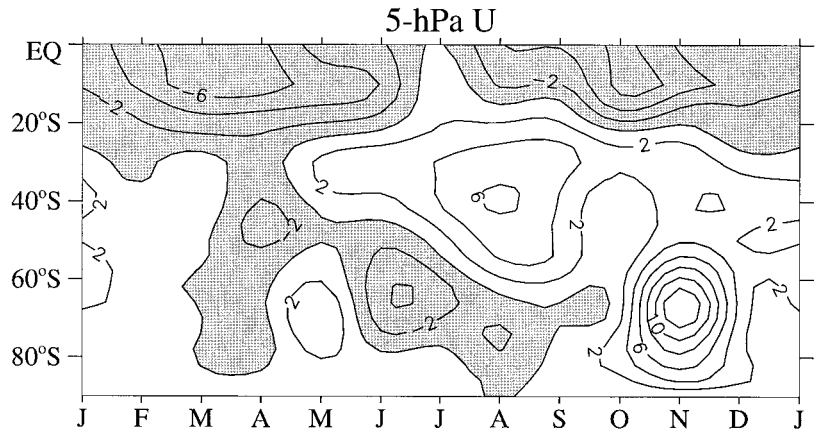

Figure 16. Southern Hemisphere (SH) 5-hPa month-latitude zonal-mean wind difference between the average of all years with westerly QBO and those with easterly QBO. The calculation is as in Figure 15, except that the phase of the QBO is optimized for the SH, which is nearly equivalent to using 25-hPa equatorial winds. From *Baldwin and Dunkerton* [1998b].

investigated in numerical experiments by *Dameris and Ebel* [1990] and *Holton and Austin* [1991]. Both studies used fairly short integrations of 3-D mechanistic models forced by idealized, rapidly growing midlatitude perturbations on a tropopause lower boundary. They found that the development of the high-latitude stratospheric flow can be strongly influenced by the tropical winds in the lower stratosphere, although this effect depends on the strength of the imposed wave forcing. Holton and Austin found that for weak wave forcing the high-latitude flow was largely unaffected by the tropical winds, but that this sensitivity increased as the strength of the wave forcing was raised. Within some range of the amplitude of the forcing, the model developed a sudden warming when there were easterly winds in the tropical stratospheric initial conditions but not when there were westerly winds. As the wave forcing was increased further, sudden warmings occurred regardless of the state of the tropical winds, and the sensitivity of the extratropical flow to tropical winds diminished.

Simplified model studies have the advantage of allowing the relevant parameters (notably the strength of the wave forcing from the troposphere) to be varied in a controlled manner. *O'Sullivan and Salby* [1990] and *Chen* [1996] used models with rather fine horizontal resolution but limited to a single layer in the vertical. Their experiments were run with simple linear relaxation of the zonal-mean state in order to simulate the effects of radiative transfer in constraining the mean flow and included an imposed wave-1 lower boundary forcing in the winter extratropics. The results showed that the models simulated high-latitude effects of the tropical QBO in the same sense as observed. *O'Sullivan and Young* [1992] and *O'Sullivan and Dunkerton* [1994] used a global 3-D mechanistic model forced with a specified wave-1 perturbation at the 10-km lower boundary. Radiative effects were parameterized with a linear relaxation of temperature to an imposed radiative state. Their simulations also included a seasonal cycle. Experiments were repeated with a range of amplitudes of the extratropical wave forcing, for initial conditions in the tropics representative of easterly and westerly QBO phases. The flow in the NH polar region in these simulations was found to be nearly unaffected by the tropical wind through November. In December, January, and February, however, there was a significant effect, with the time-mean polar vortex in the stratosphere being stronger when the tropical winds were westerly. The contrast in the winter-mean stratospheric polar vortex strength between easterly and westerly QBO phases depended strikingly on the amplitude of the wave forcing adopted. The modeling results of *O'Sullivan and Dunkerton* [1994] were broadly similar to the observations shown in Figures 15 and 16.

In a GCM the tropospheric forcing of the stratosphere (and its interannual variation) is generated self-consistently within the model. *Hamilton* [1998b] used a GCM run for a continuous 48-year period with a time-varying tropical momentum forcing that produced a 27-month QBO in the equatorial zonal wind with shear zones of realistic magnitude and descending at a realistic speed. Figure 17 shows the January composite zonal mean wind for 20 years with westerly 40-hPa equatorial winds minus that for 20 years with easterly 40-hPa winds. The results show the tendency for a weaker polar vortex in the easterly QBO phase. Outside the tropics the general features of the composite difference in Figure 17 compare well with the observed January composite shown as Figure 14. Figure 18 shows the easterly and westerly phase composite 28-hPa North Pole temperature for each month from October through April in the model integration. The systematic effects of the tropical QBO on NH polar stratospheric temperature in the model seem to be largely confined to the period December through March. The midwinter differences in Figure 18 are ~4°–5°C, which are comparable to those seen in

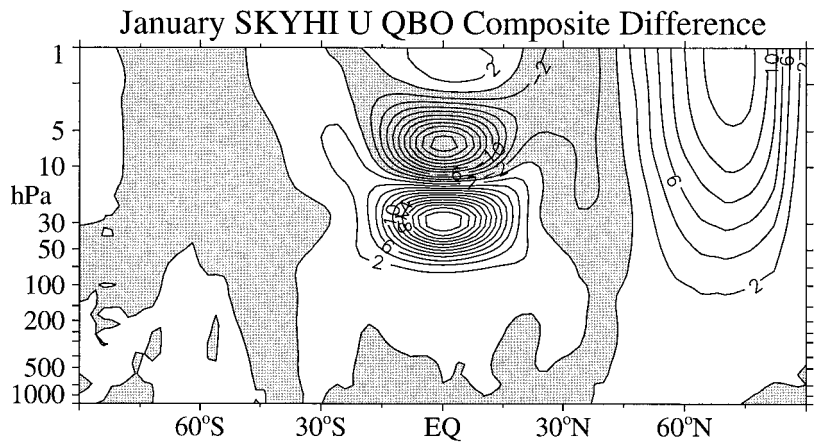

Figure 17. Westerly minus easterly phase composite of the zonal-mean zonal wind in January from the 48-year general circulation model (GCM) integration described by *Hamilton* [1998b]. The composite was based on the 20 Januarys with most westerly equatorial 40-hPa winds and the 20 Januarys with most easterly equatorial 40-hPa winds. Results are shown here to 1 hPa, but the model domain actually extends to 0.01 hPa.

the observed easterly minus westerly phase composite of *Dunkerton and Baldwin* [1991].

Niwano and Takahashi [1998] investigated the stratospheric extratropical variability in a version of the Japanese Center for Climate System Research model, which spontaneously produces a QBO-like oscillation in the tropics with a period of about 1.4 years. They analyzed a 14-year integration and calculated January–March composites based on the five most easterly and five most westerly QBO phases as judged by the equatorial zonal wind averaged between 7 and 50 hPa. The results show that, on average, the NH polar vortex was weaker in the easterly QBO phase, by ~15 m s^{-1}, near 70°N at 1 hPa.

In summary, a wide range of models has been used to study the influence of the QBO on the extratropical stratosphere. Thus far most studies have focused on the NH in late autumn through early spring, since this is the period when observations indicate the strongest influence. The published model studies are unanimous in showing at least some tendency for the strength of the polar vortex through the stratosphere to be positively correlated with the equatorial zonal wind near 40 hPa. These model results thus lend credence to the reality of the Holton-Tan effect. All the model studies are idealized to one degree or another, but the one that is most complete (and hence bears detailed comparison with

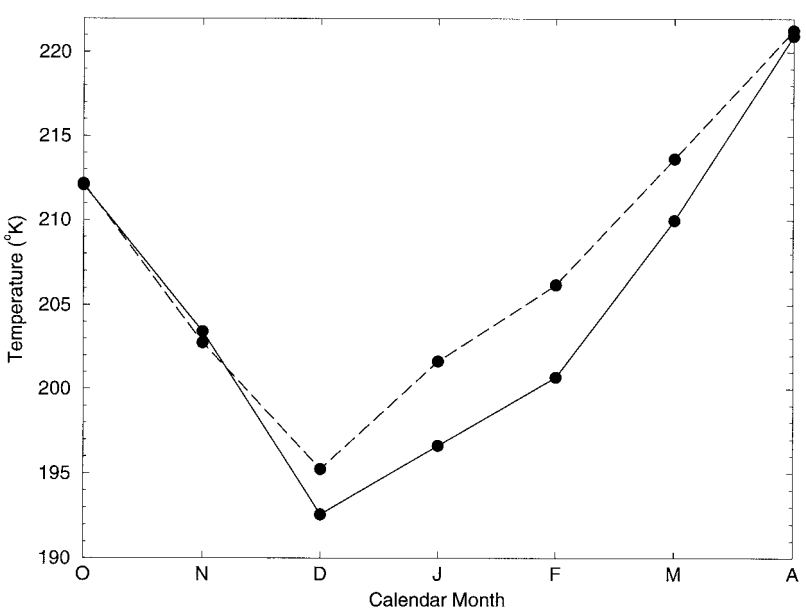

Figure 18. Average North Pole 28-hPa temperatures for each month from October through April in the 48-year GCM experiment of *Hamilton* [1998b] composited by QBO phase. Results are shown averaged over the 20 years with most easterly (dashed curve) 40-hPa equatorial winds (for the December–February period) and for the 20 years with most westerly equatorial 40-hPa winds (solid curve).

observations) is that of *Hamilton* [1998b]. The results from this study are generally in reasonable agreement with available observations, suggesting that even GCMs with an artificially imposed, but not explicitly simulated, QBO can have a realistic representation of the wave-modulated interactions between the low- and high-latitude stratosphere.

4.4. Interaction of the QBO With Other Low-Frequency Signals

The extratropical QBO signal may be identified statistically in a long data record, but it is only part of the large interannual variability of the northern winter stratosphere. Several other signals contribute to variability or interact with the QBO signal to produce other frequencies of variability in the observed data record. *Baldwin and Tung* [1994] showed that the QBO modulates the extratropical annual cycle signal so that the signature of the QBO in angular momentum, rather than having only a single spectral frequency peak at ~28 months, includes two additional spectral peaks at the annual frequency plus or minus the QBO frequency. These studies demonstrated that the "three-peak QBO" spectrum [*Tung and Yang*, 1994a] can be expected from the Holton-Tan effect acting to modulate the annual cycle. Tung and Yang considered a harmonic with the period of the QBO that acts to modulate a signal consisting of an annual mean plus a sinusoid with an annual period. The combined signal of the QBO in the extratropics together with the annual cycle can be represented mathematically as

$$(A + B \sin \Omega_{12} t) \times \sin \Omega_{\mathrm{QBO}} t \cong A \sin \Omega_{\mathrm{QBO}} t + B/2 \cos (\Omega_{12} - \Omega_{\mathrm{QBO}}) t - B/2 \cos (\Omega_{12} + \Omega_{\mathrm{QBO}}) t,$$

where Ω_{12} and Ω_{QBO} denote the annual and tropical QBO frequencies, respectively. With a QBO period of 30 months (the average QBO period during 1979–1992, used by Tung and Yang) the last two terms of the above equation represent variations with periods of 20 and 8.6 months. The 30-, 20-, and 8.6-month spectral peaks were found in ozone [*Tung and Yang*, 1994a, 1994b], angular momentum and Eliassen-Palm flux [*Baldwin and Tung*, 1994], and isentropic potential vorticity [*Baldwin and Dunkerton*, 1998a].

Studies using time series of stratospheric temperatures [e.g., *Salby et al.*, 1997] suggest that low-frequency variability of the middle and upper stratosphere includes a biennial mode with a period of exactly 24 months. Such a purely biennial signal cannot be the result of quasi-biennial forcing. Salby et al. as well as *Baldwin and Dunkerton* [1998a] speculated that a biennial mode might propagate into the stratosphere from the upper troposphere. It is unclear why a biennial mode, which may be found in the troposphere, would be amplified to become important in the polar stratosphere. Baldwin and Dunkerton could find no explanation for such a biennial mode and noted that the statistical significance of the biennial spectral peak is not high; the mode may simply be an artifact of using a short (32-year) data record that happened to have biennial variability. They noted that the Holton-Tan mechanism would tend to make polar anomalies in potential vorticity (PV) change sign from year to year. This tendency, together with random chance, could account for the observed biennial mode. If this interpretation is correct, then the biennial mode, in all likelihood, will not continue.

Several researchers have considered that remote effects from El Niño–Southern Oscillation (ENSO) could influence the extratropical stratosphere. Such an influence could masquerade as a QBO signal, or at least be difficult to separate from a QBO signal. *Wallace and Chang* [1982] were unable to separate the effects of ENSO and the QBO on the tropical stratosphere in 21 winters of NH 30-hPa geopotential. *Van Loon and Labitzke* [1987] also found that the phases of the QBO and ENSO tended to coincide. By removing cold and warm ENSO years (keeping years only with weak ENSO anomalies), they displayed results similar to those of Holton and Tan. Subsequent observational studies [e.g., *Hamilton*, 1993; *Baldwin and O'Sullivan*, 1995] and modeling [*Hamilton*, 1995] show a consistent picture in which the influence of ENSO on the zonal-mean structure of the vortex is largely confined to the troposphere. In the lower stratosphere, ENSO appears to modulate the amplitudes of large-scale stationary waves.

Decadal variability, possibly related to the 11-year solar cycle, clearly exists in data records which began in the 1950s. *Labitzke* [1987] and *Labitzke and van Loon* [1988] studied the observed late-winter NH circulation classified by both the level of solar activity and the QBO phase. They found a strong relation to the solar cycle during late winter. *Naito and Hirota* [1997] confirmed this relationship and found that early winter is dominated by a robust QBO signal. Figure 19 summarizes the solar-QBO results as scatterplots of mean 30-hPa geopotential heights during January and February above the North Pole versus 10.7-cm solar radio flux (a proxy for the 11-year cycle in solar activity). The data set can be grouped into four categories based on the QBO phase and solar activity level. In years with low solar activity the polar winter vortex tends to be disturbed and weak when the QBO is easterly, but deeper and undisturbed when the QBO is westerly. In years with strong solar activity, however, westerly phases of the QBO are associated with disturbed winters, whereas easterly phases of the QBO are accompanied by deep and undisturbed polar vortices. Hence the QBO acts as predicted by *Holton and Tan* [1980] in years with low solar activity but appears to reverse its behavior during years with high solar activity. Only two cases do not fit this scheme: 1989 and 1997.

It is the subject of active debate whether or not decadal variability is caused by the 11-year solar cycle, but there is increasing evidence through modeling that the solar cycle has a significant influence on winds and

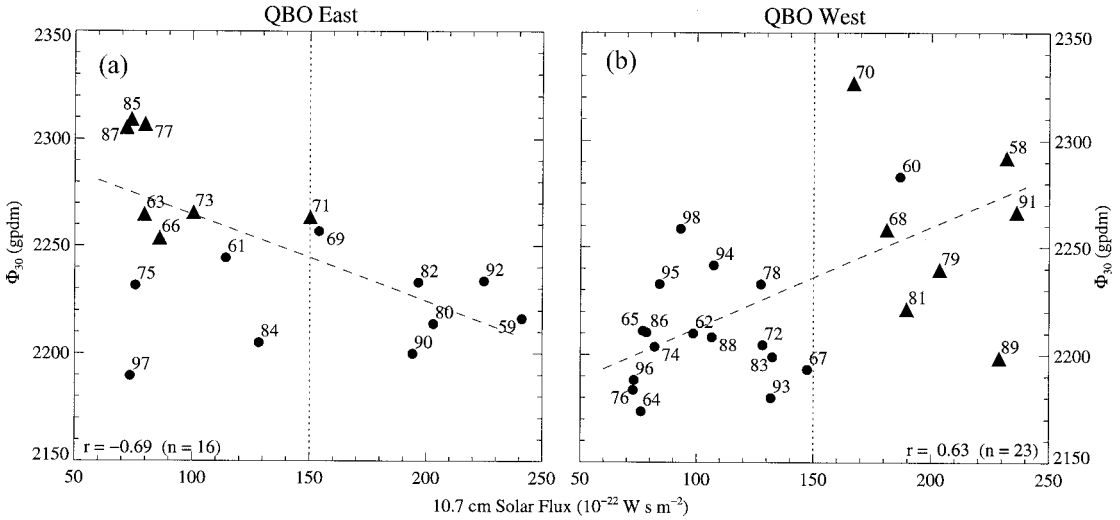

Figure 19. Scatterplots of mean January and February 30-hPa geopotential heights at the North Pole between 1958 and 1998 for years with (a) easterly tropical QBO and (b) westerly tropical QBO (after *van Loon and Labitzke* [1994], updated). Years during which major midwinter or final warmings occurred in January or February are denoted by triangles. Linear correlations are given in the lower left and right corner of each plot, and the linear fit through each of the data sets is denoted by the dashed lines. Two outliers (1989 and 1997) were not used in the statistical calculations.

temperatures in the upper stratosphere. Over the 11-year solar cycle, the solar "constant" (i.e., the radiative energy input into the Earth's atmosphere summed over the entire spectrum) varies by less than 0.1% [*Willson et al.*, 1986]. Variability in the UV responsible for most of ozone heating is less than 1% [*Rottman*, 1999]. The variability rises to 8% only at wavelengths shorter than 200 nm, but these wavelengths may affect indirectly the ozone chemistry through enhanced production of odd oxygen, which in turn could affect middle atmospheric heating rates and dynamics.

Following earlier solar cycle modeling [*Haigh*, 1994, 1996, 1999] and solar cycle–QBO modeling [*Rind and Balachandran*, 1995; *Balachandran and Rind*, 1995], *Shindell et al.* [1999] used a troposphere-stratosphere-mesosphere GCM with interactive ozone and realistic values of UV forcing to show that ozone changes amplify irradiance changes to affect climate. Circulation changes introduced in the stratosphere penetrated downward, even reaching the troposphere. The modeling studies found a more intense Hadley circulation during solar maximum conditions. They concluded that the observed record of geopotential height variations in the NH are, in part, driven by solar variability.

Figure 15 showed that the observed QBO modulation of zonal wind in the NH middle stratosphere is essentially over by February, and the observations show decadal variability coherent with the solar cycle during January and February. The possibility exists for the QBO to dominate early winter, while solar influence (or interaction between the QBO and the solar cycle) is manifest during late winter [*Dunkerton and Baldwin*, 1992]. Because of the strong absorption of ozone in the UV occurring in the upper stratosphere and mesosphere, a solar influence on the thermal structure in these regions of the atmosphere is plausible. This, in turn, might affect the strength of the planetary wave driven "extratropical pump" [*Holton et al.*, 1995]. A mechanism involving downward propagation of stratospheric anomalies, through modification of planetary wave propagation from below, is discussed in section 6.2.

Salby and Callaghan [2000] showed that the QBO westerlies below 30 hPa vary with the solar cycle, as do the easterlies above 30 hPa. Changes in the duration of westerly or easterly winds were found to introduce a systematic drift in the QBO phase during northern winter.

Various hypotheses have been proposed to explain the observed stratospheric decadal variability without reference to the solar cycle. These hypotheses rely on the QBO interacting with other signals. *Teitelbaum and Bauer* [1990] and *Salby and Shea* [1991] argued that the wintertime 11-year variability is a byproduct of the analysis procedure which involves the stratification of the data into years with respect to the QBO. *Gray and Dunkerton* [1990] showed the possibility of an 11-year cycle arising from the interaction of the QBO with the annual cycle. *Salby et al.* [1997] and *Baldwin and Dunkerton* [1998a] suggested that a modulation of the tropical QBO by a biennial extratropical signal (which exists but has not yet been explained) would result in a period of 11 years. These would provide an explanation of the 11-year variability without reference to the solar cycle, although the observed inphase relation to the solar cycle remains unexplained.

The observed biennial and decadal variability, and

uncertainty of its origin, does not overshadow the direct influence of the QBO on the extratropical stratosphere. The debate centers on the solar and biennial signals and whether or not the observed decadal variability could arise in the absence of solar influence.

5. EFFECTS OF THE QBO ON CHEMICAL CONSTITUENTS

5.1. Background

There is a substantial body of evidence for the influence of the QBO on chemical constituents in the atmosphere. Initial evidence came from ground-based observations of column ozone at two subtropical stations reported by *Funk and Garnham* [1962], which were shown by *Ramanathan* [1963] to be associated with the stratospheric wind oscillation. In an examination of historical ozone data, *Angell and Korshover* [1964] showed that a QBO signal is evident in Shanghai data (31°N) in the 1930s. Subsequent information about the temporal, latitudinal, and vertical structure of the ozone QBO has come primarily from satellite observations, due to their global nature and better temporal and spatial sampling. Although no single satellite has been operational for the whole period, the large-scale pattern and evolution of the ozone QBO, including its height structure, have been well characterized over this period, often with overlapping measurements from two or more instruments.

The first simulation of the ozone QBO was carried out by *Reed* [1964] using a simplified linearized model. However, it was not until 1986 that the QBO was studied in a full photochemical model. *Ling and London* [1986] included the QBO variation of zonal wind in a 1-D radiative-dynamical-photochemical model of the stratosphere. This was soon followed by a 2-D simulation [*Gray and Pyle*, 1989] including the latitudinal structure and interaction with the annual cycle and subsequently by 3-D simulations [*Hess and O'Sullivan*, 1995] which included a better representation of the wave-driven transport. Subsequent studies employing both 2-D and 3-D models have increased our understanding of the mechanisms of the ozone QBO, and these are described in more detail in the following sections.

In their 2-D QBO simulation, *Gray and Chipperfield* [1990] also noted QBOs in many of the other trace gases carried in the model, some of which were substantial. Some of these model predictions were confirmed by the subsequent analysis of Stratospheric Aerosol and Gas Experiment (SAGE) II NO_2 measurements [*Zawodny and McCormick*, 1991] and, more recently, by measurements of CH_4, H_2O, HF, HCl, and NO from the Halogen Occultation Experiment (HALOE) [*Luo et al.*, 1997; *Ruth et al.*, 1997; *Randel et al.*, 1998; *Dunkerton*, 2001]. Additionally, there is a well-documented QBO modulation of volcanic aerosol in the lower stratosphere [*Trepte and Hitchman*, 1992; *Hitchman et al.*, 1994; *Grant et al.*, 1996; *Choi et al.*, 1998].

5.2. Ozone: The Equatorial Anomaly

The close association of variations in equatorial column ozone with the zonal wind QBO is illustrated by Figure 20a, which shows a time series of solar backscattered ultraviolet (SBUV) and SBUV/2 equatorial ozone anomalies together with a reference QBO wind time series. The signal varies between ±10 Dobson units (DU), approximately ±4% of the background total column amount. The reference QBO wind time series was calculated by multiplying the observed equatorial stratospheric wind profile by the weighting profile shown in Figure 20b. The latter profile was derived empirically to optimize the fit to column ozone, neglecting volcanic periods. Note the excellent correspondence between the observed ozone anomaly and the reference wind series. Positive anomalies are present when the zonal winds in the lower stratosphere are westerly, while negative anomalies correspond to easterlies. The strongest correlations with column ozone are achieved with the weighting profile biased toward the winds around 20- to 30-hPa winds rather than the 40- to 50-hPa reference wind normally used in correlations with the extratropical zonal wind [*Dunkerton and Baldwin*, 1991].

The variable period of the equatorial ozone QBO is clearly evident in Figure 21, which shows a latitude-time section of the column ozone anomaly. Note that the equatorial QBO signal is not synchronized with the annual cycle since there is no apparent preferred season in which the anomalies change sign or reach their maximum amplitude.

A mechanism to explain the equatorial column ozone QBO anomaly was first suggested by *Reed* [1964]. The timing of the maximum westerly vertical wind shear at a particular level corresponds to the warmest phase of the temperature QBO on the equator. This phase is therefore the time of maximum diabatic cooling, which will induce relative sinking of air parcels through isentropic surfaces. This vertical motion occurs in a region of the atmosphere where the ozone mixing ratio increases with height and where the lifetime of ozone is rapidly changing. Below about 28 km the chemical lifetime is relatively long compared with dynamical processes and ozone may be regarded as a long-lived tracer. Above 28 km its chemical lifetime shortens considerably. The relative descent of air through this region produces an increase in the total column of ozone, since at levels above 28 km ozone is replaced by chemical production on relatively short timescales. Thus the maximum column ozone occurs when the column has been displaced farthest downward into the lower stratosphere. This will occur after the descent of westerly shear to the lowermost stratosphere, i.e., around the time of maximum westerlies at 20–30 hPa (Figure 21). The converse is true of an easterly shear situation. Mass continuity also requires there to be a return arm to this circulation in the subtropics with upwelling associated with westerly equatorial shear and downwelling associated with easterly equatorial shear.

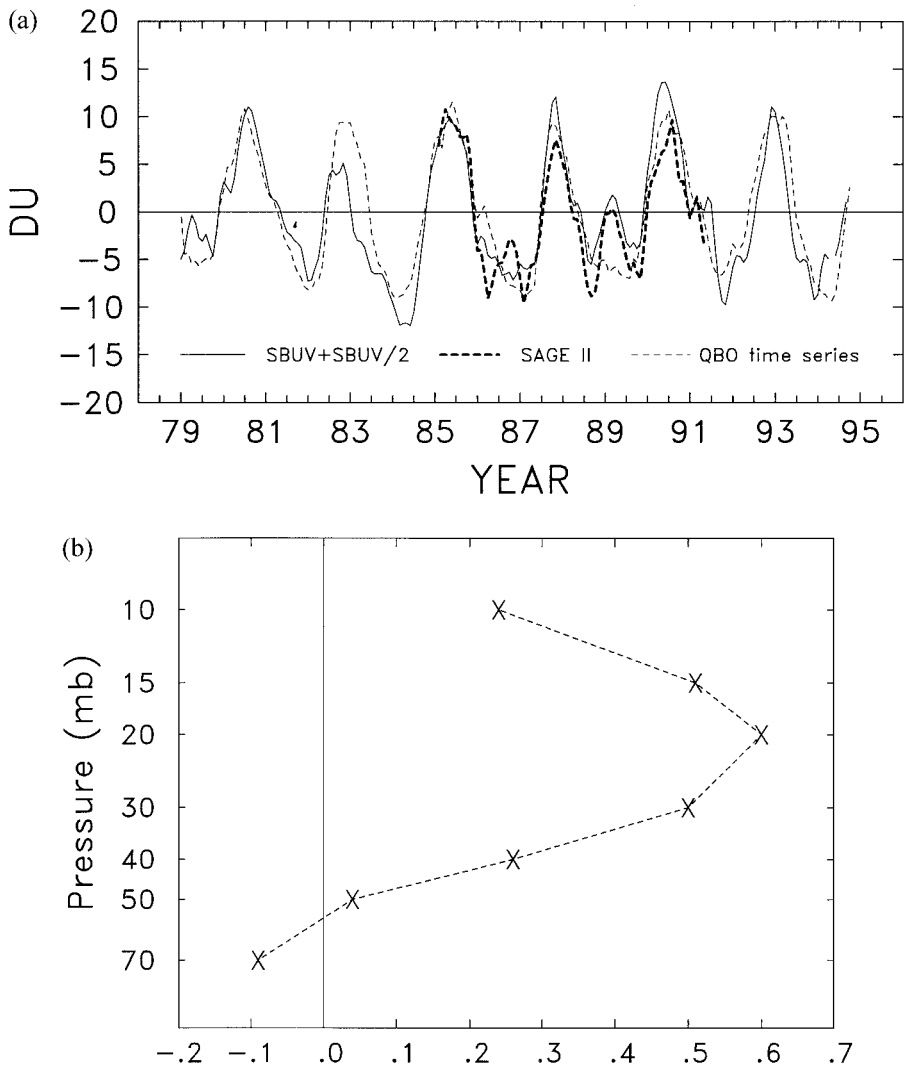

Figure 20. (a) Time series of equatorial ozone anomaly in Dobson units (DU, solid line) from solar backscattered ultraviolet (SBUV) and SBUV/2 together with a reference QBO wind time series (dotted curve) compiled by multiplying the observed winds at Singapore by the weighting profile shown in Figure 20b. Reprinted from *Randel and Wu* [1996] with permission from the American Meteorological Society.

While this conventionally accepted mechanism accounts for a large component of the variability, there are nevertheless additional important factors contributing to the column anomaly. Figure 22 shows a time-height cross section of the QBO ozone density anomaly (DU km^{-1}) from the SAGE II data set. A regression analysis has been applied in order to isolate the QBO variability. Ozone density can be used to visually determine contributions to the column ozone anomaly (simply a sum in the vertical of the ozone density anomalies). The QBO dominates the ozone variability at the equator, with alternating positive and negative anomalies which propagate downward with time [*Zawodny and McCormick*, 1991; *Hasebe*, 1994; *Randel and Wu*, 1996]. There are two regions of maximum ozone perturbation: in the lower stratosphere (20–27 km) and the middle stratosphere (30–37 km). The anomalies at these two levels are approximately a quarter cycle out of phase. There is therefore a small contribution to the column from the region above 28 km, which also influences the timing of the maximum column ozone anomaly. The equatorial QBO column ozone signal is simulated reasonably well by models [*Ling and London*, 1986; *Gray and Pyle*, 1989; *Tung and Yang*, 1994b; *Chipperfield and Gray*, 1992; *Chipperfield et al.*, 1994; *Kinnersley and Tung*, 1998; *Jones et al.*, 1998; *Hess and O'Sullivan*, 1995; *Nagashima et al.*, 1998] particularly when the observed winds are used to force a realistic zonal wind QBO period [*Gray and Ruth*, 1993] and when the effect of the ozone anomaly on heating rate is included [*Hasebe*, 1994; *Li et al.*, 1995; *Huang*, 1996].

The ozone QBO anomaly above 28 km has been shown to be controlled by changes in the photochemical sources and sinks of ozone, primarily via transport-induced variations of NO_y (the total reactive nitrogen reservoir) [*Chipperfield and Gray*, 1992; *Chipperfield et*

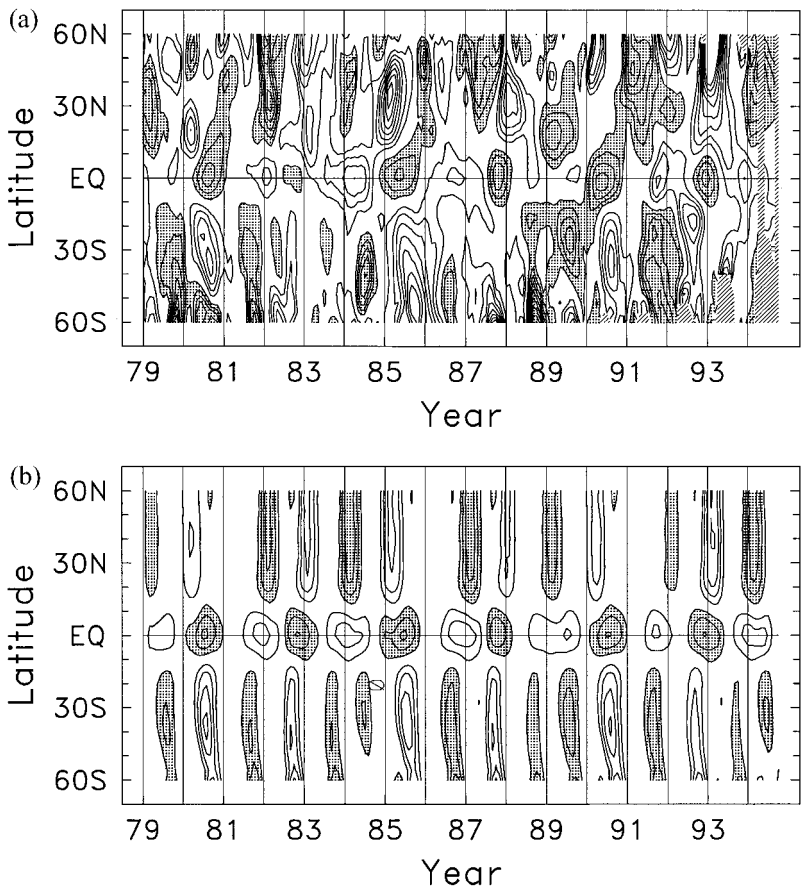

Figure 21. Latitude-time sections of column ozone anomalies from combined SBUV-SBUV/2 data: (a) full anomalies defined as deseasonalized and detrended over 1979–1994, and (b) the QBO component derived by seasonally varying regression analysis. Data in all panels were multiplied by cos (latitude) to account for area weighting. Contour interval is 3 DU, with 0 contours omitted and positive values shaded. Diagonal hatching denotes unreliable data. Vertical lines denote January of each year. Reprinted from *Randel and Wu* [1996] with permission from the American Meteorological Society.

al., 1994; *Politowicz and Hitchman*, 1997; *Jones et al*., 1998].

5.3. Ozone: Subtropical and Higher Latitudes

A QBO signal in the subtropics that extends to middle and high latitudes is clearly evident in Figure 21. There is a 180° phase change at around 15° in each hemisphere, with the higher-latitude anomaly extending to at least 60°N but with its maximum at approximately 30°–40° latitude. Broadly, this concurs with the presence of a return arm of the local equatorial QBO circulation described above, with ascent (descent) in the subtropics associated with westerly (easterly) equatorial shear. However, there are two significant departures from the signature expected from this simple explanation. First, the theoretical equatorial QBO circulation is confined to low latitudes and cannot explain the ozone QBO signal poleward of about 30°. Second, the timing of the subtropical anomalies is such that they are not symmetric about the equator. The subtropical and higher-latitude anomaly maxima and minima in the two hemispheres are approximately 6 months apart and coincide with the local late winter/spring. This timing is confirmed in Figure 23, in which we show a regression fit of the Total Ozone Mapping Spectrometer (TOMS) column ozone amounts to the 30-hPa Singapore winds [*Randel and Cobb*, 1994]. On average, the subtropical regression anomalies reach their maximum in March and August in the NH and SH, respectively. However, note from Figure 21b that occasionally there is a "missed" subtropical anomaly, for example, in 1981, 1986, and 1991 in the NH and in 1993 in the SH. There is therefore a change in the period of the column ozone QBO as one moves to higher latitudes [*Hilsenrath and Schlesinger*, 1981], with a phase relationship between the equatorial and subtropical anomalies that is constantly changing and is more complicated than a symmetric QBO circulation would imply.

The timing of the subtropical and high-latitude anomalies in late winter/spring suggests a modulation of the ozone QBO by the annual cycle [*Bowman*, 1989; *Hamilton*, 1989; *Lait et al*., 1989]. Early proposed mechanisms for the seasonal synchronization of the subtropical anomalies centered on a modulation of the low-latitude

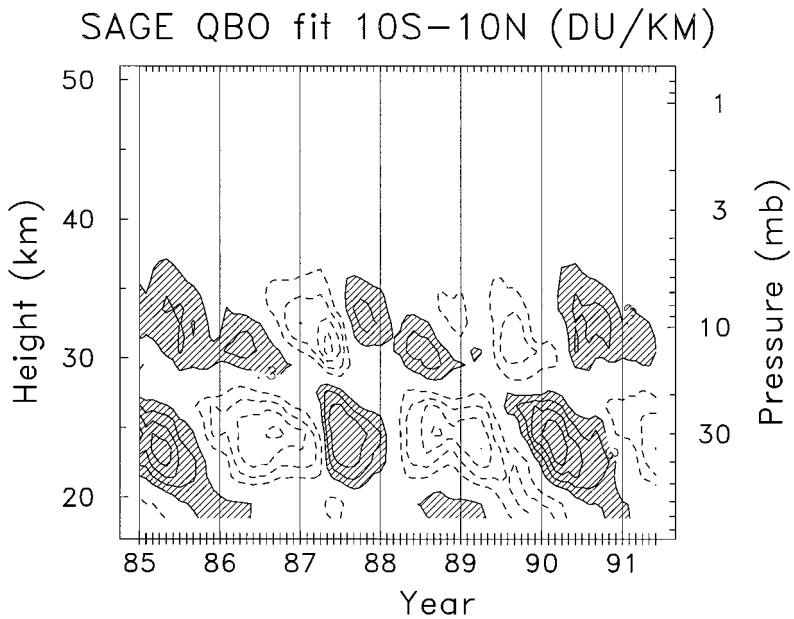

Figure 22. Height-time series of interannual anomalies in ozone density (DU km^{-1}) derived using a regression analysis to isolate the QBO variation. Contour intervals are 0.3 DU km^{-1}, with 0 contours omitted and positive values shaded. Reprinted from *Randel and Wu* [1996] with permission from the American Meteorological Society.

ozone anomalies once they had been produced by the classic symmetric QBO circulation. For example, *Holton* [1989] proposed that transport of the equatorial anomaly by the poleward winter circulation could explain the seasonality, while *Gray and Dunkerton* [1990] suggested that downwelling during winter would preserve the subtropical ozone anomaly while upwelling in summer would destroy it. On the other hand, *Hamilton* [1989] suggested the possibility of a modulation of the seasonally varying eddy transport of ozone into the subtropics. However, *Jones et al.* [1998] and *Kinnersley* [1999] have shown that there is a significant modulation of the mean meridional circulation induced by the QBO itself. This seasonal dependence of the circulation occurs primarily

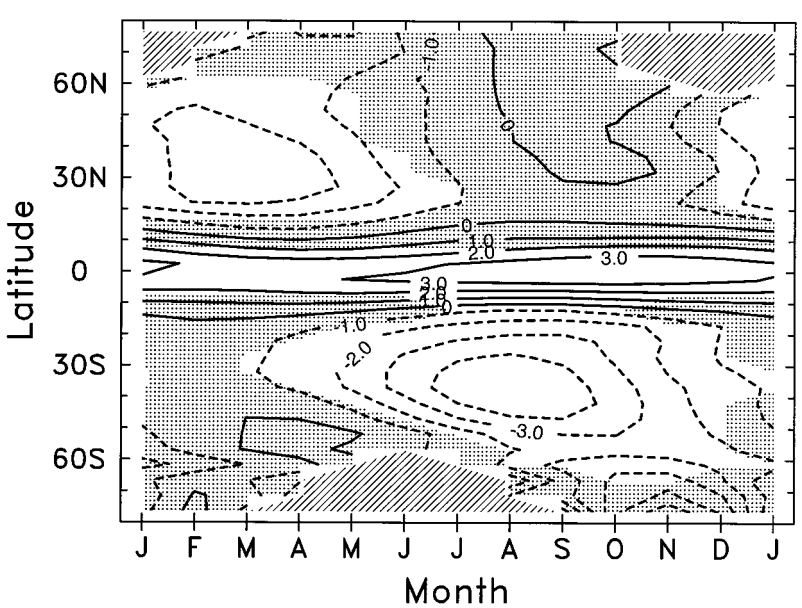

Figure 23. Latitude-time section of QBO-associated regression fit of zonal-mean Total Ozone Mapping Spectrometer (TOMS) column ozone (DU) to the 30-hPa Singapore winds for the period 1979–1994. Shading denotes regions where the statistical fits are not different from zero at the 2σ level. Hatched regions denote the polar night, where no ozone data are available. Updated from *Randel and Cobb* [1994].

because of nonlinear horizontal advection of zonal momentum in the tropics and subtropics by the mean meridional circulation, which is highly asymmetric during solstice periods. This results in a strongly asymmetric QBO circulation in which the winter hemisphere circulation is substantially reinforced and the summer hemisphere circulation is weakened (Plate 3). Thus the classic symmetric QBO circulation, first described by *Plumb and Bell* [1982a] and shown in Figure 13, may not be present except, perhaps, in the very low stratosphere where horizontal advection by the asymmetric mean circulation is thought to be weak and at equinox when the mean circulation is weakest. The asymmetry in subtropical ozone anomalies therefore arises primarily through its formation by an asymmetric QBO circulation rather than by the subsequent disruption of a symmetric ozone pattern.

The missed subtropical and midlatitude anomalies in 1981, 1986, and 1991 in the NH and in 1993 in the SH (Figure 21b) are thought to be due to the timing of the equatorial QBO relative to the annual cycle. The formation of a significant winter subtropical anomaly requires not only a strong vertical wind shear at the equator so that a strong QBO circulation is induced, but also the presence of strong background horizontal advection which will strengthen the winter side of the induced QBO circulation as described above. These conditions need to last for a month or two to allow the ozone distribution to respond to the induced circulation. If either of these requirements is not present for a sufficient length of time, a significant subtropical anomaly is unlikely to form in that year.

Similarly, if the timing and duration of the equatorial wind QBO is such that it persists in the same phase for two successive winters of either hemisphere, then two anomalies of the same sign will occur in successive winters in the subtropics of that hemisphere. The latter is evident in the SH in 1983–1984 and 1988–1989. This phenomenon can be thought of as a nonlinear interaction between the annual cycle and the QBO [*Gray and Dunkerton*, 1990], which results in a low-frequency modulation of the amplitude of the subtropical and midlatitude ozone anomaly on a timescale of ~5–13 years. Over the period of data used in Figure 23 this causes the SH regression anomaly to be coincidentally larger on average than the NH anomaly. Over a longer time span, both anomalies would presumably be of similar size.

A typical latitude-height cross section of the modeled QBO in ozone from the *Jones et al.* [1998] model is shown in Figure 24 for winter solstice in the NH with an eastward QBO wind maximum at about 26 km in the tropics. In both the tropics and subtropics the ozone QBO consists of two maxima centered in the lower and middle stratosphere with the tropical and subtropical anomalies approximately 180° out of phase, in agreement with observations. Also in agreement with observations, the modeled anomalies are large in the winter hemisphere and small in the summer hemisphere in both

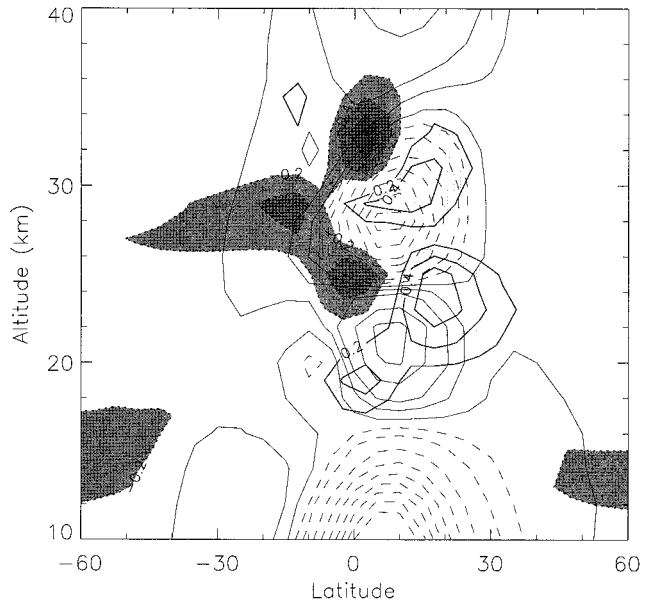

Figure 24. QBO anomaly in ozone (DU km^{-1}) in January from the 2-D model of *Jones et al.* [1998] together with the corresponding mass stream function. Contour intervals are 0.2 DU km^{-1}, with 0 contours omitted. Positive (negative) ozone anomaly values have lighter (darker) shading. Solid contours indicate positive stream function.

the photochemically and dynamically controlled regions. This is due to the asymmetry in the QBO-induced circulation, as illustrated by the corresponding mass stream function also shown in Figure 24. The asymmetric ozone anomaly arises directly through advection of ozone at the lower levels and indirectly though the advection of NO_y at the upper levels.

The *Jones et al.* [1998] model did not include extratropical influences such as the QBO modulation of planetary wave breaking. While it produces a good simulation in the tropics and subtropics, the modeled ozone anomalies do not extend as far poleward as suggested by observations. The upper level anomalies inferred from observations maximize between 10° and 40°, whereas those in the lower stratosphere extend to at least 60° [*Randel and Wu*, 1996]. The mechanism for the poleward extension of the dynamically controlled ozone anomaly is not well understood, although it likely involves an interaction between the planetary waves and the equatorial QBO. The modulation of planetary wave forcing by the equatorial wind QBO results in a stronger large-scale mean circulation in easterly phase years. Stronger downwelling in the winter midlatitudes will produce a relatively larger column ozone anomaly in easterly years than westerly years, as observed [*Tung and Yang*, 1994b]. On the other hand, the extension of the ozone anomalies to middle and high latitudes in the models of *Gray and Pyle* [1989] and *Kinnersley and Tung* [1998] is a result of the seasonally varying eddy transports in their models, which transfer the subtropical anomalies to higher latitudes. Figure 25 shows the correlation between the sim-

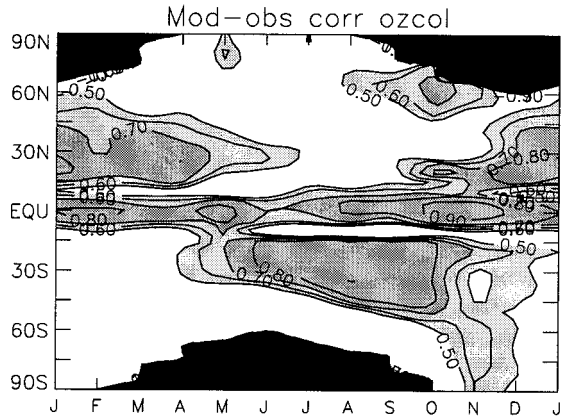

Figure 25. Correlation of detrended TOMS monthly-mean ozone column with the ozone column from the model of *Kinnersley and Tung* [1998], forced by the observed Singapore wind, covering the period November 1978 to April 1993 (contour interval is 0.1). Reprinted with permission from the American Meteorological Society.

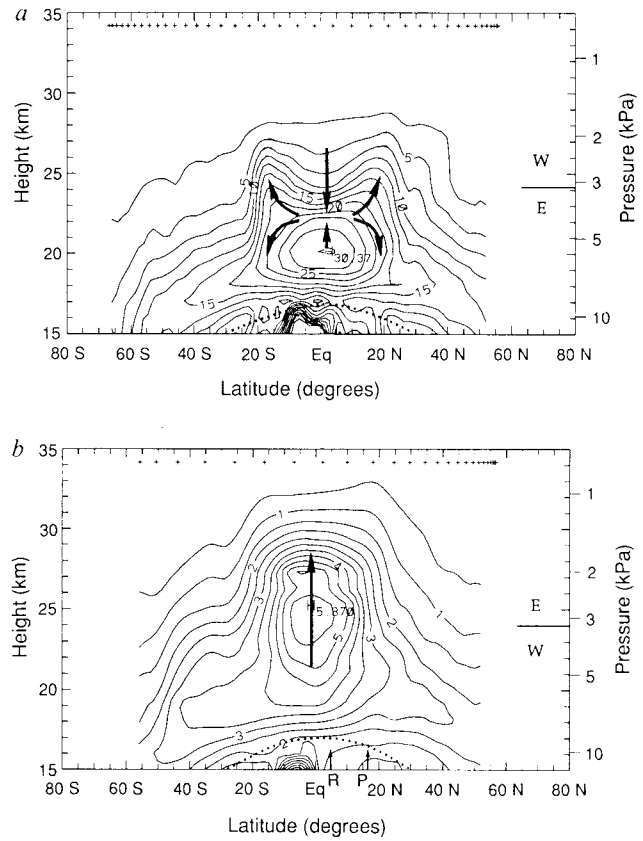

Figure 26. Latitude-height cross sections of observed aerosol extinction ratio for two 40-day periods representative of the two phases of the QBO. (a) Westerly shear phase centered on November 11, 1984 (contour interval is 2.5). (b) Easterly shear phase centered on October 4, 1988 (contour interval is 0.5). From *Trepte and Hitchman* [1992]. Reprinted with permission from *Nature*.

ulated ozone anomaly of *Kinnersley and Tung* [1998] and the observed anomaly between 1978 and 1993. At midlatitudes, therefore, a number of factors and feedback processes are found to contribute to the final ozone QBO, and the QBO may actually be responsible for a larger part of the observed ozone anomaly than a simple correlation with the wind QBO would suggest.

In addition to the QBO signals in the tropics and midlatitudes, analysis of TOMS data and other long-term records suggest an additional region of QBO influence in the winter polar regions [*Oltmans and London*, 1982; *Garcia and Solomon*, 1987; *Bowman*, 1989; *Lait et al.*, 1989; *Randel and Cobb*, 1994]. The polar ozone QBO is approximately in phase with midlatitudes and is seasonally synchronized in the same way, with maximum amplitude in springtime. Observational evidence for the polar ozone QBO is less statistically significant than that in the tropics or midlatitudes, partly due to the high level of interannual variability in the springtime vortex associated with planetary wave forcing from the troposphere [*Kinnersley and Tung*, 1998]. There is a suggestion of a feedback loop between the modulation of extratropical temperature by the QBO, the formation of polar stratospheric clouds and hence with the underlying chemical destruction that gives rise to the ozone hole [*Poole et al.*, 1989; *Mancini et al.*, 1991; *Butchart and Austin*, 1996].

5.4. QBO Anomalies in Other Trace Species

The QBO influences many other trace gases in the atmosphere, including methane, water vapor, volcanic aerosol, and shorter lived species such as NO_2 and N_2O_5. Volcanic aerosol distributions following major eruptions in equatorial latitudes illustrate the different circulation patterns associated with the two QBO phases, as shown in Figure 26, from *Trepte and Hitchman* [1992]. In a descending westerly phase (Figure 26a) the aerosol shows a distinctive "double peak" with relative maxima in the subtropics and a minimum at the equator in the region 20–50 hPa; the descending easterly phase (Figure 26b) has a single equatorial peak. The bold arrows indicate the approximate sense of induced QBO circulations. The near-symmetry of the double peak in the aerosol distribution, in contrast to the hemispheric asymmetry discussed in the previous section, is probably a consequence of these observations having been obtained near equinox, when the cross-equatorial flow is weak, and perhaps also due to the fact that the aerosol layer is located in the lower equatorial stratosphere, where the influence of the asymmetrical mean circulation is relatively small.

Figure 27 shows the interannual anomalies of H_2O at the equator, from HALOE observations [*Randel et al.*, 1998]. The QBO anomaly in H_2O ascends slowly with time, at approximately the rate of background mean upwelling, in contrast to the slow descent of the ozone anomaly. Outside of the equatorial lower and middle stratosphere, variations of H_2O anomaly mimic those observed in CH_4, but with opposite sign. In the upper

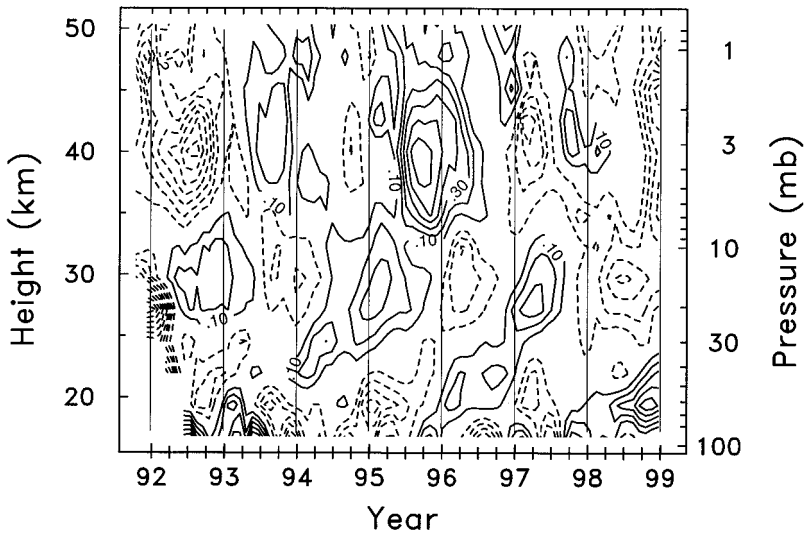

Figure 27. Time-height cross sections of interannual anomalies in H_2O over the equator from the Halogen Occultation Experiment (HALOE) instrument. The contour interval is 0.1 ppmv, with 0 contour omitted. Updated from *Randel et al*. [1998].

stratosphere (35–45 km) these anomalies are approximately in phase with QBO winds near 30 km. The CH_4 and H_2O variations over this region cancel to a large degree, such that there are much smaller variations of $H_2O + 2 \times CH_4$ (the variable part of total hydrogen). This cancellation confirms the production of water vapor via methane oxidation and is evidence that these stratospheric anomalies arise from variations in transport.

One region where large differences between CH_4 and H_2O anomalies are observed is in the tropical middle stratosphere, where H_2O and $H_2O + 2 \times CH_4$ show QBO variations over approximately 25–35 km, but none are observed for CH_4. These patterns are equatorially centered (~15°N–15°S) and are highly correlated with the QBO zonal wind near 20 hPa. One possible mechanism for the tropical H_2O signal is that QBO temperature variations modulate tropical tropopause temperatures [e.g., *Reid and Gage*, 1985] and hence the magnitude of water vapor entering the lower stratosphere [*Mote et al*., 1996]. However, the HALOE H_2O anomalies do not show strong coherence between 100- and 30-hPa levels in Figure 27, and the variations at the lowest levels do not exhibit a strong QBO behavior. The mechanism of the middle stratosphere QBO signal in H_2O awaits clarification.

Measurements of long-lived tracers also indicate the large effects of the QBO in midlatitudes. Figure 28 shows the January and April CH_4 distributions from HALOE in 1993 (westerly phase) and 1994 (easterly phase). In January 1994 the isolines form a distinctive "staircase" pattern between the tropics and NH midlatitudes that is very different from January 1993; this structure is also seen in Microwave Limb Sounder (MLS) and Cryogenic Limb Array Etalon Spectrometer (CLAES) data [*Dunkerton and O'Sullivan*, 1996; *O'Sullivan and Dunkerton*, 1997; *Gray and Russell*, 1999; *Gray*, 2000]. *Gray* [2000] has shown that this large asymmetry in QBO anomalies between the hemispheres in 1994 is consistent with the asymmetric QBO circulation of *Jones et al*. [1998] and *Kinnersley* [1999] discussed earlier. The detailed staircase pattern in Figure 28c nevertheless results from a complicated interaction of advection by the local QBO circulation and the effects of isentropic mixing at midlatitudes.

In April 1993 (Figure 28b) the distribution displays a distinct double-peak feature near 0.3–5 hPa, significantly higher than that displayed by the volcanic aerosol in Figure 26. This double peak results from vertical advection by the circulation associated with westerly shear of the semiannual oscillation (SAO) [*Gray and Pyle*, 1986; *Sassi and Garcia*, 1997]. The HALOE observations show a distinct QBO variation in the amplitude of this SAO double peak, with a prominent double peak in westerly phase years (Figure 28b) but a barely discernible one in easterly phase years (Figure 28d) [*Ruth et al*., 1997; *Randel et al*., 1998]. This observation is counterintuitive, since during an easterly QBO phase there is enhanced vertical propagation of eastward propagating waves and hence a stronger SAO westerly wind shear. However, in a 2-D modeling study, *Kennaugh et al*. [1997] showed that the enhanced eastward wave forcing also caused the westerly SAO phase to descend much more rapidly during an easterly QBO phase. Hence the SAO circulation that produces the double peak does not remain at any one level long enough for the tracers to respond to its presence.

In the January CH_4 distributions, there is also a distinct QBO signal in the steepness of the isolines in the subtropics around 30 hPa. In 1993 (Figure 28a) they slope gently from equator to midlatitudes, but in 1994

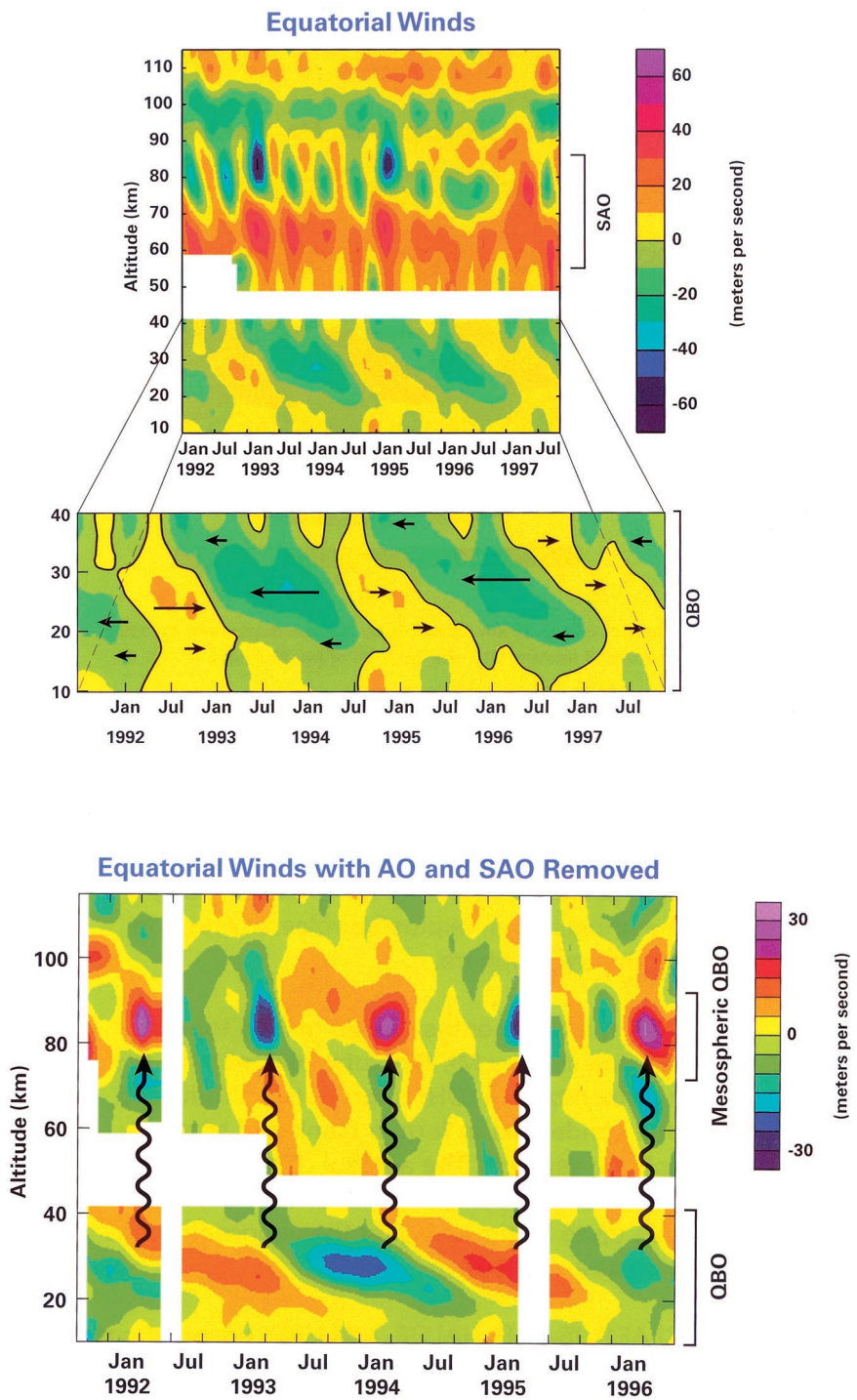

Plate 6. (top) High Resolution Doppler Imager (HRDI) measurements of the zonally averaged zonal wind in the tropical stratosphere and mesosphere from 1992 to 1998. The lower panel shows the QBO from 20 to 40 km as descending easterly (green to blue) and westerly (red to yellow) winds. In the lower mesosphere (60–80 km) the wind structure is dominated by the semiannual oscillation (SAO). (bottom) Removing the SAO and the annual oscillation (upper panel) shows that the influence of the QBO extends into the mesosphere (80 km). Mesospheric wind changes coincide with the change of the QBO winds near 30 km. This coupling between the mesosphere and the stratosphere is believed to be caused by small-scale upward propagating gravity waves, indicated by wavy arrows. From the UARS brochure, modified from the original provided by M. Burrage and D. Ortland. Courtesy M. Schoeberl.

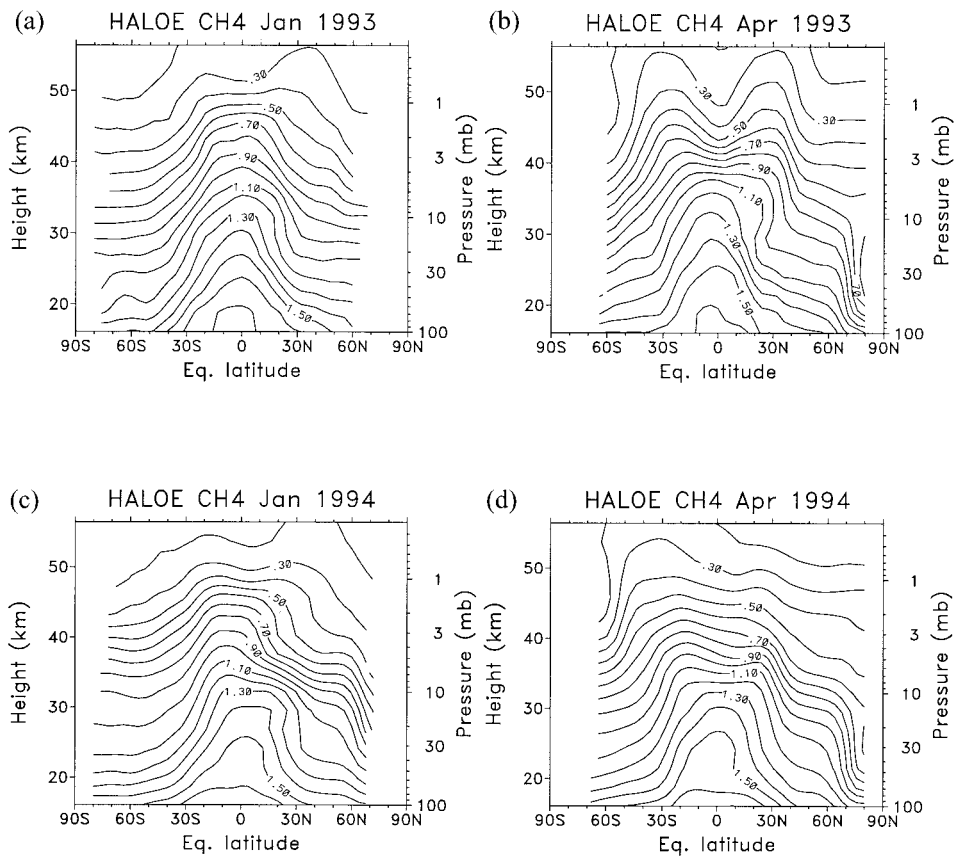

Figure 28. Height versus equivalent latitude cross sections of methane in January and April, 1993 and 1994, from HALOE observations. Contour interval is 0.1 ppbv.

(Figure 28c) the isolines are almost vertical [*Gray and Russell*, 1999]. This difference is not so apparent in the aerosol distributions of Figure 26, probably due to the unusual distribution of tracer gradients immediately after a volcanic eruption, but it is more apparent in composite aerosol measurements [*Hitchman et al.*, 1994]. Again, it is not clear whether this is due to advection by the QBO circulation or to the QBO's influence on the equatorward extent of Rossby-wave mixing and hence on the sharpness of PV and tracer gradients at the subtropical edge of the surf zone. Some studies suggested a sensitivity of isentropic mixing to the QBO [*Dunkerton and Baldwin*, 1991; *O'Sullivan and Young*, 1992; *O'Sullivan and Chen*, 1996; *O'Sullivan and Dunkerton*, 1997], and there is evidence of this in satellite measurements [*Grant et al.*, 1996]. On the other hand, *Waugh* [1996] used analyzed winds and contour advection techniques to make quantitative estimates of mixing in the subtropics, but found no sensitivity to the QBO, which may be due to a lack of reliable wind data in the subtropics. *Gray and Russell* [1999] noted that the stronger QBO signature is in the steepness of isolines and not in the isentropic gradients, which suggests that advection by the QBO circulation is important in setting up this feature. This inference is supported by the modeling of *Jones et al.* [1998] and *Kinnersley* [1999] which reproduces some aspects of this steepening using advective transport only.

The QBO anomalies in a shorter-lived species, NO_2, as measured by HALOE, are shown in Figure 29. The general pattern of anomalies in NO is similar to that of NO_2 and reflects QBO-induced changes in the abundance of NO_y in the stratosphere [*Gray and Chipperfield*, 1990; *Jones et al.*, 1998]. Anomalies of NO_y are produced through the influence of vertical advection on the vertical gradient in NO_y [*Chipperfield et al.*, 1994; *Politowicz and Hitchman*, 1997; *Jones et al.*, 1998]. Below about 5 hPa, the amplitude of the QBO in NO_2 is larger than in NO as a result of the influence of QBO temperature anomalies on the ratio of the abundance of NO to NO_2, through the reaction $NO + O_3 \rightarrow NO_2 + O_2$ [*Gray and Chipperfield*, 1990]. The reason for a large QBO signal in NO above 5 hPa has not yet been determined. However, it is likely due to the dominant contribution of NO to NO_y at these altitudes.

The pattern of QBO anomaly in HCl observed by HALOE (not shown) is similar to that of NO and NO_2. In their modeling study, *Gray and Chipperfield* [1990] found a similarity between the QBO anomalies of NO_y and Cl_y (the total inorganic chlorine reservoir). The anomalies were produced by vertical advection of the positive vertical gradients in Cl_y and NO_y in the lower and middle stratosphere. In the upper stratosphere, where the vertical gradient in Cl_y is weak, QBO anomalies in HCl are also weak, providing evidence for this mechanism.

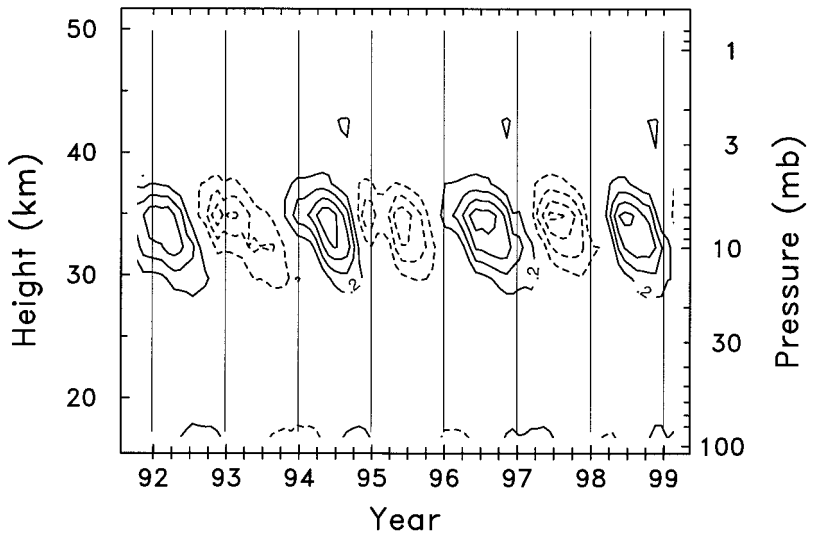

Figure 29. Height-time cross section of the QBO anomalies in NO_2 in the 10°S–10°N latitude band derived from HALOE sunset observations. The contour interval is 0.2 ppbv, with 0 contours omitted. These anomalies were derived from regression analyses, following *Randel and Wu* [1996].

6. THE QBO ABOVE AND BELOW THE STRATOSPHERE

6.1. Mesospheric QBO

Rawinsonde measurements of equatorial winds (to ~30 km, since the 1950s) and rocketsonde wind observations from stations near 8°S and 8°N (to ~60 km, since the 1960s) provide data only up to the lower mesosphere, as shown in Plate 1. Satellite measurements from the High Resolution Doppler Imager (HRDI) on the Upper Atmosphere Research Satellite (UARS), beginning in November 1991, provide equatorial wind data from 10–40 and 50–115 km. The HRDI data revealed a QBO in the upper mesosphere [*Burrage et al.*, 1996] called the MQBO. Monthly mean HRDI equatorial winds are shown in Plate 6 (top panel), confirming the QBO up to 40 km, and the mesospheric SAO from ~55–85 km. After removing the annual and semiannual harmonics, an MQBO centered near 85 km becomes apparent, as shown in the lower panel of Plate 6. The wind variations have been confirmed by radar observations at Christmas Island (2°N) during the HRDI period. The HRDI data show that the MQBO extends out to ±30° latitude, with a 180° phase difference relative to the stratospheric QBO at 40 hPa.

The HRDI record is too short to reliably confirm that the MQBO is linked to the stratospheric QBO. *Garcia et al.* [1997] suggested that the easterly phase of the mesospheric SAO is usually stronger only when deep westerlies are present in the stratospheric QBO. This relationship held during 1992–1995 in both satellite and radar data, but exceptions are found when the radar data from 1990–1991 are examined. Mesospheric westerlies do not show marked interannual variability, and they are not correlated with the QBO.

The possibility of a connection to the QBO is strengthened by modeling and theoretical evidence. *Mayr et al.* [1997] used a 2-D model to simulate oscillations in the equatorial stratosphere and mesosphere resulting from vertically propagating gravity waves. The modeled QBO was not confined to the stratosphere, but showed a QBO in the upper mesosphere, similar to that observed in HRDI data and Christmas Island radar data. The theoretical explanation involves selective critical-layer absorption or wave filtering of small-scale gravity waves as they traverse the underlying winds in the stratosphere, together with the complementary wave breaking at higher levels in the upper mesosphere. This process also generates the SAO in the upper mesosphere.

The amplitudes of the various equatorial oscillations in zonal wind, as a function of height, are summarized in Figure 30. The annual cycle (dotted curve) is relatively small in the stratosphere (~5 m s^{-1}). The stratospheric QBO is shown from 16 to 40 km, peaking near 20 m s^{-1} at about 25 km. The amplitude in the troposphere is negligible. The amplitude of the QBO between 40 and 70 km is not shown due to the uncertainty in defining what part of the variability is related to the QBO (see Plate 1).

6.2. Effect of the QBO on the Extratropical Troposphere

In section 4 it was shown that the QBO, by modulating the wave guide for vertically propagating planetary waves, affects the circulation of the extratropical winter stratosphere. This modulation is more easily seen in the NH, where wave amplitudes are larger and the stratospheric circulation is disrupted by major warmings. Figure 14 showed that modulation of the zonal wind by the QBO in the NH in January extends below the tropopause. *Angell and Korshover* [1975] showed a strong correlation between Balboa 50-hPa zonal wind and the

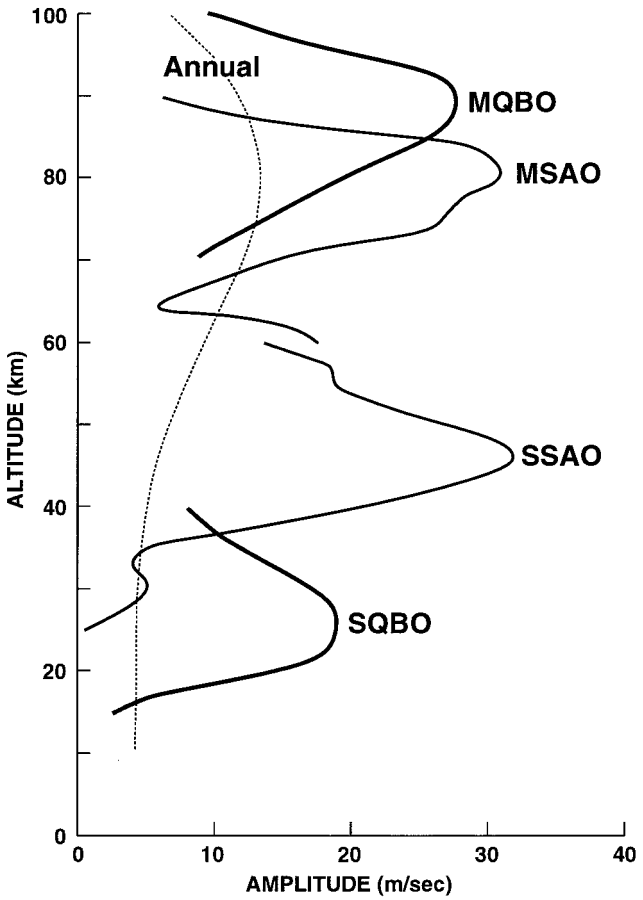

Figure 30. Vertical distribution of the amplitude of the MQBO, MSAO, SSAO, SQBO, and annual component at the equator. The MQBO is based on UARS/HRDI observations [*Burrage et al.*, 1996]. The SAO is based on rocket observations at Ascension Island [*Hirota*, 1978], and the annual component is after COSPAR International Reference Atmosphere (1986).

displacement of the northern vortex at 300 hPa, near the tropopause. The surface signature of the QBO was first examined by *Holton and Tan* [1980], who showed the difference between 1000-hPa geopotential for the two phases of the QBO. An update of Holton and Tan's calculation, for 1964–1996 data, is shown in Figure 31. The pattern is characterized by modulation of the strength of the polar vortex and anomalies of opposite sign at low to middle latitudes. The pattern in Figure 31 is similar to that shown by Holton and Tan. *Hamilton* [1998b], in a 48-year GCM simulation with an imposed QBO, found that the QBO composite difference in the strength of the upper tropospheric polar vortex, while small, was statistically significant.

There is increasing evidence from observations, numerical models, and conceptual models that stratospheric anomalies do indeed influence the troposphere. (It is not necessary to limit our discussion to the influence of the QBO, but to think of any circulation anomaly in the stratosphere: for example, due to solar influence, the QBO, a volcanic eruption, etc.) *Boville* [1984] showed, using a GCM, that a change in the high-latitude zonal wind structure in the stratosphere introduced changes in the zonal-mean flow down to the Earth's surface, as well as in planetary wave structures. He concluded that the degree of trapping of planetary waves in the troposphere is determined by the strength and structure of the stratospheric zonal-mean wind, resulting in sensitivity of the troposphere to the stratospheric zonal wind structure. *Boville* [1986] explained further that when high-latitude winds in the lower stratosphere are strong, they tend to inhibit vertical propagation of wave activity into the polar stratosphere. If winds are weak, on the other hand, wave activity can propagate more effectively into the polar stratosphere. The process was found to be tightly coupled to the tropospheric generation of vertically propagating planetary waves.

Kodera et al. [1990] used both observations and a GCM to show that anomalies in the midlatitude upper stratosphere (1 hPa) in December tend to move poleward and downward, reaching the troposphere approximately 2 months later. In general, these effects can be understood in terms of the modification of the zonal-mean zonal wind, which acts as a waveguide for planetary wave propagation. Stratospheric anomalies tend to induce changes in wave propagation at lower levels, which affect the convergence of the waves, which further modifies the zonal-mean flow. Over time, the net effect appears as a downward and poleward movement of anomalies.

A complementary approach to understanding the downward link to the troposphere has been to examine "modes of variability." Such modes may be thought of as patterns which tend to recur and which account for a large fraction of variance; patterns should be robust and be found through different analysis schemes. For example, the NH winter zonal wind tends to vary in a dipole pattern (Figure 14). This coupled mode of variability between the northern winter stratosphere and troposphere was discussed by *Nigam* [1990], who examined rotated EOFs of zonal-mean zonal wind. Nigam's result showed that the dominant mode of variability in zonal-mean wind appears as a deep north-south dipole with a node near 40°–45°N (similar to Figure 14). The poleward part of the dipole represents fluctuations in the strength of the polar vortex.

Coupling between the stratosphere and troposphere was further explored by *Baldwin et al.* [1994], who examined geopotential patterns in the middle troposphere linked to the stratosphere. Using singular value decomposition (also called maximum covariance analysis) between 500-hPa geopotential and zonal-mean wind, they showed that the leading mode had a strong dipole signature in zonal-mean wind, extending from the surface to above 10 hPa. The north-south dipole mode accounts for a large fraction of the variance in zonal wind and is found by a variety of techniques.

The leading mode of variability of the northern extratropical troposphere/stratosphere is characterized by

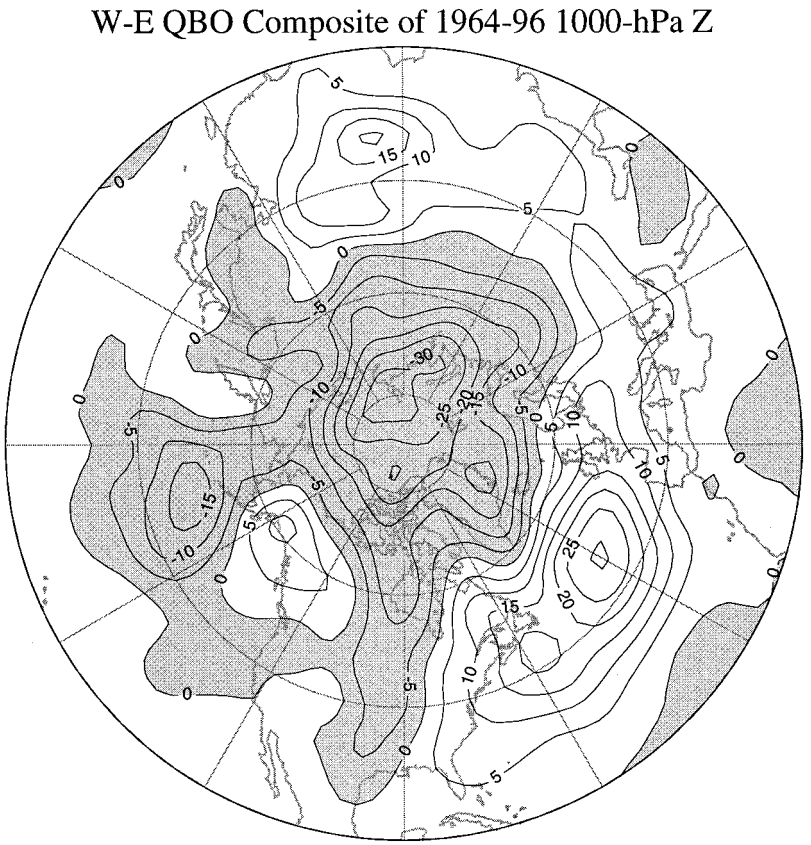

Figure 31. Difference in 1000-hPa geopotential height composites (meters) between westerly and easterly QBO composites. December–February monthly-mean National Centers for Environmental Prediction data for 1964–1996 were used.

a deep, zonally symmetric or "annular" structure [*Thompson and Wallace*, 2000]. This dipole mode in zonal-mean zonal wind is coupled to a horizontal wave structure of geopotential anomalies in the troposphere. The surface pattern resembles the North Atlantic Oscillation, but is more symmetric in longitude. *Thompson and Wallace* [1998] showed that the surface pattern corresponds to the leading EOF of wintertime monthly-mean sea level pressure. The mode, at any level, is known as the Northern Annular Mode (NAM). The surface NAM pattern is also known as the Arctic Oscillation [*Thompson and Wallace*, 1998] and is broadly similar to the QBO signature shown in Figure 31, suggesting that the QBO may act to modulate the NAM. It is now becoming clear that all studies of modes of NH variability produce patterns that are, in essence, slight variants of the NAM. The NAM represents a dominant, robust, naturally occurring mode of variability, and if the QBO can affect the NAM in the stratosphere, it can be expected that there would also be a surface signature of the QBO.

The NAM is closely linked to stratospheric sudden warmings [*Baldwin and Dunkerton*, 1999], and every major warming shows a clear signature in the magnitude of the stratospheric NAM. This relationship can be expected because both phenomena, in the stratosphere, relate to the strength of the polar vortex. As the strength of the stratospheric polar vortex changes, the surface NAM signature tends to vary. Baldwin and Dunkerton examined this relationship and demonstrated that large, sustained variations in the strength of the stratospheric polar vortex tend to propagate downward to the Earth's surface. The time to propagate from 10 hPa to the surface was found to vary, averaging about 3 weeks. They also examined the relationship between the QBO and the NAM, which was found to be strongest during December in the middle stratosphere and weaker as winter progressed. The QBO is one of several factors that influences the NAM, modulating the strength of the polar vortex from the lower mesosphere to the Earth's surface.

6.3. Effects of the QBO on the Tropical Troposphere

Because the QBO has its maximum amplitude over the equator, it is natural to inquire whether this oscillation has any effect on the underlying tropical troposphere. Here it is important to keep two things in mind. First, the zonal wind and temperature anomalies of the QBO do not penetrate significantly below the tropopause. The temperature QBO at the tropopause is small relative to the annual cycle. Second, it is known that the tropical troposphere has a quasi-biennial oscillation of

its own, uncorrelated with the stratospheric QBO [*Yasunari*, 1985; *Gutzler and Harrison*, 1987; *Kawamura*, 1988; *Lau and Sheu*, 1988; *Moron et al.*, 1995; *Shen and Lau*, 1995]. Unlike the stratospheric QBO, the "tropospheric QBO" is irregular in time, asymmetric in longitude, and propagates slowly eastward, with largest amplitude near Indonesia.

Although *Yasunari* [1989] suggested that the tropospheric oscillation is coherent with the stratospheric QBO, his results and those of other authors tend to disprove the claim. For example, the Hovmoller plot of biennially filtered upper tropospheric winds has an irregular variation in longitude and time, with two apparently distinct oscillations in the Pacific and Atlantic sectors, neither of which correlate well with the stratospheric QBO. The oscillation is a bit too fast over the Atlantic, and a bit too slow over the Pacific. On the basis of a longer record, some authors view the stratospheric and tropospheric QBOs as completely unrelated [*Barnett*, 1991; *Xu*, 1992]. As far as linear correlations are concerned, tropospheric and stratospheric QBOs do not exhibit a consistent phase relationship over several decades. Their morphologies are so different that it is difficult to see any obvious connection.

On the other hand, a more subtle relationship (either nonlinear or multivariate) might exist between these phenomena. There is evidence that ENSO warm events enhance the rate of QBO westerly descent [*Maruyama and Tsuneoka*, 1988]. This effect is dynamically plausible [*Dunkerton*, 1990; *Geller et al.*, 1997] but would not result in any linear correlation. Perhaps in a similar way, the stratospheric QBO influences the underlying troposphere, its effect mixed with that of other phenomena or occurring only at certain times and places.

The most promising connection between the stratospheric QBO and tropical troposphere is found in the interannual variation of Atlantic hurricane activity [*Gray*, 1984a, 1984b; *Shapiro*, 1989; *Hess and Elsner*, 1994; *Landsea et al.*, 1998; *Elsner et al.*, 1999]. Strong hurricanes originating in the tropical Atlantic occur significantly more often in seasons when the overlying QBO is westerly or becoming westerly near 50 hPa. The reverse is true in the opposite phase of the QBO. The stratospheric QBO remains one of several predictors of Atlantic hurricane activity in seasonal forecasts issued by W. Gray and collaborators at Colorado State University (http://typhoon.atmos.colostate.edu/forecasts/).

It is unclear whether the QBO has a similar influence on typhoons in the western Pacific [*Chan*, 1995; *Baik and Paek*, 1998; *Lander and Guard*, 1998]. The dynamics of hurricane formation are somewhat different in the two regions.

A convincing explanation of the QBO's effect on hurricane activity has not been given. Various authors have noted the effect of lower stratospheric vertical wind shear on penetrative convection associated with strong storms [*Gray et al.*, 1992a, 1992b], the effect on lower stratospheric static stability [*Knaff*, 1993], and the effect of QBO winds on the position of critical levels for tropical easterly waves [*Shapiro*, 1989]. Evidence supporting a role of the QBO in hurricane activity is derived from multiple regression in which the predictors are chosen subjectively from experience. The possibility that other forms of quasi-biennial variability might equally well explain the Atlantic hurricane connection has not been explored [*Shapiro*, 1989].

Other apparent effects of the QBO in the troposphere include the remarkable finding of *Chao* [1989] that the Earth's length of day has an interannual variation coherent with the stratospheric QBO's angular momentum. This result is consistent with the fact that atmospheric angular momentum is intimately connected to the rotation rate of the Earth. The connection between the stratosphere and solid Earth is unclear, however. In a similar vein, *Del Rio and Cazenave* [1994] discuss a possible effect on polar motion. *Fontaine et al.* [1995] found that contrasting precipitation regimes in west Africa are associated with the stratospheric QBO. *Collimore et al.* [1998] showed a correlation, although imperfect, between the QBO and deep convective activity in regions of strong convection. In the realm of much smaller signals, *Hamilton* [1983] found quasi-biennial variability in the amplitude of the semidiurnal surface pressure oscillation. These and other published and unpublished evidence of the QBO's effect on the tropical troposphere motivate further study and demonstrate that the stratospheric QBO should be properly simulated in models of the tropical atmosphere.

7. CONCLUSIONS

In a paper summarizing work on the then recently discovered QBO, *Reed* [1967, p. 393] stated

> Perhaps a simple explanation will soon be found, and what now seems an intriguing mystery will be relegated to the category of a meteorological freak. Or perhaps the phenomenon will prove to have a greater significance than we now might envisage, either because of some intrinsic property it possesses or because of its effect on other related areas of research.

With the benefit of more than 3 decades of QBO-related research, we can now say assuredly that the QBO is more than a meteorological "freak." Indeed, as demonstrated in this review, the QBO has a much larger role beyond that envisaged in the 1960s, both for its inherent fluid dynamical characteristics and its relevance to issues of global atmospheric chemistry and climate.

The QBO is a spectacular demonstration of the role of wave, mean-flow interactions in the fluid dynamics of a rotating stratified atmosphere. As elegantly argued by *McIntyre* [1993], what makes the dynamics of a rotating stratified atmosphere special is the ubiquitous occurrence of wave motions and the fact that wave propagation and refraction are generally accompanied by a transport of momentum. The QBO would not exist were it not for momentum transfer by wave propagation and

refraction. The dependence of wave refraction on the mean flow provides the mechanism whereby wave-induced momentum fluxes in the equatorial stratosphere can produce a feedback onto the mean flow. In the QBO, not only do the oscillating waves interact with the mean flow to produce a flow rectification, but also the rectified flow itself oscillates on a period completely different from that of the driving waves.

Plate 1 shows that the QBO (which in the 1960s was regarded by some as most likely a transient phenomenon) is a persistent feature of the circulation of the equatorial stratosphere. We have observed directly 20 full cycles of the oscillation, and there is indirect evidence covering a much longer time. By study of long-term variations in the solar semidiurnal tidal signal in surface pressure at equatorial stations (which is sensitive to the zonal winds in the stratosphere), *Hamilton* [1983] and *Teitelbaum et al*. [1995] argued that the QBO must have existed for at least the past 120 years.

This robust nature of the QBO suggests that similar phenomena should be present on other planets with rotating stratified atmospheres and equatorial convection zones. Indeed, an analogous oscillation, the quasi-quadrennial oscillation (QQO), has been documented in the equatorial atmosphere of Jupiter [*Leovy et al*., 1991; *Friedson*, 1999]. The observed meridional scale of the QQO on Jupiter ($\sim 7°$) is about half that of the terrestrial QBO. For the parameters given by Friedson, this is consistent with the transition scale discussed in section 3.1, provided that the vertical scale of forcing is set at 12 km, rather than the 4-km value appropriate for the terrestrial QBO. *McIntyre* [1994] suggested that a similar oscillation may occur in the solar interior.

The possibility of broader implications of the QBO for other areas of research, as suggested by *Reed* [1967] in the above quotation, has certainly proved to be true. As discussed in section 6.2, the influence of the QBO on interannual climate variations in the extratropical troposphere and stratosphere is a major subject of current interest. Attempts to better understand and predict trends and variability of atmospheric ozone require careful consideration of direct and indirect effects of the equatorial QBO on the ozone layer (see section 5). Thus models of interannual climate variability and of global stratospheric chemistry both should include the effects of the QBO either explicitly or through some parameterization.

Unfortunately, simulation of the QBO remains a great challenge for general circulation models. Such models are currently being used for prediction of climate trends and variability associated with human-induced changes in the concentrations of various greenhouse gases. Yet, as discussed in section 3.3.2, many models are unable to spontaneously generate a realistic QBO. The atmosphere, however, has no such difficulties. A skeptic might argue that the absence of such a robust global-scale dynamical phenomenon demonstrates that models are still far from reality. It would be more accurate to say that the QBO places stringent requirements on a numerical model, requiring an accurate computational method, fine spatial resolution, and low diffusion. The need for accurate parameterization of subgrid-scale momentum fluxes is also clear.

The arguments presented above suggest that gravity waves generated by equatorial convection are essential to forcing of the QBO. This implies that among other things, better modeling of the dynamics of mesoscale convective systems, and the synoptic-scale tropical waves in which these systems are embedded, is required if GCMs are to routinely reproduce the fascinating wave, mean-flow feedback interactions that result in the equatorial QBO.

GLOSSARY

β-plane: An approximation of the Coriolis parameter in which $f = f_0 + \beta y$, where beta is a constant. The Coriolis parameter is assumed to vary linearly in the north-south direction.

Boussinesq limit: A simplification in which density is treated as a constant except where it is coupled to gravity in the buoyancy term of the vertical momentum equation.

Coriolis parameter *f*: Equal to $2\Omega \sin \phi$, where Ω is the rotation rate of the Earth and ϕ is latitude.

Critical level or line: For a wave propagating on a background flow, the location at which the phase speed of the wave in the flow direction is equal to the flow speed. Waves tend to dissipate or break near such locations.

Easterly: From the east.

Eastward: To the east.

Eliassen-Palm (EP) flux: A measure of the propagation of wave activity in the latitude-height plane [*Eliassen and Palm*, 1961; *Edmon et al*., 1980]. The convergence of EP flux is a measure of the westward (or easterly) force exerted by the waves on the zonal-mean flow.

Gravity waves: Oscillations usually of high frequency and short horizontal scale, relative to synoptic-scale motions, that arise in a stably stratified fluid when parcels are displaced vertically.

Inertia-gravity waves: Low-frequency gravity waves that are substantially affected by the Coriolis force.

Kelvin waves: At the equator, eastward propagating waves with negligible meridional velocity component and Gaussian latitudinal structure in zonal velocity, geopotential, and temperature, symmetric about the equator.

Log-pressure height: A vertical coordinate proportional to the logarithm of pressure, approximately equal to physical height.

Meridional plane: The latitude-height plane. The mean meridional circulation is the zonally averaged circulation in the meridional plane.

Phase of the QBO: Easterly or westerly as defined by the equatorial winds at a specified level. Historically, the level has been chosen in the range 50–25 hPa.

Planetary-scale waves: Tropical or extratropical disturbances with low zonal wave number (1–3), for example, equatorial Kelvin waves, or Rossby waves in the winter stratosphere.

Planetary waves and planetary-wave breaking: Planetary waves are planetary-scale *Rossby waves*. In the wintertime stratosphere the polar vortex creates steep meridional gradients of PV, surrounded by weak gradients. Outside the vortex, there is overturning (in the latitudinal direction) of PV contours by Rossby waves as their amplitudes become large. This is a kind of "wave breaking," and the region where it takes place is therefore referred to as the stratospheric "surf zone." The wave breaking results in long, drawn-out tongues of PV and irreversible mixing of PV to small scales.

Rossby waves: A generic term for waves that owe their existence to latitudinal gradients of potential vorticity. Such gradients provide a restoring mechanism to allow propagation of the waves.

Rossby-gravity waves: Westward propagating waves with Gaussian latitudinal structure in meridional velocity symmetric about the equator. Zonal wind, temperature, and geopotential are antisymmetric.

Semiannual oscillation: Oscillation with a period of approximately 6 months.

Surf zone: See planetary-wave breaking.

Waveguide: A region in which waves propagate and are spatially confined by reflecting boundaries or internal turning points. The propagation of planetary waves is approximately analogous to the propagation of light through a medium with a variable index of refraction. For planetary Rossby waves the index of refraction depends on the zonally averaged zonal wind, and vertical propagation is allowed for waves propagating westward relative to the mean flow.

Westerly: From the west.

Westward: To the west.

Zonal: Longitudinal. By convention, the zonal wind is positive when it is from the west.

ACKNOWLEDGMENTS. This review was the outgrowth of a workshop held in March 1998 in La Jolla, California, sponsored by the World Climate Research Program (WCRP) Stratospheric Processes and Their Role in Climate (SPARC) Initiative and NASA's Atmospheric Chemistry Modeling and Analysis Program (ACMAP). We thank Sandy Grant and Susan Ball for preparing the manuscript and Michael McIntyre and Charles McLandress for comments. The NCEP/NCAR Reanalysis data were provided by the NOAA-CIRES Climate Diagnostics Center. The Singapore zonal wind data were provided by Barbara Naujokat (Free University Berlin). M.P.B. and T.J.D. were supported by the Climate Dynamics and Large-Scale Dynamic Meteorology Programs of the NSF, the NASA ACMAP and SR&T Programs, and the NOAA Office of Global Programs. M.J.A. was supported by NSF's Physical Meteorology Program. W.J.R. was supported by NCAR (sponsored by NSF) and NASA's ACMAP and UARS Programs.

Jim Smith was the Editor responsible for this paper. He and the authors thank two anonymous technical reviewers and one anonymous cross-disciplinary reviewer.

REFERENCES

Alexander, M. J., and J. R. Holton, A model study of zonal forcing in the equatorial stratosphere by convectively induced gravity waves, *J. Atmos. Sci.*, *54*, 408–419, 1997.

Alexander, M. J., and L. Pfister, Gravity wave momentum flux in the lower stratosphere over convection, *Geophys. Res. Lett.*, *22*, 2029–2032, 1995.

Alexander, M. J., J. R. Holton, and D. R. Durran, The gravity wave response above deep convection in a squall line simulation, *J. Atmos. Sci.*, *52*, 2212–2226, 1995.

Alexander, M. J., J. Beres, and L. Pfister, Tropical stratospheric gravity waves and cloud correlations, *J. Geophys. Res.*, *105*, 22,299–22,310, 2000.

Allen, S. J., and R. A. Vincent, Gravity wave activity in the lower atmosphere: Seasonal and latitudinal variations, *J. Geophys. Res.*, *100*, 1327–1350, 1995.

Andrews, D. G., and M. E. McIntyre, Planetary waves in horizontal and vertical shear: The generalized Eliassen-Palm relation and the mean zonal acceleration, *J. Atmos. Sci.*, *33*, 2031–2048, 1976.

Andrews, D. G., J. R. Holton, and C. B. Leovy, *Middle Atmosphere Dynamics*, 489 pp., Academic, San Diego, Calif., 1987.

Angell, J. K., and J. Korshover, Quasi-biennial variations in temperature, total ozone, and tropopause height, *J. Atmos. Sci.*, *21*, 479–492, 1964.

Angell, J. K., and J. Korshover, Evidence for a quasi-biennial variation in eccentricity of the North Polar vortex, *J. Atmos. Sci.*, *32*, 634–635, 1975.

Baik, J.-J., and J.-S. Paek, A climatology of sea surface temperature and the maximum intensity of western North Pacific tropical cyclones, *J. Meteorol. Soc. Jpn.*, *76*, 129–137, 1998.

Balachandran, N. K., and D. Rind, Modeling the effects of UV variability and the QBO on the troposphere-stratosphere system, part I, The middle atmosphere, *J. Clim.*, *8*, 2058–2079, 1995.

Baldwin, M. P., and T. J. Dunkerton, Quasi-biennial oscillation above 10 mbar, *Geophys. Res. Lett.*, *18*, 1205–1208, 1991.

Baldwin, M. P., and T. J. Dunkerton, Biennial, quasi-biennial, and decadal oscillations of potential vorticity in the northern stratosphere, *J. Geophys. Res.*, *103*, 3919–3928, 1998a.

Baldwin, M. P., and T. J. Dunkerton, Quasi-biennial modulations of the Southern Hemisphere stratospheric polar vortex, *Geophys. Res. Lett.*, *25*, 3343–3346, 1998b.

Baldwin, M. P., and T. J. Dunkerton, Propagation of the Arctic Oscillation from the stratosphere to the troposphere, *J. Geophys. Res.*, *104*, 30,937–30,946, 1999.

Baldwin, M. P., and D. O'Sullivan, Stratospheric effects of ENSO-related tropospheric circulation anomalies, *J. Clim.*, *4*, 649–667, 1995.

Baldwin, M. P., and K.-K. Tung, Extratropical QBO signals in angular momentum and wave forcing, *Geophys. Res. Lett.*, *21*, 2717–2720, 1994.

Baldwin, M. P., X. Cheng, and T. J. Dunkerton, Observed correlation between winter-mean tropospheric and stratospheric circulation anomalies, *Geophys. Res. Lett.*, *21*, 1140–1144, 1994.

Barnett, T. P., The interaction of multiple time scales in the tropical climate system, *J. Clim.*, *4*, 269–285, 1991.

Barnston, A. G., and R. E. Livezey, A closer look at the effect of the 11-year solar cycle and the QBO on the Northern

Hemisphere 700 mb height and extratropical North American surface temperature, *J. Clim.*, *2*, 1295–1313, 1987.

Belmont, A. D., and D. G. Dartt, Variation with longitude of the quasi-biennial oscillation, *Mon. Weather Rev.*, *96*, 767–777, 1968.

Bergman, J. W., and M. L. Salby, Equatorial wave activity derived from fluctuations in observed convection, *J. Atmos. Sci.*, *51*, 3791–3806, 1994.

Booker, J. R., and F. P. Bretherton, The critical layer for internal gravity waves in a shear flow, *J. Fluid Mech.*, *27*, 513–539, 1967.

Boville, B. A., The influence of the polar night jet on the tropospheric circulation in a GCM, *J. Atmos. Sci.*, *41*, 1132–1142, 1984.

Boville, B. A., Wave-mean flow interactions in a general circulation model of the troposphere and stratosphere, *J. Atmos. Sci.*, *43*, 1711–1725, 1986.

Boville, B. A., and W. J. Randel, Equatorial waves in a stratospheric GCM: Effects of vertical resolution, *J. Atmos. Sci.*, *49*, 785–801, 1992.

Bowman, K. P., Global patterns of the quasi-biennial oscillation in total ozone, *J. Atmos. Sci.*, *46*, 3328–3343, 1989.

Boyd, J. P., The effects of latitudinal shear on equatorial waves, part 1, Theory and methods, *J. Atmos. Sci.*, *35*, 2236–2258, 1978.

Bretherton, F. P., Momentum transport by gravity waves, *Q. J. R. Meteorol. Soc.*, *95*, 213–243, 1969.

Burrage, M. D., R. A. Vincent, H. G. Mayr, W. R. Skinner, N. F. Arnold, and P. B. Hays, Long-term variability of the equatorial middle atmosphere zonal wind, *J. Geophys. Res.*, *101*, 12,847–12,854, 1996.

Butchart, N., and J. Austin, On the relationship between the quasi-biennial oscillation, total chlorine and the severity of the Antarctic ozone hole, *Q. J. R. Meteorol. Soc.*, *122*, 183–217, 1996.

Cadet, D., and H. Teitelbaum, Observational evidence of internal inertia-gravity waves in the tropical stratosphere, *J. Atmos. Sci.*, *36*, 892–907, 1979.

Canziani, P. O., and J. R. Holton, Kelvin waves and the quasi-biennial oscillation: An observational analysis, *J. Geophys. Res.*, *103*, 31,509–31,521, 1998.

Canziani, P. O., J. R. Holton, E. Fishbein, and L. Froidevaux, Equatorial Kelvin wave variability during 1992 and 1993, *J. Geophys. Res.*, *100*, 5193–5202, 1995.

Chan, J. C. L., Tropical cyclone activity in the western North Pacific in relation to the stratospheric quasi-biennial oscillation, *Mon. Weather Rev.*, *123*, 2567–2571, 1995.

Chao, B. F., Length-of-day variations caused by El Niño–Southern Oscillation and quasi-biennial oscillation, *Science*, *243*, 923–926, 1989.

Charney, J. G., and P. G. Drazin, Propagation of planetary-scale disturbances from the lower into the upper atmosphere, *J. Geophys. Res.*, *66*, 83–109, 1961.

Chen, P., The influences of zonal flow on wave breaking and tropical-extratropical interaction in the lower stratosphere, *J. Atmos. Sci.*, *53*, 2379–2392, 1996.

Chipperfield, M. P., and L. J. Gray, Two-dimensional model studies of interannual variability of trace gases in the middle atmosphere, *J. Geophys. Res.*, *97*, 5963–5980, 1992.

Chipperfield, M. P., L. J. Gray, J. S. Kinnersley, and J. Zawodny, A two-dimensional model study of the QBO signal in SAGE II NO_2 and O_3, *Geophys. Res. Lett.*, *21*, 589–592, 1994.

Choi, W., W. B. Grant, J. H. Park, K.-M. Lee, H. Lee, and J. M. Russell III, Role of the quasi-biennial oscillation in the transport of aerosols from the tropical stratosphere reservoir to midlatitudes, *J. Geophys. Res.*, *103*, 6033–6042, 1998.

Collimore, C. C., M. H. Hitchman, and D. W. Martin, Is there a quasi-biennial oscillation in tropical deep convection?, *Geophys. Res. Lett.*, *25*, 333–336, 1998.

Cornish, C. R., and M. F. Larsen, A review of synoptic scale wave perturbations in the equatorial stratosphere, *J. Atmos. Terr. Phys.*, *47*, 769–780, 1985.

Dameris, M., and A. Ebel, The quasi-biennial oscillation and major stratospheric warmings: A three-dimensional model study, *Ann. Geophys.*, *8*, 79–85, 1990.

Del Rio, R. A., and A. Cazenave, Interannual variations in the Earth's polar motion for 1963–1991: Comparison with atmospheric angular momentum over 1980–1991, *Geophys. Res. Lett.*, *21*, 2361–2364, 1994.

Dunkerton, T. J., The evolution of latitudinal shear in Rossby-gravity wave, mean flow interaction, *J. Geophys. Res.*, *88*, 3836–3842, 1983a.

Dunkerton, T. J., Laterally-propagating Rossby waves in the easterly acceleration phase of the quasi-biennial oscillation, *Atmos. Ocean*, *21*, 55–68, 1983b.

Dunkerton, T. J., A two-dimensional model of the quasi-biennial oscillation, *J. Atmos. Sci.*, *42*, 1151–1160, 1985.

Dunkerton, T. J., Annual variation of deseasonalized mean flow acceleration in the equatorial lower stratosphere, *J. Meteorol. Soc. Jpn.*, *68*, 499–508, 1990.

Dunkerton, T. J., Nonlinear propagation of zonal winds in an atmosphere with Newtonian cooling and equatorial wavedriving, *J. Atmos. Sci.*, *48*, 236–263, 1991a.

Dunkerton, T. J., Intensity variation and coherence of 3- to 6-day equatorial waves, *Geophys. Res. Lett.*, *18*, 1469–1472, 1991b.

Dunkerton, T. J., Observation of 3–6 day meridional wind oscillations over the tropical Pacific, 1973–1992: Vertical structure and interannual variability, *J. Atmos. Sci.*, *50*, 3292–3307, 1993.

Dunkerton, T. J., Horizontal buoyancy flux of internal gravity waves in vertical shear, *J. Meteorol. Soc. Jpn.*, *73*, 747–755, 1995.

Dunkerton, T. J., The role of gravity waves in the quasi-biennial oscillation, *J. Geophys. Res.*, *102*, 26,053–26,076, 1997.

Dunkerton, T. J., Quasi-biennial and subbiennial variations of stratospheric trace constituents derived from HALOE observations, *J. Atmos. Sci.*, *58*, 7–25, 2001.

Dunkerton, T. J., and M. P. Baldwin, Quasi-biennial modulation of planetary-wave fluxes in the Northern Hemisphere winter, *J. Atmos. Sci.*, *48*, 1043–1061, 1991.

Dunkerton, T. J., and M. P. Baldwin, Modes of interannual variability in the stratosphere, *Geophys. Res. Lett.*, *19*, 49–51, 1992.

Dunkerton, T. J., and D. P. Delisi, Climatology of the equatorial lower stratosphere, *J. Atmos. Sci.*, *42*, 376–396, 1985.

Dunkerton, T. J., and D. J. O'Sullivan, Mixing zone in the tropical stratosphere above 10 mbar, *Geophys. Res. Lett.*, *23*, 2497–2500, 1996.

Ebdon, R. A., Notes on the wind flow at 50 mb in tropical and subtropical regions in January 1957 and in 1958, *Q. J. R. Meteorol. Soc.*, *86*, 540–542, 1960.

Ebdon, R. A., and R. G. Veryard, Fluctuations in equatorial stratospheric winds, *Nature*, *189*, 791–793, 1961.

Edmon, H. J., B. J. Hoskins, and M. E. McIntyre, Eliassen-Palm cross sections for the troposphere, *J. Atmos. Sci.*, *37*, 2600–2616, 1980.

Eliassen, A., and E. E. Palm, On the transport of energy in stationary mountain waves, *Geophys. Publ.*, *22*, 1–23, 1961.

Elsner, J. B., A. B. Kara, and M. A. Owens, Fluctuations in North Atlantic hurricane frequency, *J. Clim.*, *12*, 427–437, 1999.

Fontaine, B., S. Janicot, and V. Moron, Rainfall anomaly patterns and wind field signals over west Africa in August, *J. Clim.*, *8*, 1503–1510, 1995.

Fovell, R., D. Durran, and J. R. Holton, Numerical simulations of convectively generated stratospheric gravity waves, *J. Atmos. Sci.*, *49*, 1427–1442, 1992.

Friedson, A. J., New observations and modelling of a QBO-like oscillation in Jupiter's stratosphere, *Icarus*, *137*, 34–55, 1999.

Funk, J. P., and G. L. Garnham, Australian ozone observations and a suggested 24 month cycle, *Tellus*, *14*, 378–382, 1962.

Garcia, R. R., On the mean meridional circulation of the middle atmosphere, *J. Atmos. Sci.*, *41*, 2113–2125, 1987.

Garcia, R. R., and S. Solomon, A possible relationship between interannual variability in Antarctic ozone and the quasi-biennial oscillation, *Geophys. Res. Lett.*, *14*, 848–851, 1987.

Garcia, R. R., T. J. Dunkerton, R. S. Lieberman, and R. A. Vincent, Climatology of the semiannual oscillation in the tropical middle atmosphere, *J. Geophys. Res.*, *102*, 26,019–26,032, 1997.

Geller, M. A., W. Shen, M. Zhang, and W.-W. Tan, Calculations of the stratospheric quasi-biennial oscillation for time-varying wave forcing, *J. Atmos. Sci.*, *54*, 883–894, 1997.

Grant, W. B., E. V. Browell, C. S. Long, L. L. Stowe, R. G. Grainger, and A. Lambert, Use of volcanic aerosols to study the tropical stratospheric reservoir, *J. Geophys. Res.*, *101*, 3973–3988, 1996.

Gray, L. J., A model study of the influence of the quasi-biennial oscillation on trace gas distributions in the middle and upper stratosphere, *J. Geophys. Res.*, *105*, 4539–4551, 2000.

Gray, L. J., and M. P. Chipperfield, On the interannual variability of trace gases in the middle atmosphere, *Geophys. Res. Lett.*, *17*, 933–936, 1990.

Gray, L. J., and T. J. Dunkerton, The role of the seasonal cycle in the quasi-biennial oscillation of ozone, *J. Atmos. Sci.*, *47*, 2429–2451, 1990.

Gray, L. J., and J. A. Pyle, The semi-annual oscillation and equatorial tracer distributions, *Q. J. R. Meteorol. Soc.*, *112*, 387–407, 1986.

Gray, L. J., and J. A. Pyle, A two-dimensional model of the quasi-biennial oscillation in ozone, *J. Atmos. Sci.*, *46*, 203–220, 1989.

Gray, L. J., and J. M. Russell III, Interannual variability of trace gases in the subtropical winter stratosphere, *J. Atmos. Sci.*, *56*, 977–993, 1999.

Gray, L. J., and S. L. Ruth, The modeled latitudinal distribution of the ozone quasi-biennial oscillation using observed equatorial winds, *J. Atmos. Sci.*, *50*, 1033–1046, 1993.

Gray, L. J., S. J. Phipps, T. J. Dunkerton, M. P. Baldwin, E. F. Drysdale, and M. R. Allen, A data study of the influence of the upper stratosphere on Northern Hemisphere stratospheric sudden warmings, *Q. J. R. Meteorol. Soc.*, in press, 2001.

Gray, W. M., Atlantic seasonal hurricane frequency, part I, El Niño and 30 mb quasi-biennial oscillation influences, *Mon. Weather Rev.*, *112*, 1649–1668, 1984a.

Gray, W. M., Atlantic seasonal hurricane frequency, part II, Forecasting its variability, *Mon. Weather Rev.*, *112*, 1669–1683, 1984b.

Gray, W. M., J. D. Sheaffer, and J. A. Knaff, Hypothesized mechanism for stratospheric QBO influence on ENSO variability, *Geophys. Res. Lett.*, *19*, 107–110, 1992a.

Gray, W. M., J. D. Sheaffer, and J. A. Knaff, Influence of the stratospheric QBO on ENSO variability, *J. Meteorol. Soc. Jpn.*, *70*, 975–995, 1992b.

Graystone, P., Meteorological office discussion—Tropical meteorology, *Meteorol. Mag.*, *88*, 113–119, 1959.

Gutzler, D. S., and D. E. Harrison, The structure and evolution of seasonal wind anomalies over the near-equatorial eastern Indian and western Pacific oceans, *Mon. Weather Rev.*, *115*, 169–192, 1987.

Haigh, J. D., The role of stratospheric ozone in modulating the solar radiative forcing of climate, *Nature*, *370*, 544–546, 1994.

Haigh, J. D., The impact of solar variability on climate, *Science*, *272*, 981–984, 1996.

Haigh, J. D., A GCM study of climate change in response to the annual 11-year solar cycle, *Q. J. R. Meteorol. Soc.*, *125*, 817–892, 1999.

Hamilton, K., The vertical structure of the quasi-biennial oscillation: Observations and theory, *Atmos. Ocean*, *19*, 236–250, 1981.

Hamilton, K., Quasi-biennial and other long-period variations in the solar semidiurnal barometric oscillation: Observations, theory and possible application to the problem of monitoring changes in global ozone, *J. Atmos. Sci.*, *40*, 2432–2443, 1983.

Hamilton, K., Mean wind evolution through the quasi-biennial cycle of the tropical lower stratosphere, *J. Atmos. Sci.*, *41*, 2113–2125, 1984.

Hamilton, K., Interhemispheric asymmetry and annual synchronization of the ozone quasi-biennial oscillation, *J. Atmos. Sci.*, *46*, 1019–1025, 1989.

Hamilton, K., An examination of observed Southern Oscillation effects in the Northern Hemisphere stratosphere, *J. Atmos. Sci.*, *50*, 3468–3473, 1993.

Hamilton, K., Interannual variability in the Northern Hemisphere winter middle atmosphere in control and perturbed experiments with the GFDL SKYHI general circulation model, *J. Atmos. Sci.*, *52*, 44–66, 1995.

Hamilton, K., Observations of tropical stratospheric winds before World War II, *Bull. Am. Meteorol. Soc.*, *79*, 1367–1371, 1998a.

Hamilton, K., Effects of an imposed quasi-biennial oscillation in a comprehensive troposphere-stratosphere-mesosphere general circulation model, *J. Atmos. Sci.*, *55*, 2393–2418, 1998b.

Hamilton, K., R. J. Wilson, and R. Hemler, Middle atmosphere simulated with high vertical and horizontal resolution versions of a GCM: Improvement in the cold pole bias and generation of a QBO-like oscillation in the tropics, *J. Atmos. Sci.*, *56*, 3829–3846, 1999.

Hasebe, F., Quasi-biennial oscillations of ozone and diabatic circulation in the equatorial stratosphere, *J. Atmos. Sci.*, *51*, 729–745, 1994.

Hayashi, Y., and D. G. Golder, Kelvin and mixed Rossby-gravity waves appearing in the GFDL "SKYHI" general circulation model and the FGGE data set: Implications for their generation mechanism and role in the QBO, *J. Meteorol. Soc. Jpn.*, *72*, 901–935, 1994.

Haynes, P. H., The latitudinal structure of the quasi-biennial oscillation, *Q. J. R. Meteorol. Soc.*, *124*, 2645–2670, 1998.

Hess, J. C., and J. B. Elsner, Extended-range hindcasts of tropical-origin Atlantic hurricane activity, *Geophys. Res. Lett.*, *21*, 365–368, 1994.

Hess, P. G., and D. O'Sullivan, A three-dimensional modeling study of the extratropical quasi-biennial oscillation in ozone, *J. Atmos. Sci.*, *52*, 1539–1554, 1995.

Hilsenrath, E., and B. M. Schlesinger, Total ozone seasonal and interannual variations derived from the 7-year Nimbus 4 BUV data set, *J. Geophys. Res.*, *86*, 12,087–12,096, 1981.

Hines, C. O., Doppler-spread parameterization of gravity wave momentum deposition in the middle atmosphere, 2, Broad and quasi-monochromatic spectra, and implementation, *J. Atmos. Terr. Phys.*, *59*, 387–400, 1997.

Hirota, I., Equatorial waves in the upper stratosphere and mesosphere in relation to the semiannual oscillation of the zonal wind, *J. Atmos. Sci.*, *35*, 714–722, 1978.

Hitchman, M. H., C. B. Leovy, J. C. Gille, and P. L. Bailey, Quasi-stationary asymmetric circulations in the equatorial lower mesosphere, *J. Atmos. Sci.*, *44*, 2219–2236, 1987.

Hitchman, M. H., M. McKay, and C. R. Trepte, A climatology of stratospheric aerosol, *J. Geophys. Res.*, *99*, 20,689–20,700, 1994.

Holton, J. R., *The Dynamic Meteorology of the Stratosphere and Mesosphere*, 319 pp., Am. Meteorol. Soc., Boston, Mass., 1975.

Holton, J. R., Influence of the annual cycle in meridional transport on the quasi-biennial oscillation in total ozone, *J. Atmos. Sci.*, *46*, 1434–1439, 1989.

Holton, J. R., and J. Austin, The influence of the QBO on sudden stratospheric warmings, *J. Atmos. Sci.*, *48*, 607–618, 1991.

Holton, J. R., and R. S. Lindzen, An updated theory for the quasi-biennial cycle of the tropical stratosphere, *J. Atmos. Sci.*, *29*, 1076–1080, 1972.

Holton, J. R., and H.-C. Tan, The influence of the equatorial quasi-biennial oscillation on the global circulation at 50 mb, *J. Atmos. Sci.*, *37*, 2200–2208, 1980.

Holton, J. R., and H.-C. Tan, The quasi-biennial oscillation in the Northern Hemisphere lower stratosphere, *J. Meteorol. Soc. Jpn.*, *60*, 140–148, 1982.

Holton, J. R., P. H. Haynes, M. E. McIntyre, A. R. Douglass, R. B. Hood, and L. Pfister, Stratosphere-troposphere exchange, *Rev. Geophys.*, *33*, 403–439, 1995.

Horinouchi, T., and S. Yoden, Excitation of transient waves by localized episode heating in the tropics and their propagation in the middle atmosphere, *J. Meteorol. Soc. Jpn.*, *74*, 189–210, 1996.

Horinouchi, T., and S. Yoden, Wave-mean flow interaction associated with a QBO-like oscillation simulated in a simplified GCM, *J. Atmos. Sci.*, *55*, 502–526, 1998.

Huang, T. Y. W., The impact of solar radiation on the quasi-biennial oscillation of ozone in the tropical stratosphere, *Geophys. Res. Lett.*, *23*, 3211–3214, 1996.

Jones, D. B. A., H. R. Schneider, and M. B. McElroy, Effects of the quasi-biennial oscillation on the zonally averaged transport of tracers, *J. Geophys. Res.*, *103*, 11,235–11,249, 1998.

Karoly, D. J., G. L. Roff, and M. J. Reeder, Gravity wave activity associated with tropical convection detected in TOGA COARE sounding data, *Geophys. Res. Lett.*, *23*, 261–264, 1996.

Kawamoto, N., M. Shiotani, and J. C. Gille, Equatorial Kelvin waves and corresponding tracer oscillations in the lower stratosphere as seen in LIMS data, *J. Meteorol. Soc. Jpn.*, *75*, 763–773, 1997.

Kawamura, R., Quasi-biennial oscillation modes appearing in the tropical sea water temperature and 700 mb zonal wind, *J. Meteorol. Soc. Jpn.*, *66*, 955–965, 1988.

Kennaugh, R., S. Ruth, and L. J. Gray, Modeling quasi-biennial variability in the semiannual double peak, *J. Geophys. Res.*, *102*, 16,169–16,187, 1997.

Kinnersley, J. S., On the seasonal asymmetry of the lower and middle latitude QBO circulation anomaly, *J. Atmos. Sci.*, *56*, 1942–1962, 1999.

Kinnersley, J. S., and S. Pawson, The descent rates of the shear zones of the equatorial QBO, *J. Atmos. Sci.*, *53*, 1937–1949, 1996.

Kinnersley, J. S., and K. K. Tung, Modeling the global interannual variability of ozone due to the equatorial QBO and to extratropical planetary wave variability, *J. Geophys. Res.*, *94*, 11,559–11,571, 1998.

Knaff, J. A., Evidence of a stratospheric QBO modulation of tropical convection, *Pap. 520*, 91 pp., Dep. of Atmos. Sci., Colo. State Univ., Fort Collins, 1993.

Kodera, K., K. Yamazaki, M. Chiba, and K. Shibata, Downward propagation of upper stratospheric mean zonal wind perturbation to the troposphere, *Geophys. Res. Lett.*, *17*, 1263–1266, 1990.

Labitzke, K., Sunspots, the QBO, and the stratospheric temperature in the North Polar region, *Geophys. Res. Lett.*, *14*, 535–537, 1987.

Labitzke, K., and H. van Loon, Association between the 11-year solar cycle, the QBO and the atmosphere, part I, The troposphere and stratosphere in the Northern Hemisphere in winter, *J. Atmos. Terr. Phys.*, *50*, 197–206, 1988.

Labitzke, K., and H. van Loon, *The Stratosphere*, 179 pp., Springer-Verlag, New York, 1999.

Lait, L. R., M. R. Schoeberl, and P. A. Newman, Quasi-biennial modulation of the Antarctic ozone depletion, *J. Geophys. Res.*, *94*, 11,559–11,571, 1989.

Lander, M. A., and C. P. Guard, A look at global tropical cyclone activity during 1995: Contrasting high Atlantic activity with low activity in other basins, *Mon. Weather Rev.*, *126*, 1163–1173, 1998.

Landsea, C. W., G. D. Bell, W. M. Gray, and S. B. Goldenberg, The extremely active 1995 Atlantic hurricane season: Environmental conditions and verification of seasonal forecasts, *Mon. Weather Rev.*, *126*, 1174–1193, 1998.

Larsen, M. F., W. E. Schwartz, and R. F. Woodman, Gravity wave generation by thunderstorms observed with a vertically pointing 430-MHz radar, *Geophys. Res. Lett.*, *9*, 571–574, 1982.

Lau, K.-M., and P. J. Sheu, Annual cycle, quasi-biennial oscillation, and Southern Oscillation in global precipitation, *J. Geophys. Res.*, *93*, 10,975–10,988, 1988.

Leovy, C. B., A. J. Friedson, and G. S. Orton, The quasi-quadrennial oscillation of Jupiter's equatorial stratosphere, *Nature*, *354*, 380–382, 1991.

Li, D., K. P. Shine, and L. J. Gray, The role of ozone-induced diabatic heating anomalies in the quasi-biennial oscillation, *Q. J. R. Meteorol. Soc.*, *121*, 937–943, 1995.

Li, X., P. L. Read, and D. G. Andrews, Mode selection, wave breaking and parametric sensitivity in the quasi-biennial oscillation, *Q. J. R. Meteorol. Soc.*, *123*, 2041–2068, 1997.

Lindzen, R. S., On the development of the theory of the QBO, *Bull. Am. Meteorol. Soc.*, *68*, 329–337, 1987.

Lindzen, R. S., and J. R. Holton, A theory of the quasi-biennial oscillation, *J. Atmos. Sci.*, *25*, 1095–1107, 1968.

Ling, X.-D., and J. London, The quasi-biennial oscillation of ozone in the tropical middle stratosphere: A one-dimensional model, *J. Atmos. Sci.*, *43*, 3122–3136, 1986.

Luo, M., J. M. Russell III, and T. Y. W. Huang, Halogen Occultation Experiment observations of the quasi-biennial oscillation and the effects of Pinatubo aerosols in the tropical stratosphere, *J. Geophys. Res.*, *102*, 19,187–19,198, 1997.

Mancini, E., G. Visconti, G. Pitari, and M. Verdecchia, An estimate of the Antarctic ozone modulation by the QBO, *Geophys. Res. Lett.*, *18*, 175–178, 1991.

Maruyama, T., Large-scale disturbances in the equatorial lower stratosphere, *J. Meteorol. Soc. Jpn.*, *45*, 196–199, 1967.

Maruyama, T., Annual and QBO-synchronized variations of lower-stratospheric equatorial wave activity over Singapore during 1961–1989, *J. Meteorol. Soc. Jpn.*, *69*, 219–232, 1991.

Maruyama, T., Upward transport of westerly momentum due to disturbances of the equatorial lower stratosphere in the period range of about 2 days—Singapore data analysis for 1983–1993, *J. Meteorol. Soc. Jpn.*, *72*, 423–432, 1994.

Maruyama, T., The quasi-biennial oscillation (QBO) and equatorial waves—A historical review, *Pap. Meteorol. Geophys.*, *48*, 1–17, 1997.

Maruyama, T., and Y. Tsuneoka, Anomalously short duration of the easterly wind phase of QBO at 50 hPa in 1987 and its relation with an El Niño event, *J. Meteorol. Soc. Jpn.*, *69*, 219–232, 1988.

Matsuno, T., Quasi-geostrophic motions in the equatorial area, *J. Meteorol. Soc. Jpn.*, *44*, 25–43, 1966.

Mayr, H. G., J. G. Mengel, C. O. Hines, K. L. Chan, N. F.

Arnold, C. A. Reddy, and H. S. Porter, The gravity wave Doppler spread theory applied in a numerical spectral model of the middle atmosphere, 2, Equatorial oscillations, *J. Geophys. Res.*, *102*, 26,093–26,105, 1997.

McIntyre, M. E., On the role of wave propagation and wave breaking in atmosphere-ocean dynamics, in *Theoretical and Applied Mechanics 1992*, *Proceedings of the XVIII International Congress on Theoretical and Applied Mechanics*, edited by S. R. Bodner et al., pp. 281–304, Elsevier Sci., New York, 1993.

McIntyre, M. E., The quasi-biennial oscillation (QBO): Some points about the terrestrial QBO and the possibility of related phenomena in the solar interior, in *The Solar Engine and Its Influence on the Terrestrial Atmosphere and Climate*, edited by E. Nesme-Ribes, pp. 293–320, Springer-Verlag, New York, 1994.

McIntyre, M. E., and T. N. Palmer, Breaking planetary waves in the stratosphere, *Nature*, *305*, 593–600, 1983.

McIntyre, M. E., and T. N. Palmer, The "surf zone" in the stratosphere, *J. Atmos. Terr. Phys.*, *46*, 825–849, 1984.

Mengel, J. G., H. G. Mayr, K. L. Chan, C. O. Hines, C. A. Reddy, N. F. Arnold, and H. S. Porter, Equatorial oscillations in the middle atmosphere generated by small-scale gravity waves, *Geophys. Res. Lett.*, *22*, 3027–3030, 1995.

Moron, V., B. Fontaine, and P. Roucou, Global equatorial variability of 850- and 200-hPa zonal winds from rawinsondes between 1963 and 1989, *Geophys. Res. Lett.*, *22*, 1701–1704, 1995.

Mote, P. W., K. H. Rosenlof, M. E. McIntyre, E. S. Carr, J. C. Gille, J. R. Holton, J. S. Kinnersley, H. C. Pumphrey, J. M. Russell, and J. W. Waters, An atmospheric tape recorder: The imprint of tropical tropopause temperatures on stratospheric water vapor, *J. Geophys. Res.*, *101*, 3989–4006, 1996.

Mote, P. W., T. J. Dunkerton, and H. C. Pumphrey, Subseasonal variations in lower stratospheric water vapor, *Geophys. Res. Lett.*, *25*, 2445–2448, 1998.

Nagashima, T., M. Takahashi, and F. Hasebe, The first simulation of an ozone QBO in a general circulation model, *Geophys. Res. Lett.*, *25*, 3131–3134, 1998.

Naito, Y., and I. Hirota, Interannual variability of the northern winter stratospheric circulation related to the QBO and the solar cycle, *J. Meteorol. Soc. Jpn.*, *75*, 925–937, 1997.

Naujokat, B., An update of the observed quasi-biennial oscillation of the stratospheric winds over the tropics, *J. Atmos. Sci.*, *43*, 1873–1877, 1986.

Nigam, S., On the structure of variability of the observed tropospheric and stratospheric zonal-mean wind, *J. Atmos. Sci.*, *47*, 1799–1813, 1990.

Niwano, M., and M. Takahashi, Notes and correspondence: The influence of the equatorial QBO on the Northern Hemisphere winter circulation of a GCM, *J. Meteorol. Soc. Jpn.*, *76*, 453–461, 1998.

Oltmans, S. J., and J. London, The quasi-biennial oscillation in atmospheric ozone, *J. Geophys. Res.*, *87*, 8981–8989, 1982.

Ortland, D. A., Rossby wave propagation into the tropical stratosphere observed by the High Resolution Doppler Imager, *Geophys. Res. Lett.*, *24*, 1999–2002, 1997.

O'Sullivan, D., Interaction of extratropical Rossby waves with westerly quasi-biennial oscillation winds, *J. Geophys. Res.*, *102*, 19,461–19,469, 1997.

O'Sullivan, D., and P. Chen, Modeling the QBO's influence on isentropic tracer transport in the subtropics, *J. Geophys. Res.*, *101*, 6811–6821, 1996.

O'Sullivan, D., and T. J. Dunkerton, Seasonal development of the extratropical QBO in a numerical model of the middle atmosphere, *J. Atmos. Sci.*, *51*, 3706–3721, 1994.

O'Sullivan, D., and T. J. Dunkerton, The influence of the quasi-biennial oscillation on global constituent distributions, *J. Geophys. Res.*, *102*, 21,731–21,743, 1997.

O'Sullivan, D., and M. L. Salby, Coupling of the quasi-biennial oscillation and the extratropical circulation in the stratosphere through planetary wave transport, *J. Atmos. Sci.*, *47*, 650–673, 1990.

O'Sullivan, D., and R. E. Young, Modeling the quasi-biennial oscillation's effect on the winter stratospheric circulation, *J. Atmos. Sci.*, *49*, 2437–2448, 1992.

Palmer, C. E., The general circulation between 200 mb and 10 mb over the equatorial Pacific, *Weather*, *9*, 3541–3549, 1954.

Pawson, S., and M. Fiorino, A comparison of reanalyses in the tropical stratosphere, part 1, Thermal structure and the annual cycle, *Clim. Dyn.*, *14*, 631–644, 1998.

Pawson, S., K. Labitzke, R. Lenschow, B. Naujokat, B. Rajewski, M. Wiesner, and R.-C. Wohlfart, Climatology of the Northern Hemisphere stratosphere derived from Berlin analyses, part 1, Monthly means, technical report, *Ser. A*, *7*(3), Freie Univ. Berlin, 1993.

Pfister, L., W. Starr, R. Craig, M. Loewenstein, and M. Legg, Small-scale motions observed by aircraft in the tropical lower stratosphere: Evidence for mixing and its relationship to large scale flows, *J. Atmos. Sci.*, *43*, 3210–3225, 1986.

Pfister, L., S. Scott, M. Loewenstein, S. Bowen, and M. Legg, Mesoscale disturbances in the tropical stratosphere excited by convection: Observations and effects on the stratospheric momentum budget, *J. Atmos. Sci.*, *50*, 1058–1075, 1993a.

Pfister, L., K. R. Chan, T. P. Bui, S. Bowen, M. Legg, B. Gary, K. Kelly, M. Proffitt, and W. Starr, Gravity waves generated by a tropical cyclone during the STEP tropical field program: A case study, *J. Geophys. Res.*, *98*, 8611–8638, 1993b.

Plumb, R. A., The interaction of two internal waves with the mean flow: Implications for the theory of the quasi-biennial oscillation, *J. Atmos. Sci.*, *34*, 1847–1858, 1977.

Plumb, R. A., Zonally symmetric Hough modes and meridional circulations in the middle atmosphere, *J. Atmos. Sci.*, *39*, 983–991, 1982.

Plumb, R. A., The quasi-biennial oscillation, in *Dynamics of the Middle Atmosphere*, edited by J. R. Holton and T. Matsuno, pp. 217–251, Terra Sci., Tokyo, 1984.

Plumb, R. A., and R. C. Bell, Equatorial waves in steady zonal shear flow, *Q. J. R. Meteorol. Soc.*, *108*, 313–334, 1982a.

Plumb, R. A., and R. C. Bell, A model of the quasi-biennial oscillation on an equatorial beta-plane, *Q. J. R. Meteorol. Soc.*, *108*, 335–352, 1982b.

Plumb, R. A., and A. D. McEwan, The instability of a forced standing wave in a viscous stratified fluid: A laboratory analogue of the quasi-biennial oscillation, *J. Atmos. Sci.*, *35*, 1827–1839, 1978.

Politowicz, P. A., and M. H. Hitchman, Exploring the effects of forcing the quasi-biennial oscillation in a two-dimensional model, *J. Geophys. Res.*, *102*, 16,481–16,497, 1997.

Poole, L. R., S. Solomon, M. P. McCormick, and M. C. Pitts, The interannual variability of polar stratospheric clouds and related parameters in Antarctica during September and October, *Geophys. Res. Lett.*, *16*, 1157–1160, 1989.

Ramanathan, K. R., Bi-annual variation of atmospheric ozone over the tropics, *Q. J. R. Meteorol. Soc.*, *89*, 540–542, 1963.

Randel, W. J., The evaluation of winds from geopotential height data in the stratosphere, *J. Atmos. Sci.*, *44*, 3097–3120, 1987.

Randel, W. J., Kelvin wave induced trace constituent oscillations in the equatorial stratosphere, *J. Geophys. Res.*, *95*, 18,641–18,652, 1990.

Randel, W. J., and J. B. Cobb, Coherent variations of monthly mean column ozone and lower stratospheric temperature, *J. Geophys. Res.*, *99*, 5433–5447, 1994.

Randel, W. J., and F. Wu, Isolation of the ozone QBO in SAGE II data by singular decomposition, *J. Atmos. Sci.*, *53*, 2546–2559, 1996.

Randel, W. J., F. Wu, J. M. Russel III, A. Roche, and J. Waters, Seasonal cycles and QBO variations in stratospheric CH_4 and H_2O observed in UARS HALOE data, *J. Atmos. Sci.*, *55*, 163–185, 1998.

Randel, W. J., F. Wu, R. Swinbank, J. Nash, and A. O'Neill, Global QBO circulation derived from UKMO stratospheric analyses, *J. Atmos. Sci.*, *56*, 457–474, 1999.

Reed, R. J., A tentative model of the 26-month oscillation in tropical latitudes, *Q. J. R. Meteorol. Soc.*, *90*, 441–466, 1964.

Reed, R. J., The structure and dynamics of the 26-month oscillation, in *Proceedings of the International Symposium on the Dynamics of Large-Scale Processes in the Atmosphere*, pp. 376–387, Russ. Acad. of Sci., Moscow, 1967.

Reed, R. J., W. J. Campbell, L. A. Rasmussen, and R. G. Rogers, Evidence of a downward propagating annual wind reversal in the equatorial stratosphere, *J. Geophys. Res.*, *66*, 813–818, 1961.

Reid, G. C., and K. S. Gage, Interannual variations in the height of the tropical tropopause, *J. Geophys. Res.*, *90*, 5629–5635, 1985.

Rind, D., and N. K. Balachandran, Modeling the effects of UV variability and the QBO on the troposphere-stratosphere system, part II, The troposphere, *J. Clim.*, *8*, 2080–2095, 1995.

Robinson, W., The application of quasi-geostrophic Eliassen-Palm flux to the analysis of stratospheric data, *J. Atmos. Sci.*, *43*, 1017–1023, 1986.

Röttger, J., Structure and dynamics of the stratosphere and mesosphere revealed by VHF radar investigations, *Pure Appl. Geophys.*, *118*, 494–527, 1980.

Rottman, G., Solar ultraviolet irradiance and its temporal variability, *J. Atmos. Sol. Terr. Phys.*, *61*, 37–44, 1999.

Ruth, S., R. Kennaugh, L. J. Gray, and J. M. Russell III, Seasonal, semiannual, and interannual variability seen in measurements of methane made by the UARS Halogen Occultation Experiment, *J. Geophys. Res.*, *102*, 16,189–16,199, 1997.

Salby, M., and P. Callaghan, Connection between the solar cycle and the QBO: The missing link, *J. Clim.*, *13*, 2652–2662, 2000.

Salby, M., and D. Shea, Correlations between solar activity and the atmosphere: An unphysical explanation, *J. Geophys. Res.*, *96*, 22,579–22,595, 1991.

Salby, M. L., D. L. Hartmann, P. L. Bailey, and J. C. Gille, Evidence for equatorial Kelvin modes in Nimbus-7 LIMS, *J. Atmos. Sci.*, *41*, 220–235, 1984.

Salby, M., P. Callaghan, and D. Shea, Interdependence of the tropical and extratropical QBO: Relationship to the solar cycle versus a biennial oscillation in the stratosphere, *J. Geophys. Res.*, *102*, 29,789–29,798, 1997.

Saravanan, R., A multiwave model of the quasi-biennial oscillation, *J. Atmos. Sci.*, *47*, 2465–2474, 1990.

Sassi, F., and R. R. Garcia, The role of equatorial waves forced by convection in the tropical semiannual oscillation, *J. Atmos. Sci.*, *54*, 1925–1942, 1997.

Sato, K., Vertical wind disturbances in the afternoon of midsummer revealed by the MU radar, *Geophys. Res. Lett.*, *19*, 1943–1946, 1992.

Sato, K., Small-scale wind disturbances observed by the MU radar during the passage of Typhoon Kelly, *J. Atmos. Sci.*, *50*, 518–537, 1993.

Sato, K., and T. J. Dunkerton, Estimates of momentum flux associated with equatorial Kelvin and gravity waves, *J. Geophys. Res.*, *102*, 26,247–26,261, 1997.

Sato, K., F. Hasegawa, and I. Hirota, Short-period disturbances in the equatorial lower stratosphere, *J. Meteorol. Soc. Jpn.*, *72*, 859–872, 1994.

Sato, K., H. Hashiguchi, and S. Fukao, Gravity waves and turbulence associated with cumulus convection observed with the UHF/VHF clear-air Doppler radars, *J. Geophys. Res.*, *100*, 7111–7119, 1995.

Scott, R. K., and P. H. Haynes, Internal interannual variability of the extratropical stratospheric circulation: The low latitude flywheel, *Q. J. R. Meteorol. Soc.*, *124*, 2149–2173, 1998.

Shapiro, L. J., The relationship of the quasi-biennial oscillation to Atlantic tropical storm activity, *Mon. Weather Rev.*, *117*, 1545–1552, 1989.

Shen, S., and K.-M. Lau, Biennial oscillation associated with the east Asian summer monsoon and tropical sea surface temperatures, *J. Meteorol. Soc. Jpn.*, *73*, 105–124, 1995.

Shimizu, A., and T. Tsuda, Radiosonde observations of equatorial atmosphere dynamics over Indonesia, *J. Geophys. Res.*, *102*, 26,159–26,172, 1997.

Shindell, D., D. Rind, N. B. Balanchandran, J. Lean, and P. Lonergan, Solar cycle variability, ozone and climate, *Science*, *284*, 305–308, 1999.

Shiotani, M., and T. Horinouchi, Kelvin wave activity and the quasi-biennial oscillation in the equatorial lower stratosphere, *J. Meteorol. Soc. Jpn.*, *71*, 175–182, 1993.

Shiotani, M., J. C. Gille, and A. E. Roche, Kelvin waves in the equatorial lower stratosphere as revealed by Cryogenic Limb Array Etalon Spectrometer temperature data, *J. Geophys. Res.*, *102*, 26,131–26,140, 1997.

Takahashi, M., A two-dimensional numerical model of the quasi-biennial oscillation, *J. Meteorol. Soc. Jpn.*, *65*, 523–535, 1987.

Takahashi, M., Simulation of the stratospheric quasi-biennial oscillation using a general circulation model, *Geophys. Res. Lett.*, *23*, 661–664, 1996.

Takahashi, M., Simulation of the stratospheric quasi-biennial oscillation in a general circulation model, *Geophys. Res. Lett.*, *26*, 1307–1310, 1999.

Takahashi, M., and B. A. Boville, A three-dimensional simulation of the equatorial quasi-biennial oscillation, *J. Atmos. Sci.*, *49*, 1020–1035, 1992.

Takahashi, M., N. Zhao, and T. Kumakura, Equatorial waves in a general circulation model simulating a quasi-biennial oscillation, *J. Meteorol. Soc. Jpn.*, *75*, 529–540, 1997.

Takayabu, Y. N., K.-M. Lau, and C.-H. Sui, Observation of a quasi-2-day wave during TOGA COARE, *Mon. Weather Rev.*, *124*, 1892–1913, 1996.

Tanaka, H., and N. Yoshizawa, A slowly-varying model of the quasi-biennial oscillation involving effects of transience, self-acceleration and saturation of equatorial waves, *J. Atmos. Sci.*, *44*, 1427–1436, 1987.

Teitelbaum, H., and P. Bauer, Stratospheric temperature eleven year variation: Solar cycle influence or stroboscopic effect?, *Ann. Geophys.*, *8*, 239–242, 1990.

Teitelbaum, H., F. Vial, and P. Bauer, The stratospheric quasi-biennial oscillation observed in the semidiurnal ground pressure data, *Ann. Geophys.*, *13*, 740–744, 1995.

Thompson, D. W. J., and J. M. Wallace, The Arctic Oscillation signature in the wintertime geopotential height and temperature fields, *Geophys. Res. Lett.*, *25*, 1297–1300, 1998.

Thompson, D. W. J., and J. M. Wallace, Annular modes in the extratropical circulation, part I, Month-to-month variability, *J. Clim.*, *13*, 1000–1016, 2000.

Tiedtke, M., A comprehensive mass flux scheme for cumulus parameterization in large-scale models, *Mon. Weather Rev.*, *117*, 1779–1800, 1989.

Trepte, C. R., and M. H. Hitchman, Tropical stratospheric circulation deduced from satellite aerosol data, *Nature*, *355*, 626–628, 1992.

Tsuda, T., Y. Murayama, H. Wiryosumarto, S. W. B. Harijono, and S. Kato, Radiosonde observations of equatorial atmospheric dynamics over Indonesia, 1, Equatorial waves and diurnal tides, *J. Geophys. Res.*, *99*, 10,491–10,506, 1994a.

Tsuda, T., Y. Murayama, H. Wiryosumarto, S. W. B. Harijono, and S. Kato, Radiosonde observations of equatorial atmospheric dynamics over Indonesia, 2, Characteristics of gravity waves, *J. Geophys. Res.*, *99*, 10,507–10,516, 1994b.

Tung, K., and H. Yang, Global QBO in circulation and ozone, part I, Reexamination of observational evidence, *J. Atmos. Sci.*, *51*, 2699–2707, 1994a.

Tung, K., and H. Yang, Global QBO in circulation and ozone, part II, A simple mechanistic model, *J. Atmos. Sci.*, *51*, 2708–2721, 1994b.

Untch, A., Simulation of the quasi-biennial oscillation with the ECMWF model, in *Research Activities in the Atmospheric and Oceanic Modelling*, pp. 6.26–6.27, World Meteorol. Organ., Geneva, 1998.

van Loon, H., and K. Labitzke, The Southern Oscillation, part V, The anomalies in the lower stratosphere of the Northern Hemisphere in winter and a comparison with the quasi-biennial oscillation, *Mon. Weather Rev.*, *115*, 357–369, 1987.

van Loon, H., and K. Labitzke, The 10–12 year atmospheric oscillation, *Meteorol. Z.*, *3*, 259–266, 1994.

Veryard, R. G., and R. A. Ebdon, Fluctuations in tropical stratospheric winds, *Meteorol. Mag.*, *90*, 125–143, 1961.

Vincent, R. A., and M. J. Alexander, Gravity waves in the tropical lower stratosphere: An observational study of seasonal and interannual variability, *J. Geophys. Res.*, *105*, 17,971–17,982, 2000.

Wada, K., T. Nitta, and K. Sato, Equatorial inertia-gravity waves in the lower stratosphere revealed by TOGA-COARE IOP data, *J. Meteorol. Soc. Jpn.*, *77*, 721–736, 1999.

Wallace, J. M., General circulation of the tropical lower stratosphere, *Rev. Geophys.*, *11*, 191–222, 1973.

Wallace, J. M., and F.-C. Chang, Interannual variability of the wintertime polar vortex in the Northern Hemisphere middle stratosphere, *J. Meteorol. Soc. Jpn.*, *60*, 149–155, 1982.

Wallace, J. M., and J. R. Holton, A diagnostic numerical model of the quasi-biennial oscillation, *J. Atmos. Sci.*, *25*, 280–292, 1968.

Wallace, J. M., and V. E. Kousky, Observational evidence of Kelvin waves in the tropical stratosphere, *J. Atmos. Sci.*, *25*, 900–907, 1968a.

Wallace, J. M., and V. E. Kousky, On the relation between Kelvin waves and the quasi-biennial oscillation, *J. Meteorol. Soc. Jpn.*, *46*, 496–502, 1968b.

Wallace, J. M., R. L. Panetta, and J. Estberg, Representation of the equatorial stratospheric quasi-biennial oscillation in EOF phase space, *J. Atmos. Sci.*, *50*, 1751–1762, 1993.

Waugh, D. W., Seasonal variation of isentropic transport out of the tropical stratosphere, *J. Atmos. Sci.*, *101*, 4007–4023, 1996.

Waugh, D. W., and W. J. Randel, Climatology of Arctic and Antarctic polar vortices using elliptical diagnostics, *J. Atmos. Sci.*, *56*, 1594–1613, 1999.

Wheeler, M., and G. N. Kiladis, Convectively coupled equatorial waves: Analysis of clouds and temperature in the wavenumber-frequency domain, *J. Atmos. Sci.*, *56*, 374–399, 1999.

Wikle, C. K., R. A. Madden, and T.-C. Chen, Seasonal variations of upper tropospheric and lower stratospheric equatorial waves over the tropical Pacific, *J. Atmos. Sci.*, *54*, 1895–1909, 1997.

Willson, R., H. Hudson, C. Frohlich, and R. Brusa, Long-term downward trend in total solar irradiance, *Science*, *234*, 1114–1117, 1986.

Xu, J.-S., On the relationship between the stratospheric quasi-biennial oscillation and the tropospheric Southern Oscillation, *J. Atmos. Sci.*, *49*, 725–734, 1992.

Yanai, M., and T. Maruyama, Stratospheric wave disturbances propagating over the equatorial Pacific, *J. Meteorol. Soc. Jpn.*, *44*, 291–294, 1966.

Yasunari, T., Zonally propagating modes of the global east-west circulation associated with the Southern Oscillation, *J. Meteorol. Soc. Jpn.*, *63*, 1013–1029, 1985.

Yasunari, T., A possible link of the QBOs between the stratosphere, troposphere and sea surface temperature in the tropics, *J. Meteorol. Soc. Jpn.*, *67*, 483–493, 1989.

Zawodny, J. M., and M. P. McCormick, Stratospheric Aerosol and Gas Experiment II measurements of the quasi-biennial oscillations in ozone and nitrogen dioxide, *J. Geophys. Res.*, *96*, 9371–9377, 1991.

Zhang, G. J., and N. A. McFarlane, Sensitivity of climate simulations to the parameterization of cumulus convection in the Canadian Climate Centre general circulation model, *Atmos. Ocean*, *33*, 407–446, 1995.

Ziemke, J. R., and J. L. Stanford, Quasi-biennial oscillation and tropical waves in total ozone, *J. Geophys. Res.*, *99*, 23,041–23,056, 1994.

M. J. Alexander, Colorado Research Associates, 3380 Mitchell Lane, Boulder, CO 80301. (alexand@colorado-research.com)

M. P. Baldwin and T. J. Dunkerton, NorthWest Research Associates, Inc., 14508 NE 20th Street, Bellevue, WA 98007-3713. (mark@nwra.com; tim@nwra.com)

L. J. Gray, Rutherford Appleton Laboratory, Chilton, Didcot, Oxon, OX11 0QX, England, UK. (lesley.gray@rl.ac.uk)

K. Hamilton, International Pacific Research Center, SOEST, University of Hawaii, 1680 East-West Road, Post 802, Honolulu, HI 96822. (kph@soest.hawaii.edu)

P. H. Haynes, Centre for Atmospheric Science, Department of Applied Mathematics and Theoretical Physics, University of Cambridge, Silver Street, Cambridge CB3 9EW, England, UK. (P.H.Haynes@damtp.cam.ac.uk)

I. Hirota, Department of Geophysics, Kyoto University, Kyoto 606-8502, Japan. (hirota@kugi.kyoto-u.ac.jp)

J. R. Holton, Department of Atmospheric Sciences, University of Washington, Box 351640, Seattle, WA 98195. (holton@atmos.washington.edu)

T. Horinouchi, Radio Atmospheric Science Center, Kyoto University, Uji 611-0011, Japan. (horinout@kurasc.kyoto-u.ac.jp)

D. B. A. Jones, Division of Engineering and Applied Sciences, Harvard University, 29 Oxford Street, Cambridge, MA 02138. (dbj@io.harvard.edu)

J. S. Kinnersley, 938 19th Street, Seattle, WA 98122.

C. Marquardt, GeoForschungsZentrum, Potsdam, Am Telegrafenberg, D-14473 Potsdam, Germany. (marq@gfz-potsdam.de)

W. J. Randel, Atmospheric Chemistry Division, National Center for Atmospheric Research, P.O. Box 3000, Boulder, CO 80307-3000. (randel@ucar.edu)

K. Sato, National Institute of Polar Research, Arctic Environment Research Center, Kaga 1-9-10, Itabashi, Tokyo 173-8515, Japan. (kaoru@nipr.ac.jp)

M. Takahashi, Center for Climate System Research, University of Tokyo, Komaba 4-6-1, Meguro-ku, Tokyo 153-8904, Japan. (masaaki@ccsr.u-tokyo.ac.jp)